

University of Louisville

ThinkIR: The University of Louisville's Institutional Repository

Electronic Theses and Dissertations

12-2016

Reflectivity of light emitting diodes (LED) and incandescent lights on concrete and asphalt pavements.

Jeremy Elliott Rice
University of Louisville

Follow this and additional works at: <https://ir.library.louisville.edu/etd>



Part of the [Civil Engineering Commons](#)

Recommended Citation

Rice, Jeremy Elliott, "Reflectivity of light emitting diodes (LED) and incandescent lights on concrete and asphalt pavements." (2016). *Electronic Theses and Dissertations*. Paper 2579.
<https://doi.org/10.18297/etd/2579>

This Master's Thesis is brought to you for free and open access by ThinkIR: The University of Louisville's Institutional Repository. It has been accepted for inclusion in Electronic Theses and Dissertations by an authorized administrator of ThinkIR: The University of Louisville's Institutional Repository. This title appears here courtesy of the author, who has retained all other copyrights. For more information, please contact thinkir@louisville.edu.

REFLECTIVITY OF LIGHT EMITTING DIODES (LED) AND INCANDESCENT
LIGHTS ON CONCRETE AND ASPHALT PAVEMENTS

By

Jeremy Elliott Rice
B.S.C.E., University of Memphis, 2015

A Thesis
Submitted to the Faculty of the
University of Louisville
J. B. Speed School of Engineering
in Partial Fulfillment of the Requirements
for the Degree of

Master of Science in Civil Engineering

Department of Civil and Environmental Engineering
University of Louisville
Louisville, Kentucky

December 2016

REFLECTIVITY OF LIGHT EMITTING DIODES (LED) AND INCANDESCENT
LIGHTS ON CONCRETE AND ASPHALT PAVEMENTS

By

Jeremy Elliott Rice
B.S.C.E., University of Memphis, 2015

A Thesis Approved on

November 21, 2016

By the Following Thesis Committee:

Young Hoon Kim, Thesis Director

Zihui Sun, Thesis Co-director

Jeffrey L. Hieb

ACKNOWLEDGEMENTS

As the great philosopher Thomas Aquinas brilliantly said:

“Better to illuminate than to merely shine,
to deliver to others contemplated truths than merely to contemplate.”

I would like to give special thanks to the financial supports from Ready Mixed Concrete Research and Education Foundation, the Kentucky Ready Mix Concrete Association (KRMCA), and the variable advice and assistance from Executive Director, Finley Messik and Mr. Greg Smith from the Kentucky Concrete Pavement Association.

I have to thank Dr. Hieb in advance for sacrificing his precious time to sit through my extremely lengthy defense presentation. A very special thank you goes to Dr. Sun for always giving her best creative solutions to problems that were constantly presented along the way. Last but not least, this document would not exist without Dr. Kim’s constant mentoring. I have always looked up to him not only as a mentor but as friend that truly understood how to motivate me.

A special thanks to my family to allowing me to bring this crazy process into their once calm and peaceful house. Thanks goes to my dog as well for keeping me remotely sane throughout this process. I could not have done it without their loving support.

ABSTRACT

REFLECTIVITY OF LIGHT EMITTING DIODES (LED) AND INCANDESCENT LIGHTS ON CONCRETE AND ASPHALT PAVEMENTS

Jeremy Elliott Rice

November 21, 2016

The purpose of this study is to investigate the reflectivity of light on concrete and asphalt pavement systems. In 1983, the Illuminating Engineering Society (IES) published the first recommended practice (RP-8) for the design of roadway and parking lot lighting. This design method implemented empirically tested factors which were defined as the “reduced luminance coefficients” or the R-Tables. The R-Tables are essential for proper design of light pole installation dimensions, required power, and the distribution of light. The originally tested pavements are not necessarily representative of modern pavement materials used today. Moreover, recent Light Emitting Diodes (LED) are a relatively new light technology consistently implemented in roadway and parking lot design. Therefore, the objective of this research is to reevaluate the reflectiveness of two pavement systems. The reflective properties of each pavements were evaluated considering angles (β and γ) of illuminated light from each varied light source (i.e., incandescent and LED). Research findings concluded that modern concrete pavement is up to 3 times more reflective than modern asphalt pavement. Furthermore, this research also indicates that the angular light reflectivity is not only influenced by the pavement system but also the light source being used to illuminate that surface with respect to varied (α , β , and γ) angles.

TABLE OF CONTENTS

APPROVAL PAGE	ii
ACKNOWLEDGEMENTS	iii
ABSTRACT	iv
LIST OF FIGURES	viii
LIST OF TABLES	xi
I. INTRODUCTION	1
A. Problem Statement	1
B. Objective of Reasearch	2
II. LITERATURE REVIEW AND BACKGROUND	3
A. Lighting Fundamentals	3
1. Illuminance	4
a. Distance Influencing Illuminance	5
b. Intensity Influencing Illuminance	6
2. Luminance.....	7
a. Defining Surface Lightness and Specularity.....	12
B. Roadway Lighting Design	16
1. Light Source Spectral Wavelength	16
2. Suface Reflectivity Design	19
a. R-Table Application.....	20

b. Limitations of Design Process	22
c. Reevaluation of R-Tables	24
III. EXPERIMENTAL PROGRAM	28
A. Lab Testing	29
1. Goniometer Prototype Concept.....	29
2. Measurement Tools.....	30
3. Lab Samples Tested	32
4. Lab Goniometer Testing Program	34
B. Field Testing	41
1. Portable Goniometer Design.....	41
a. Observation Angle of 15 Degrees.....	42
b. Observation Angle of 35 Degrees.....	43
2. Field Samples Tested	44
3. Portable Goniometer Testing Program	45
IV. TEST RESULTS AND ANALYSIS	48
A. Test Results.....	48
1. Luminance Results.....	48
a. Lab Results.....	49
b. Field Results.....	51
c. Summary	53
2. Luminance Results at Varied Angles.....	55
a. Lab Results.....	56
b. Field Results.....	60

B. Analysis.....	64
1. R-Values of Selected Samples	65
a. Lab R-Values	66
b. Field R-Values	69
2. R-Values Compared to Original R1 and R3	72
3. S1 Values Compared to Original R1, R2, R3, and R4.....	76
4. Specular and Diffused at Varied Observation Angles	78
V. CONCLUSION AND RECOMMENDATIONS	82
A. Conclusion	82
B. Recommendations.....	84
REFERENCES	85
APPENDIX.....	87
CURRICULUM VITA	103

LIST OF FIGURES

FIGURE 1. PAVEMENT SYSTEMS VS. LIGHT SOURCES.....	2
FIGURE 2. PHASES OF LIGHT REFLECTIVITY	3
FIGURE 3. ILLUMINANCE DECREASE AS DISTANCE INCREASES	5
FIGURE 4. ORIENTATION OF ANGLES	8
FIGURE 5. FIELD LUMINANCE CALCULATION	10
FIGURE 6. LABORATORY LUMINANCE MEASUREMENT	11
FIGURE 7. LIGHT REFLECTANCE VALUE (LRV).....	12
FIGURE 8. DIFFUSED AND SPECULAR REFLECTION	13
FIGURE 9. LIGHTNESS (Q_0) AND SPECULARITY (S_1).....	14
FIGURE 10. R CLASSIFICATION BY Q_0 AND S_1	15
FIGURE 11. LIGHT WAVELENGTHS CORRELATED TO REFLECTIVITY.....	17
FIGURE 12. SPECTRAL WAVELENGTHS OF COMMON LIGHT TYPES.....	18
FIGURE 13. PARKING LOT OBSERVATION ANGLES	22
FIGURE 14. REFLECTANCE COMPARED TO PAVEMENT AGE.....	23
FIGURE 15. ROAD SURFACE R3 – ASPHALT	27
FIGURE 16. LAB (LEFT) AND FIELD (RIGHT) PROGRAMS	28
FIGURE 17. GONIOMETER PROTOTYPE DESIGN	29
FIGURE 18. ILLUMINANCE METER	30
FIGURE 19. LUMINANCE METER	30

FIGURE 20. DATA MANAGEMENT PROGRAM (CS-S20)	31
FIGURE 21. LAB SPECIMEN ID	33
FIGURE 22. GONIOMETER PROTOTYPE STRUCTURE	34
FIGURE 23. LED LIGHTS AND INCANDESCENT LIGHTS	35
FIGURE 24. CALIBRATION OF TRADITIONAL LIGHTS	37
FIGURE 25. CALIBRATION OF LED LIGHTS	37
FIGURE 26. FINAL LAB GONIOMETER DESIGN	38
FIGURE 27. VISUAL OF ANGLE COMBINATIONS	39
FIGURE 28. PORTABLE GONIOMETER MIRROR SYSTEM	42
FIGURE 29. PORTABLE GONIOMETER DESIGN	43
FIGURE 30. FIELD SPECIMEN ID.....	44
FIGURE 31. FINAL PORTABLE GONIOMETER	45
FIGURE 32. UPPER LEVEL POWER CONTROL SECTION.....	46
FIGURE 33. INITIAL CALIBRATION PROCESS	47
FIGURE 34. LAB LUMINANCE RESULTS	49
FIGURE 35. FIELD LUMINANCE RESULTS	51
FIGURE 36. SUMMARY OF LUMINANCE RESULTS	53
FIGURE 37. INCANDESCENT LUMINANCE ON LAB CONCRETE	57
FIGURE 38. LED LUMINANCE ON LAB CONCRETE.....	57
FIGURE 39. INCANDESCENT LUMINANCE ON LAB ASPHALT.....	58
FIGURE 40. LED LUMINANCE ON LAB ASPHALT	58
FIGURE 41. INCANDESCENT LUMINANCE ON FIELD CONCRETE.....	61
FIGURE 42. LED LUMINANCE ON FIELD CONCRETE	61

FIGURE 43. INCANDESCENT LUMINANCE ON FIELD ASPHALT	62
FIGURE 44. LED LUMINANCE ON FIELD ASPHALT.....	62
FIGURE 45. INCANDESCENT R-VALUE ON LAB CONCRETE	67
FIGURE 46. LED R-VALUE ON LAB CONCRETE	67
FIGURE 47. INCANDESCENT R-VALUE ON LAB ASPHALT.....	68
FIGURE 48. LED R-VALUE ON LAB ASPHALT	68
FIGURE 49. INCANDESCENT R-VALUE ON FIELD CONCRETE.....	70
FIGURE 50. LED R-VALUE ON FIELD CONCRETE	70
FIGURE 51. INCANDESCENT R-VALUE ON FIELD ASPHALT	71
FIGURE 52. LED R-VALUE ON FIELD ASPHALT	71
FIGURE 53. INCANDESCENT LIGHT COMPARING R1 (CONCRETE)	73
FIGURE 54. INCANDESCENT LIGHT COMPARING R3 (ASPHALT).....	73
FIGURE 55. LED LIGHT COMPARING R1 (CONCRETE).....	74
FIGURE 56. LED LIGHT COMPARING R3 (ASPHALT)	74
FIGURE 57. R1 VS. INCANDESCENT VS. LED.....	75
FIGURE 58. SPECULAR CONCRETE CONTOUR PLOTS.....	79
FIGURE 59. DIFFUSED CONCRETE CONTOUR PLOTS.....	80

LIST OF TABLES

TABLE 1. R-TABLE STANDARDS	19
TABLE 2. R-TABLE PAVEMENT CLASSIFICATION	20
TABLE 3. ORIGINAL R1 TABLE	21
TABLE 4. LIGHT REFLECTION OF ASPHALT AND CONCRETE	25
TABLE 5. COMPARISON OF R-TABLES TO MEASURED VALUES	26
TABLE 6. STATISTICAL ANALYSIS.....	26
TABLE 7. LAB TRADITIONAL LIGHT SPECIMEN ID.....	32
TABLE 8. LAB LED LIGHT SPECIMEN ID	32
TABLE 9. SPECIFIED LUMINOUS FLUX.....	36
TABLE 10. ANGLE COMBINATION POINTS.....	40
TABLE 11. FIELD TRADITIONAL LIGHT SPECIMEN ID	44
TABLE 12. FIELD LED LIGHT SPECIMEN ID	44
TABLE 13. SELECTED LAB SAMPLES.....	56
TABLE 14. SELECTED FIELD SAMPLES	60
TABLE 15. CONVERTING LUMINANCE TO R-VALUES.....	64
TABLE 16. SIMPLIFIED FACTORS FOR RESPECTIVE Γ ANGLE	65
TABLE 17. S1 VALUES OF ORIGINAL R-TABLES	76
TABLE 18. S1 VALUES OF CONSTANT OBSERVATION ANGLE	76
TABLE 19. S1 VALUES OF VARIED OBSERVATION ANGLES	76
TABLE 20. SPECULAR VS. DIFFUSED AT VARIED OBSERVATION ANGLES	78

I. INTRODUCTION

The following chapter presents an introduction to the problem statement and the objective of the following research document.

A. Problem Statement

The human eye performs the best during the daytime when natural sun light is illuminating the world around us. According to Lutkevich, McLean, and Cheung (2012): “the nighttime fatality rate is three times the daytime rate.” In order to reduce roadway and parking lot accident rates proper light design is essential. The proper illumination of all pavements are important to adequately light sidewalks, bus stops, and parking lots. Current light design practices rely on outdated research findings on older pavement materials and conventional lighting systems. Not only has pavement drastically changed over time but the entire lighting market is being replaced by new light emitting diodes or LED lights. Van Bommel (2015) summarized this recent lighting market transition by stating: “With further improvements to be expected, they (LED) surely will become the dominant light source of the future.” LED lights are no doubt the light source of the future due to their extreme energy efficiency, but little research has been conducted on their reflective behavior compared to more traditional lighting technology. Therefore, further research is required to provide practical and fundamental data to establish the design guidelines of new light systems interacting with modern pavement systems.

B. Objective of Research

The objective of this research is to measure luminance values of two light sources on two different pavement systems. The two evaluated light sources are incandescent and LED lights. The traditional light source used for establishing the original road light design tables (R-Values) is unknown. Each R-Value is expressed as a function of the three angles (i.e., α , β , and γ) between the light sources, the surface, and the luminance meter. This test program is to establish the data base of luminance values to reconstruct R-Tables using LED and traditional (incandescent) lights. The two variables compared in this test program are different pavement systems and varying light sources.



Figure 1. Pavement Systems vs. Light Sources

Figure 1 depicts both variables that are further evaluated in this test program. The upper two quadrants show the variability of reflected light from different pavement systems. The bottom two quadrants illustrate the drastic color variation provided by two different sources of light. The interaction of these two variables is analyzed in this testing program by measuring the luminance values of multiple combinations of these variables. Finally, the measured luminance values are used to establish the relationship between different variations of two lighting angles, β and γ (angular incidence light).

II. LITERATURE REVIEW AND BACKGROUND

The first section of this chapter is intended to fundamentally explain the physics of light reflectivity through the mathematical theoretical concepts. The second section will look at the engineering design method in which these theoretical concepts are applied.

A. Lighting Fundamentals

In order to understand the fundamental mechanics of light, this section will begin by outlining each of the two interactive “phases” of light reflectivity: illuminance and luminance. Within each “phase” of lighting, the theoretical equations and contributing factors will be defined in further detail. **Figure 2** illustrates the two interactive phases of the light reflectivity process. In section 1, Illuminance, the quantity of light illuminating a surface area (lux), will be discussed. In section 2, Luminance, the quantity of reflected light received at a central viewing point (cd/m^2), will be discussed.

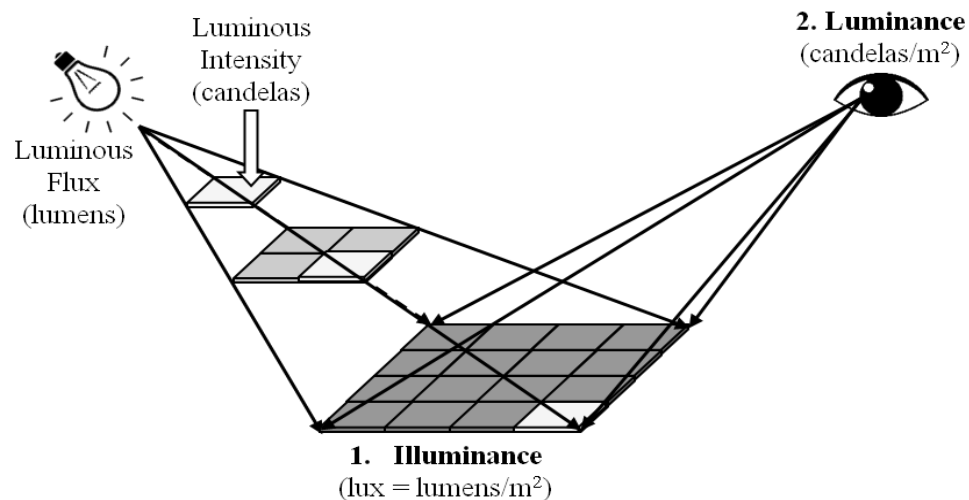


Figure 2. Phases of Light Reflectivity

1. Illuminance

The first phase of lighting, Illuminance, can be defined as the amount of light evenly distributed over a particular surface area. The illumination of a surface area, E, can be defined in the following equation:

$$E = \left(\frac{I}{D^2} \right) \quad (1)$$

where:

E = illuminance (lux)

I = light intensity (candelas or cd)

D = distance of light to illuminated surface area (m)

The quantity of light illuminating a surface is dependent on two factors: the intensity (I) of the light source itself and the distance (D) between the light source and the surface area being illuminated. The intensity of the light source is dependent on the power supplied to the light as well as on the efficiency of the light source. Light intensity will be discussed further in section b and the effect of distance is discussed in section a.

a. Distance Influencing Illumination

The influence of the distance factor (D) on the surface area being illuminated is illustrated in **Figure 3** below.

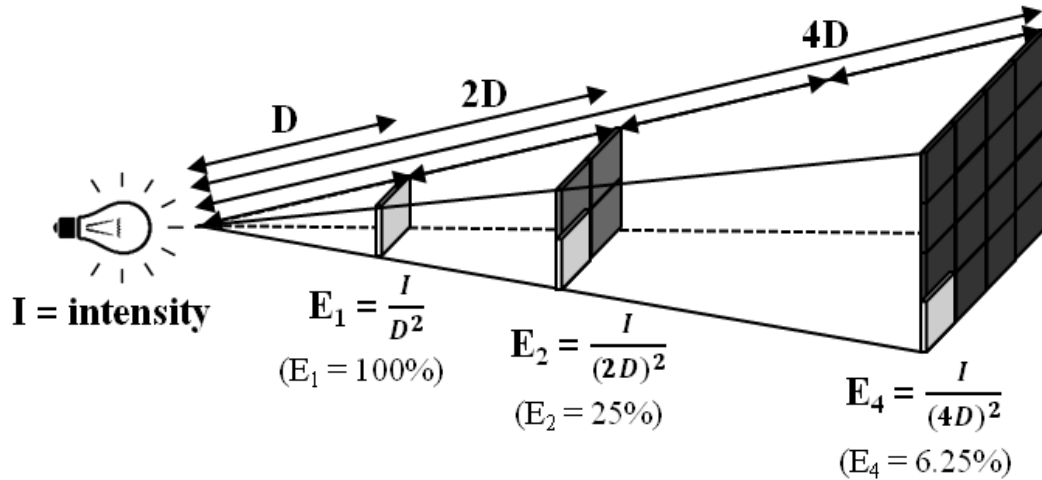


Figure 3. Illuminance Decrease as Distance Increases

For example, at a distance (D) there is 100% of the illumination intensity at that level of surface area. The value of E₂ decreases 75% from that of E₁ as the distance (D) increases two times (doubles). Similarly, the value of E₄ reduces to 6.25% of the initial E₁ illumination at a distance of four times. Where the intensity is inversely proportional to the square of the distance between the light source and the illuminated surface area. This physical mathematic concept is defined as the inverse-square law.

b. Intensity Influencing Illumination

The second factor, light intensity (I), is not only determined by the amount of power supplied to the source but also the manner in which that power is used. Lighting intensity (energy output) is dependent on the power input as well as the light efficiency. For example, two different light sources require very different amounts of power supply in order to achieve the same light intensity (energy output). LED lights are so popular because they achieve the same light intensity compared to traditional sources but require substantially less energy (cost). Therefore, intensity is directly proportional to efficiency.

There is substantial evidence that LED lighting is more energy-efficient than traditional lighting. For example, the California Energy Commission's Public Interest Energy Research Program (PIER Buildings Program, 2011) conducted a cost analysis comparing the use of High Pressure Sodium (HPS) lights with bi-level LED lights (16 to 77 Watts for low demand hours and 47 to 165 Watts for high demand hours) for illuminating parking garages in California State University (CSU Sacramento and CSU Long Beach) and San Marcos Civic Center. Examining multiple variables (energy consumption, energy cost, and maintenance cost) their analysis revealed a total annual cost savings of \$113 per unit for CSU Sacramento's bi-level LED lights as compared to HPS lights. Similar analysis comparing CSU Long Beach's lower wattage LED lights with HPS lights revealed even greater annual savings of \$232 per unit. This analysis also documented the lifespan of HPS lights as 24,000 hours, while CSU Sacramento's bi-level LED (77 W and 165 W) lifespan was 70,000 hours and CSU Long Beach's bi-level LED (16 W and 47 W) lifespan was 100,000 hours. These research studies indicate that the total lifespan of bi-level LED lights is 2.9 to 4.2 times the lifespan of HPS lights.

2. Luminance

The second phase of lighting, luminance, can be defined as the amount of light reflected from a particular surface area and being projected to a concentrated viewing point. Therefore, luminance is not only dependent on all the previously discussed illuminance parameters but also the reflective properties of the surface area that is being illuminated.

Each different pavement system has unique reflective properties. Light behavior can be mathematically defined using an “empirical approach” to categorize groups with similar reflective properties. This empirical approach is entirely defined by testing the luminance values (reflected light) of selected samples. Each categorized pavement type has different luminance values with respect to illuminated light and observation angles. Therefore, luminance can be calculated utilizing an empirically developed luminance coefficient (q) and the illuminance (E) defined as:

$$L = [(q)(E)] = \left[(q) \left(\frac{I}{D^2} \right) \right] \quad (2)$$

where:

L = luminance (cd/m^2)

q = luminance coefficient

E = illumination (lux)

The luminance coefficient (q) is dependent on the angular interaction between light and surface. **Figure 4** visually defines the “angles” that will be further defined in the form of mathematical equations.

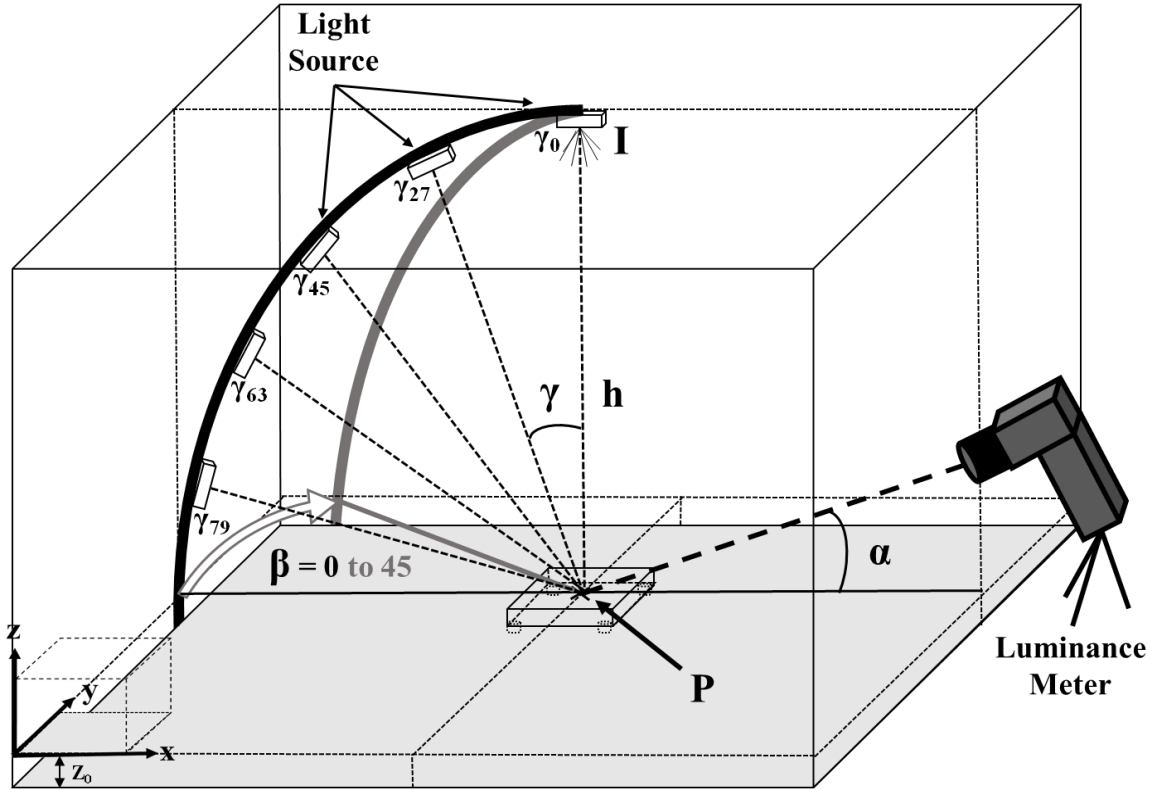


Figure 4. Orientation of Angles

Figure 4 defines the β angle as the angle along the horizontal plane at the intersection of the light and the luminance meter. This intersection point (P) can also be defined as the incidence point. The γ angle is defined as the downward angle along the vertical plane between the perpendicular direction of the surface (h) and the light. Observation Angle (α) is defined as the luminance meter viewing angle on the vertical plane between the parallel direction of the surface and the incidence point. Based on these angles the luminance coefficient (q) can more accurately be defined in the following equation:

$$q = f(\beta, \gamma) \quad (3)$$

where:

q = luminance coefficient as a function of the β and γ angles

β = β angle (refer to **Figure 4**)

γ = γ angle (refer to **Figure 4**)

The luminance coefficient (q) is commonly adjusted to represent the actual luminance value with the multiplier of $\cos^3\gamma$. The reduced luminance coefficient (R), also referred to as the R-value, is mathematically defined by the following equation:

$$R = [(q)(\cos^3\gamma)] = \left[\frac{(h^2)(L)}{(I)} \right] \quad (4)$$

Where all the variables are previously defined in **Figure 4** on the previous page and the luminance (L) is defined as the reflected light measured from the Luminance Meter.

Every individual pavement surface has a different reduced luminance coefficient as a function of angles β and γ . This R-value is utilized by designers to calculate the luminance (L) accordingly. Luminance (reflected light) is dependent on the angular reflective properties of a given surface. The reduced luminance coefficient (R) can be empirically found from the measurement of luminance values. The R-Value or the reduced luminance coefficient accounts for the amount of light which does not reach the viewer due to surface granular redirection (diffusion) or surface (lightness) absorption. The R-Values are intended to represent a general category of pavement. Utilizing these empirical factors a corresponding luminance value can easily be calculated accordingly. Therefore, the quantity of reflected light or luminance (L) can be calculated by utilizing the following equation:

$$L = \left[\frac{(R)(I)}{(h^2)} \right] \quad (5)$$

where:

R = reduced luminance coefficient

I = light intensity (cd)

h = height of light source (m)

For example, consider a scenario where there is a minimal amount of light (L) required for a parking lot area. Assuming the light has a set intensity, a standard pole height of 25 ft, and the designer intends to use a concrete pavement. Computer software is then typically used to generate all the specific (Concrete) R-Values corresponding to all possible incident light points. A specific R-Value can then be defined for every individual horizontal grid location on the respective surface underneath the light source. Therefore, light (L) can be calculated for each respective grid point. Once that calculated light (L) value drops below the desired quantity another light pole (source) is required.

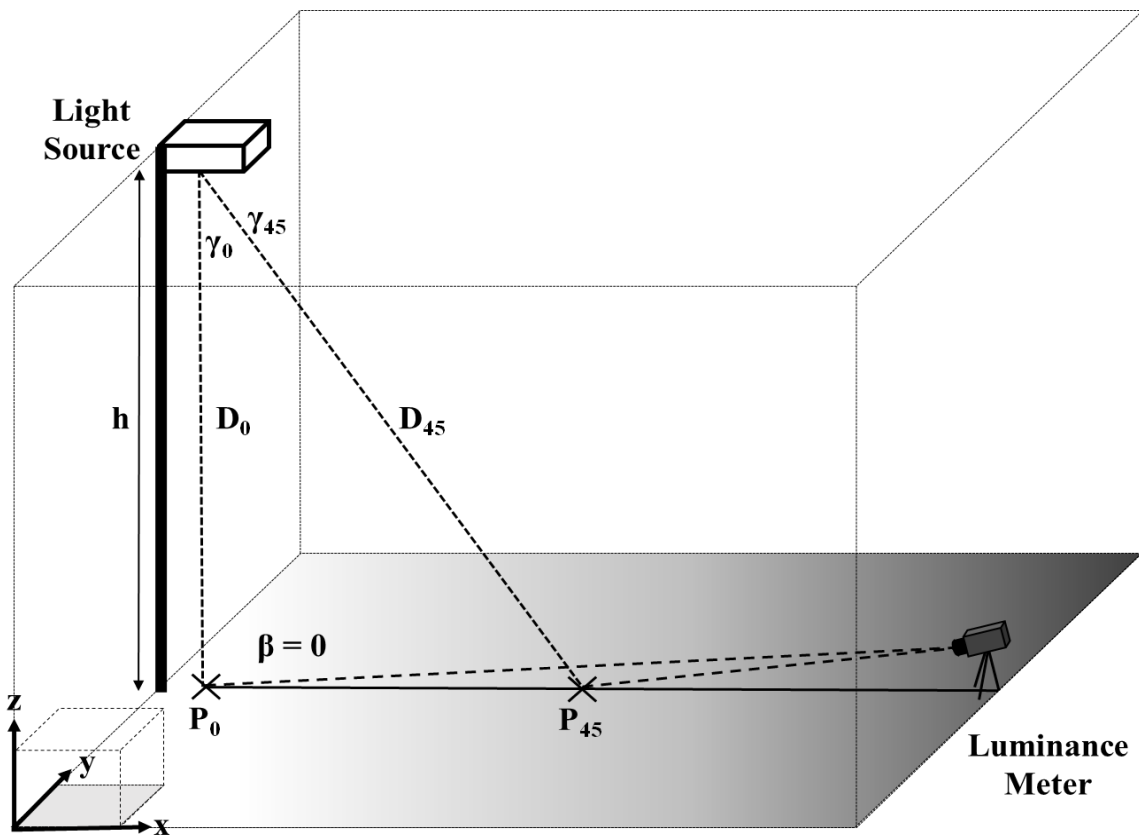


Figure 5. Field Luminance Calculation

Figure 5 visually expands on the previous example field design scenario. A much smaller R-Value corresponds with the P_{45} than with P_0 , hence the light to dark color. Therefore, both measured and calculated luminance (L) values correlate in a proportional manner.

Figure 5 shows the field application in which R-Values can be utilized to easily calculate corresponding luminance values. R-Values are only measured in a laboratory scenario in which the light angles can be easily manipulated. Dimensions depicted in **Figure 5** show a constant height (h) with varying distance (D) for each measurement. The laboratory has angled lights mounted along an arch and therefore has different measurement dimensions. This dimension difference is mathematically accounted for in the following equation:

$$h = [(\cos \gamma)(D)] \quad (6)$$

Where the height (h) of each light source is calculated based on the corresponding γ angle with a constant distance (D) as defined in **Figure 6**.

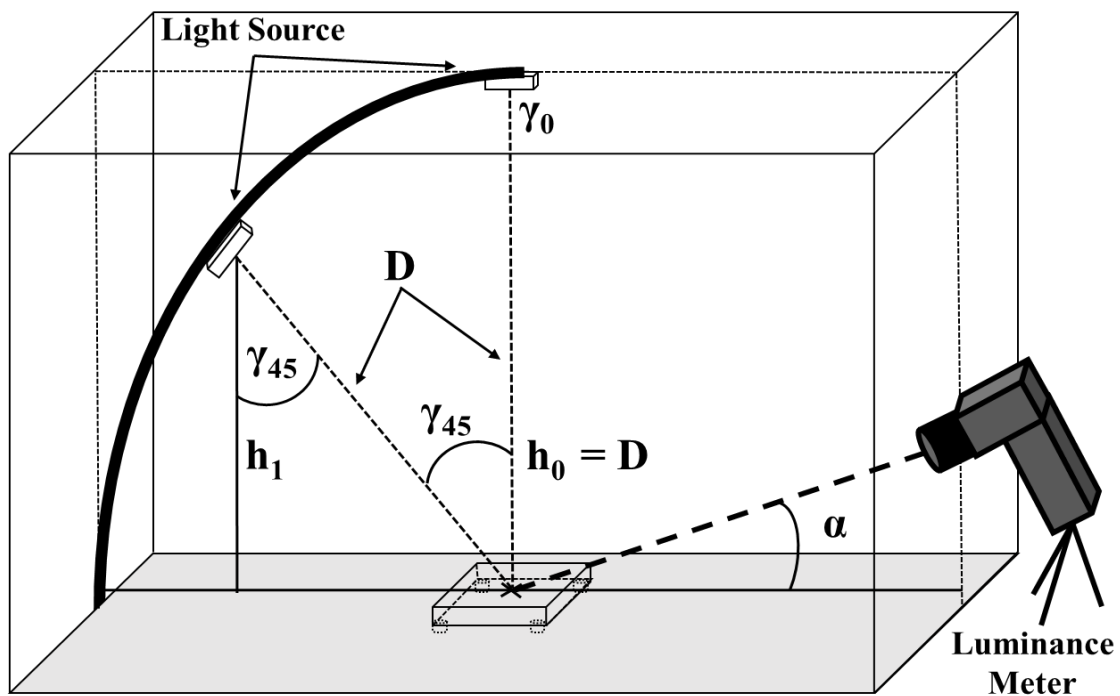


Figure 6. Laboratory Luminance Measurement

Figure 6 depicts the dimensions utilized in the laboratory measurement scenario. The laboratory scenario is more feasible for taking luminance measurements. Measurements are much more difficult in the field scenario. This is why R-Values are developed in the laboratory scenario and applied to calculations out in field.

a. Defining Surface Lightness and Specularity

In 1983, the International Commission on Illumination (CIE) developed a system for classifying pavement types according to a surface's diffuse and specular reflection. The R-Tables, developed later, used these basic parameters with respect to the angular interaction. This is why luminance calculations are dependent on the horizontal and vertical angles (β and γ). This angular interaction can be further examined as two fundamental properties, lightness (Q_0) and specularity (S_1). Lightness is a parameter that describes surface "lightness" or the grey-scaled amount of reflective color. Lightness (Q_0) is the primary reason lighter concrete surfaces reflect more light than darker asphalt surfaces. **Figure 7** is a Light Reflectance Value (LRV) lightness scale that directly correlates the lightness of a material to the amount of light that will reflect from that given surface.

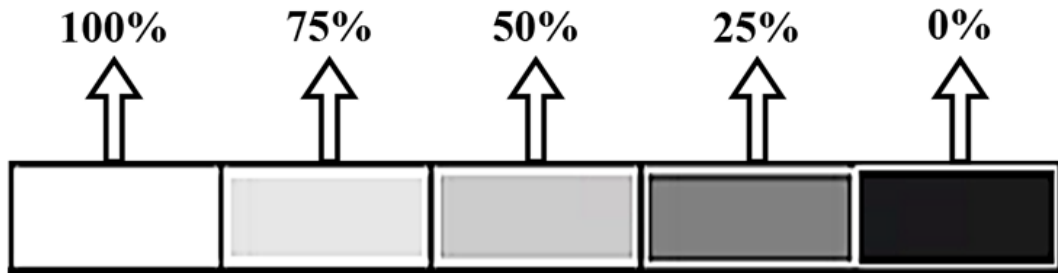


Figure 7. Light Reflectance Value (LRV)

The Lightness (Q_0) is calculated from the reduced reflection table as shown in the following equation:

$$Q_0 = \frac{1}{\Omega} \times \iint_{\Omega} q(d\beta)(d\gamma) \quad (7)$$

where:

Ω = solid angle being measured from incidence point on the surface

Specularity (S1) is dependent on the actual “texture” of the surface and material properties. Smooth surfaces tend to be more “glossy” than rougher, more textured, less “glossy” surfaces. One example of a perfectly specular surface is a mirror since a mirror perfectly reflects light. The opposite of specularity is a diffused or rough surface that reflects angular light poorly. A surface that is rough and does not reflect light well is defined as a “diffused” surface. In contrast, the surface that is very smooth and does reflect light well is defined as a “specular” surface. This concept of specularity and diffusion is better illustrated at the granular level in **Figure 8**.

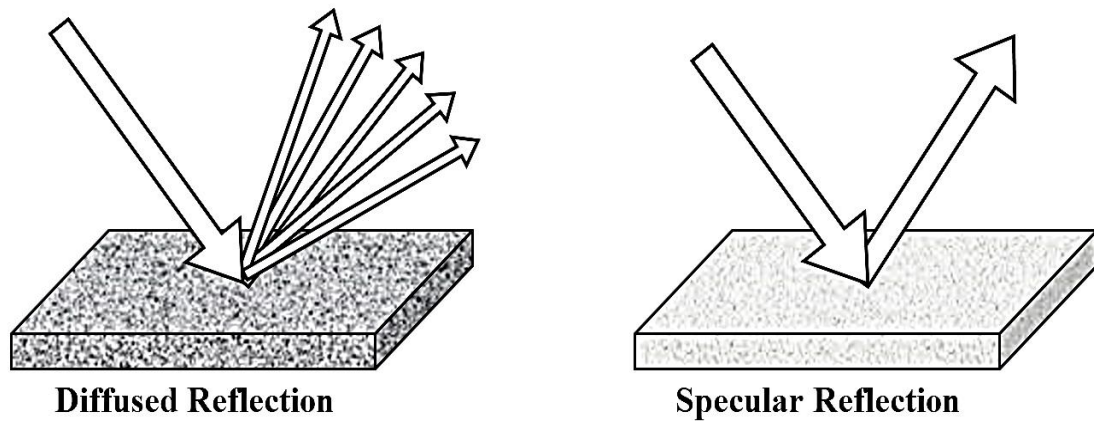


Figure 8. Diffused and Specular Reflection

The specularity (S1) is calculated from two R-values as shown in the following equation:

$$S1 = \frac{R(\beta = 0, \tan \gamma = 2)}{R(\beta = 0, \tan \gamma = 0)} \quad (8)$$

where:

Angles β and γ previously defined in **Figure 4**

($\tan \gamma = 2$) or ($\gamma \approx 63^\circ$)

($\tan \gamma = 0$) or ($\gamma \approx 0^\circ$)

R-Values are developed based on the amount of light reflecting from the surface at a given incidence angle. Specularity (S1) is defined by the texture of a given surface. One example of a perfectly specular surface is a mirror. A mirror allows all the light to be reflected at the same incidence angle. Whereas, a rough surface would diffuse (redirect) the light. Lightness (Q_0) is another influential factor of how much light reflects from the pavement surface. The darker the pavement the more light it absorbs and does not reflect.

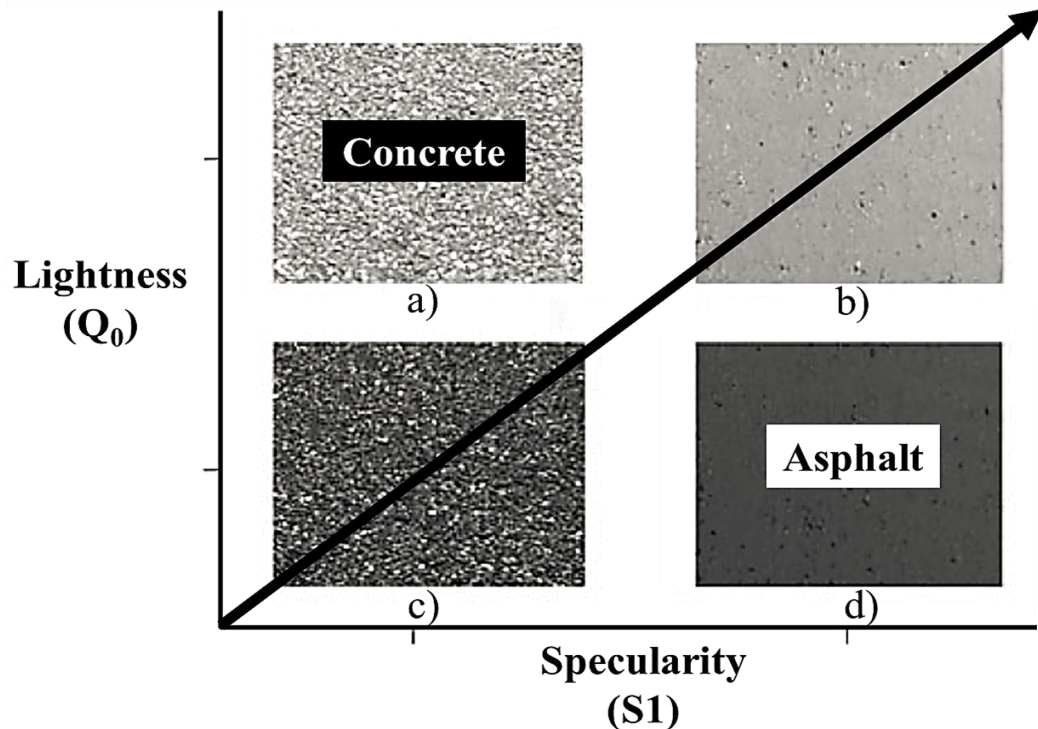


Figure 9. Lightness (Q_0) and Specularity (S1)
(Source: van Bommel, 2015)

Surfaces a) and b) in **Figure 9** look brighter in color and seem to reflect light better than surfaces c) and d). The pavements b) and d) in **Figure 9** are very smooth and therefore reflect light better than rougher surfaces a) and c). Pavement a) in **Figure 9** is the typical representation of concrete pavement, whereas pavement d) best represents typical asphalt. Considering the interaction of lightness and specularity, the pavement c) in **Figure 9** is the least reflective, while the pavement b) is the most reflective.

These factors are more explicitly defined with respect to similar pavement types. Each R-Table is meant to represent a common pavement surface and therefore can be categorized the corresponding lightness (Q_0) and specularity (S_1) values. These values have been designated for each R-Table (R1, R2, R3, and R4) and are shown **Figure 10**.

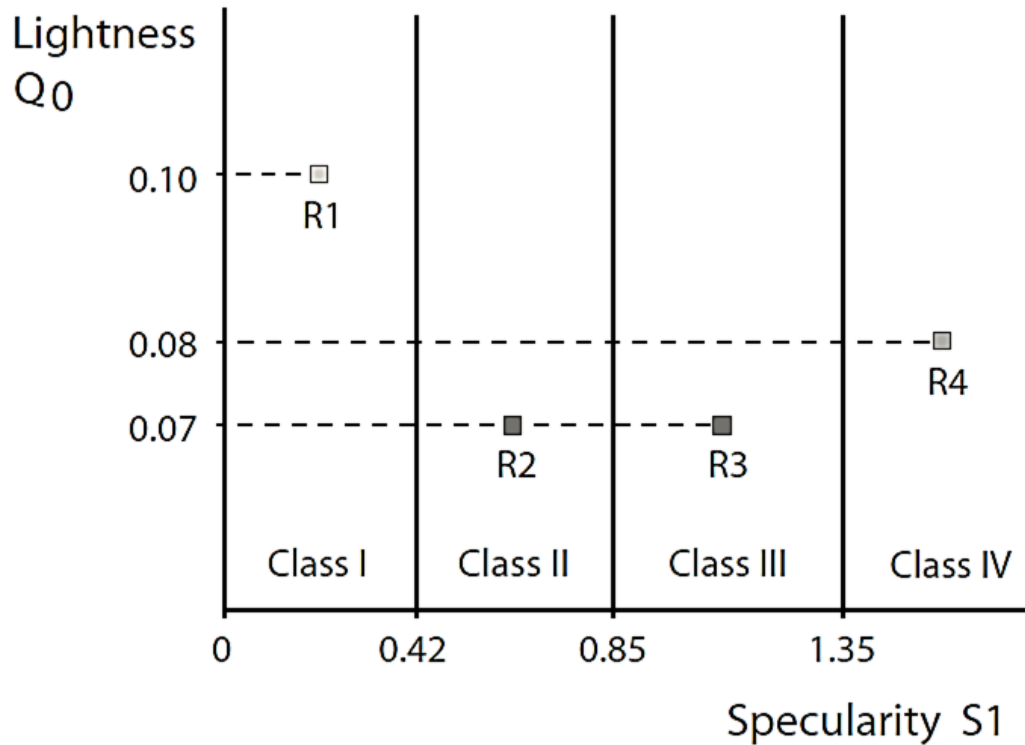


Figure 10. R Classification by Q_0 and S_1
(Source: van Bommel, 2015)

For example in **Figure 10** the R1 class is displayed on the left side of the graph. R1 is intended to represent concrete pavements that are “light” in color but tend to have a more “rough” surface texture than typical asphalt pavements (R2, R3, and R4). Therefore, while concrete’s “light” color contributes to better reflectivity the “rough” surface texture decreases the amount of reflected light. Application of these concepts are discussed in more detail in the following section.

B. Roadway Lighting Design

Section A defined the fundamentals of light in two “phases” involving the light source itself (illuminance) and the reflective surface (luminance). This section will discuss the practical application of each “phase” that is utilized in the roadway lighting design practice. First, light sources having different wavelength characteristics and exhibiting different reflectiveness will be discussed. Second, the utilized roadway light design methodology will be discussed.

1. Light Source Spectral Wavelength

Comparing eleven pavement types with High Pressure Sodium (HPS) lights and Metal Halide (MH) lights, Ekrias and colleagues (2008) examined the influence of aggregate color and aggregate lightness on pavement reflectivity. The results of this study suggest that both aggregate lightness and color significantly impact surface reflection properties. For example, compared to other surface samples, stone mastic asphalt samples with white aggregates demonstrated significantly greater reflectance values. Research results also indicated that relative reflectance’s exhibited higher values for longer wavelengths. Research concluded that the longer wavelength HPS lights are typically more effective than MH lights.

Similar to the research conducted by Ekrias and colleagues (2005), Adrian and Jobanputra (2005) also compared the reflectance properties of concrete with that of asphalt surfaces using HPS lights and MH lights. Adrian and Jobanputra found that longer wavelength HPS lights were more effective than shorter wavelength MH lights.

A Comparison of Total Reflectance between Asphalt and Concrete

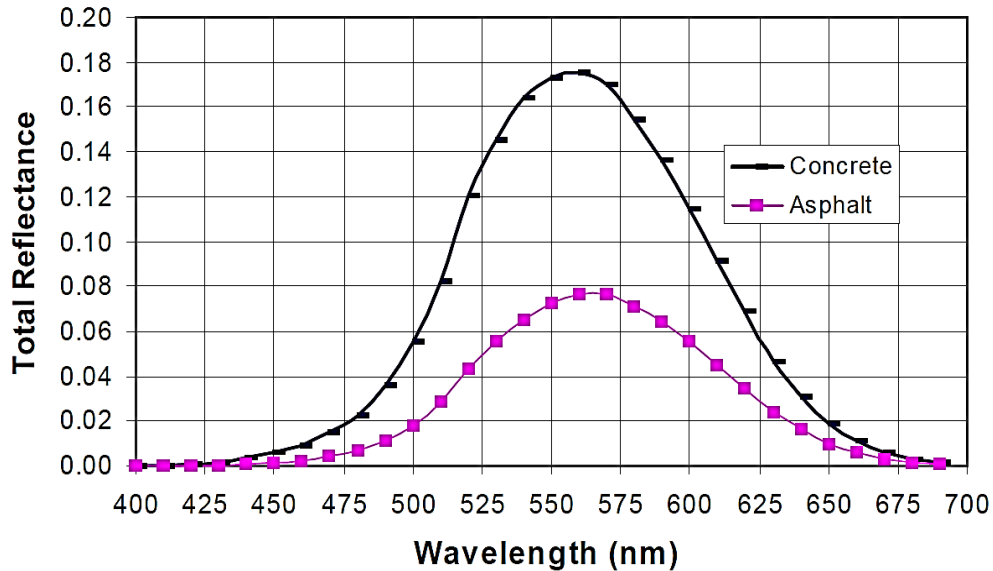


Figure 11. Light Wavelengths Correlated to Reflectivity
(Source: Adrian and Jobanputra, 2005)

Figure 11 demonstrates the relationship between light wavelengths and reflectivity of a given surface. Light sources with wavelengths between 500nm and 600nm achieve the greatest surface reflectance. Within this wavelength range, the surface reflectance exhibited much higher values on concrete than on asphalt. It is important to note that Adrian and Jobanputra's (2005) research examined only traditional light sources (HPS and MH); LED lights were not included in their study.

Wout van Bommel (2015) reported that compact fluorescent lights (CFLs) became available as an alternative to incandescent light sources in the 1980s. This indicates that incandescent light was still dominantly used when the original lighting design guidelines were developed during the same decade.

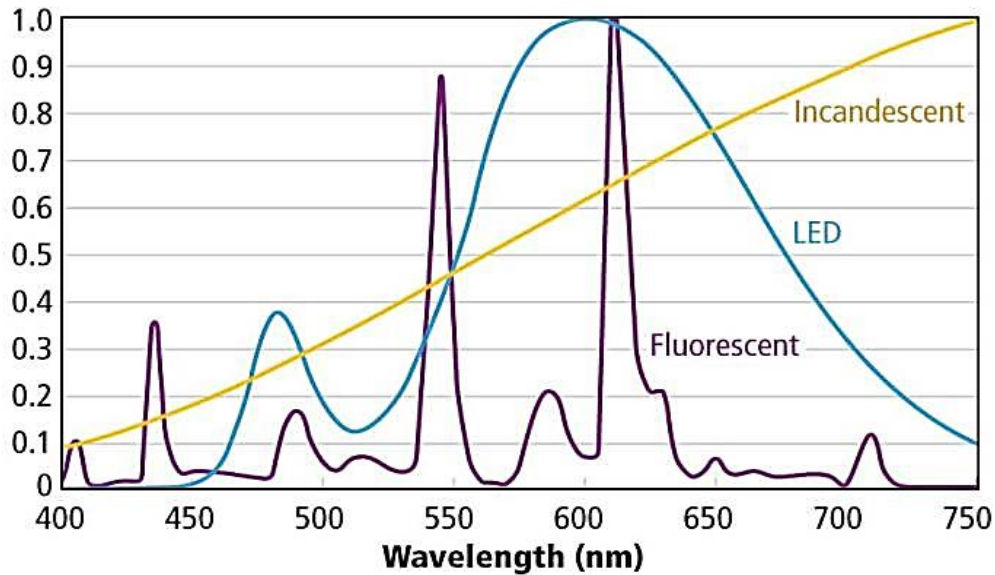


Figure 12. Spectral Wavelengths of Common Light Types
(Source: Kelly, 2013)

Figure 12 demonstrates the unpredictable wavelength pattern of traditional fluorescent type lights. Where the y-axis is defined as the relative spectral distribution. Fluorescent type lights are typically used in roadway lighting mainly due to their energy efficiency but do not have a consistent wavelength spectrum. Incandescent lights are the oldest light source and are so inefficient many countries are no longer using these for roadway lighting design. The incandescent lights have the most consistent wavelength spectrum which makes these lights behave in a similar manner to natural sunlight.

Adrian and Jobanputra (2005) concluded that peak reflective behavior occurs at about 500nm. **Figure 12** demonstrates at 500nm incandescent, fluorescent and LED lighting groups intersect and share similar wavelength characteristics around this wavelength. Incandescent type lights have a more predictable behavior and therefore were selected as the “traditional” light source to be further evaluated in the experimental program. In addition, the earlier R-Table (that will be discussed later) seems to have been developed based on the incandescent type light.

2. Surface Reflectivity Design

To define the reflectivity of a pavement surfaces, a road reflection classification system was developed in 1983 by the International Commission on Illumination. This system established standard parameters for classifying surfaces considering multiple variables, including lightness (Q_0) and specularity ($S1$). The road reflection classification system is commonly referred to as the “reduced luminance coefficient tables” (R-Tables).

Table 1. R-Table Standards

(Source: International Commission on Illumination RP-8)

Class	Limitation	Standard	$S1$	Q_0
RI	$S1 < 0.42$	R1	0.25	0.10
RII	$0.42 \leq S1 < 0.85$	R2	0.58	0.07
RIII	$0.85 \leq S1 < 1.35$	R3	1.11	0.07
RIV	$S1 \geq 1.35$	R4	1.55	0.08
CI	$S1 < 0.4$	C1	0.24	0.10
CII	$S1 \geq 0.4$	C2	0.97	0.07

Table 1 shows shortly after the four class R system was proposed, an alternative more simplistic approach was also proposed. The C-Classes were proposed in which C1 was representative of R1. The C2 class represents a general class to include R1, R2, and R3. While this proposed method has been accepted, the original four class R-Table system is still typically used in current light design (RP-8). There are also varied derivations to the R-Tables which are used when considering the surface as “wet”. These wet classes are an extension to the R-Table system but are defined as W1, W2, W3, and W4. To simplify discussion in the proceeding sections, W1, W2, W3, and W4 (as well as C1 and C2) will not be further discussed.

3. R-Table Application

The Recommended Practice (RP-8), currently used in lighting design and initially proposed in 1983 by De Boer and Vermeulen, was the first method that incorporated light reflectivity as one of the primary factors of roadway lighting design. Pavements were categorized into four separate classification groups based on extensive testing of many different road surface samples collected in 1983 by IESNA.

Table 2. R-Table Pavement Classification
(Source: International Commission on Illumination RP-8)

Class	Q_0	Description	Mode of reflectance
R1	0.10	Portland cement concrete road surface. Asphalt road surface with a minimum of 15 % of the aggregates composed or artificial brightener aggregates (labrodorite, quartzite)	Mostly diffuse
R2	0.07	Asphalt road surface with an aggregate composed of minimum 60 % gravel (size greater than 10 mm). Asphalt road surface with 10 to 15 % artificial brightener in aggregate mix. (Not normally used in North America)	Mixed (Diffuse and specular)
R3	0.07	Asphalt road surface (regular and carpet seal) with dark aggregate (e.g. traprock, blast furnace slag) rough structure after months in use (typical highway)	Slight specular
R4	0.08	Asphalt road surface with a very smooth texture	Mostly specular

Fotios, Boyce and Ellis (2006) described materials and construction method of both “established” and “new” asphalt-based and concrete-based pavement materials. These authors identified established surfaces as hot rolled asphalt, brushed concrete and surface dressing. New surfaces included exposed aggregate concrete, porous asphalt, stone mastic asphalt and several forms of thin surfacing asphalt. Brightening additives contribute to pavement options as well. This (2006) description of modern materials appears to have many variations to those displayed in **Table 2** which were the original R-Table pavement classification material descriptions.

The only feasible method of calculating light reflectivity (L) is by using an “empirical” factor (R). These values assume all incoming light (wavelength spectrum) will produce the same factors determined in RP-8. One of the four tables (R1) used to calculate light reflectivity is displayed in **Table 3** below.

Table 3. Original R1 Table
(Source: International Commission on Illumination RP-8)

θ tan γ	0	2	5	10	15	20	25	30	35	40	45	60	75	90	105	120	135	150	165	180
0	655	655	655	655	655	655	655	655	655	655	655	655	655	655	655	655	655	655	655	655
0.25	619	619	619	619	610	610	610	610	610	610	610	610	610	601	601	601	601	601	601	601
0.5	539	539	539	539	539	539	521	521	521	521	521	503	503	503	503	503	503	503	503	503
0.75	431	431	431	431	431	431	431	431	431	431	395	386	371	371	371	371	371	386	395	395
1	341	341	341	341	323	323	305	296	287	287	278	269	269	269	269	269	269	278	278	278
1.25	269	269	269	260	251	242	224	207	198	189	189	180	180	180	180	180	189	198	207	224
1.5	224	224	224	215	198	180	171	162	153	148	144	144	139	139	139	144	148	153	162	180
1.75	189	189	189	171	153	139	130	121	117	112	108	103	99	99	103	108	112	121	130	139
2	162	162	157	135	117	108	99	94	90	85	85	83	84	84	86	90	94	99	103	111
2.5	121	121	117	95	79	66	60	57	54	52	51	50	51	52	54	58	61	65	69	75
3	94	94	86	66	49	41	38	36	34	33	32	31	31	33	35	38	40	43	47	51
3.5	81	80	66	46	33	28	25	23	22	22	21	21	22	22	24	27	29	31	34	33
4	71	69	55	32	23	20	18	16	15	14	14	14	15	17	19	20	22	23	25	27
4.5	63	59	43	24	17	14	13	12	12	11	11	11	12	13	14	14	16	17	19	21
5	57	52	36	19	14	12	10	9.0	9.0	8.8	8.7	8.7	9.0	10	11	13	14	15	16	16
5.5	51	47	31	15	11	9.0	8.1	7.8	7.7	7.7										
6	47	42	25	12	8.5	7.2	6.5	6.3	6.2											
6.5	43	33	22	10	6.7	5.8	5.2	5.0												
7	40	34	19	8.1	5.6	4.8	4.4	4.2												
7.5	37	31	15	6.9	4.7	4.0	3.8													
8	35	28	14	5.7	4.0	3.6	3.2													
8.5	33	25	12	4.8	3.6	3.1	2.9													
9	31	23	10	4.1	3.2	2.8														
9.5	30	22	9.0	3.7	2.8	2.5														
10	29	20	8.2	3.2	2.4	2.2														
10.5	28	18	7.3	3.0	2.2	1.9														
11	27	16	6.6	2.7	1.9	1.7														
11.5	26	15	6.1	2.4	1.7															
12	25	14	5.6	2.2	1.6															

*All values have been multiplied by 10,000.

Q0 = 0.10; S1 = 0.25; S2 = 1.53

Table 3 shows a visual picture of the original R1-Table which is the table (data) still currently used to define the behavior of any and all concrete type pavements. Pictures of each of the original R-Tables were found and translated into a simplified digital Excel version (can be found at the end of the appendix). These equivalent Excel tables are simplified down to the selective angles experimentally tested for comparison purposes.

a. Limitations of Design Process

The R-Tables were measured under a 1° observation angle. One of the critical issues of a 1° observation angle is that such a small angle is impractical to set up for laboratory testing. In addition, not only is a 1° observation angle impractical for testing but it also does not necessarily apply to all situations. For example, compared to roadway drivers, drivers in parking lots are not focusing on far horizontal distances, but more towards the ground looking for open parking spaces; therefore, the observation angles of parking lot drivers tend to be greater than observation angles of roadway drivers. In addition, the speed of drivers in parking lots is also much lower than freeways and therefore much shorter stopping sight distances (SSD) are required (smaller X distance). Slower speeds and shorter stopping distances increase the observation angle of drivers in parking lots and should be considered accordingly in the design. **Figure 13** illustrates the difficulties presented when an observation angle (α) of 1° is required.

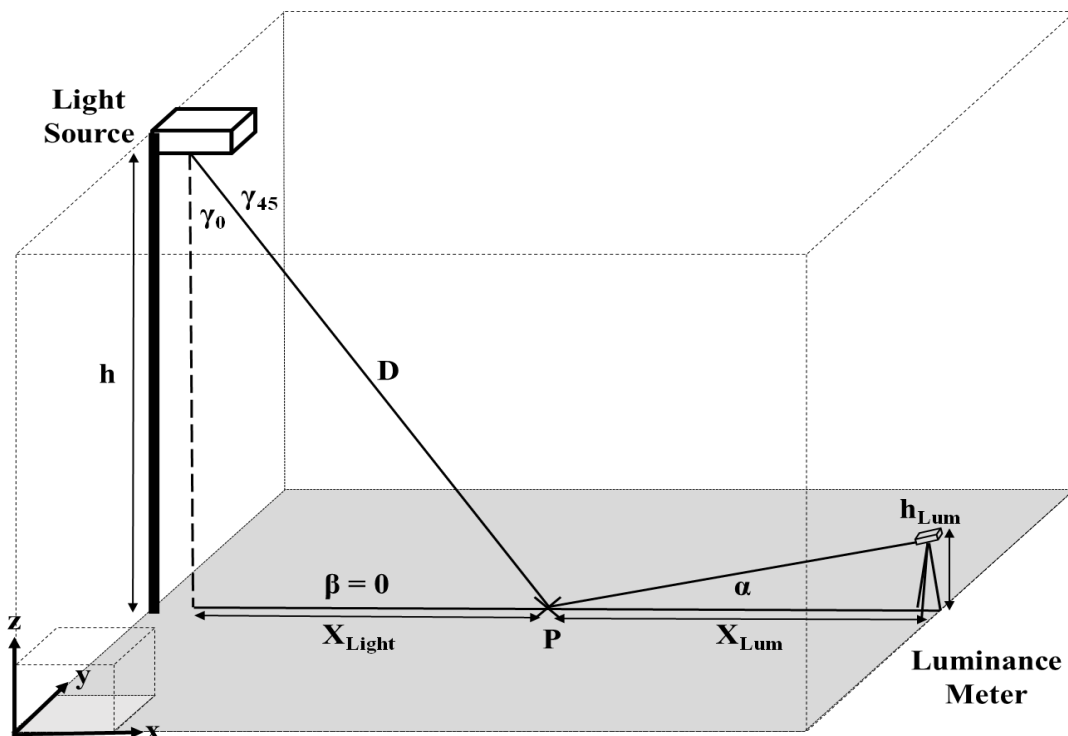


Figure 13. Parking Lot Observation Angles

Another limitation in the design process is that road surfaces age over time and therefore their properties do not remain constant as time passes. For example, when asphalt is freshly paved the color is dark black. However, asphalt slowly loses the black binding filler as it ages and subsequently shows the lighter color of the aggregates used. Aging has an opposite impact on concrete as concrete becomes slightly darker over time.

Figure 14 shows the impact of pavement aging on solar reflectance.

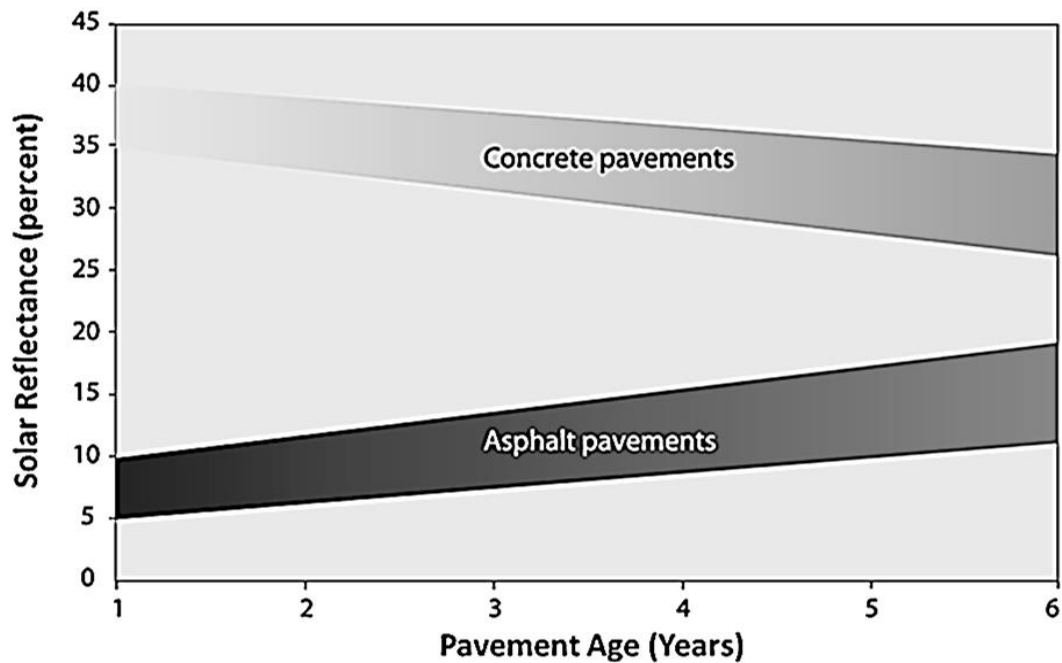


Figure 14. Reflectance Compared to Pavement Age
(Source: EPA, 2008)

In summary, design considers the pavement is brand new but over time the reflective properties of that surface does not remain constant. Furthermore, the comparison of age shown in **Figure 14** is not a fair comparison since concrete and asphalt pavements typically have a completely different life expectancy. For example, concrete is usually designed to last much longer than asphalt, which tends to need continual resurfacing.

b. Reevaluations of R-Tables

Reflectance properties of different pavement types depend on a variety of factors, such as dryness level and pavement wear. Several studies have been conducted to explore the reflective interaction of traditional light sources on varying pavement types. Despite the universal acceptance of this method, multiple research studies have examined the validity of these R-Tables and have determined that the R-Tables are not representative of reflectance properties of modern pavement types.

For example, Dumont and colleagues (2008) completed a series of tests on the reflectance properties of various roadway pavement types in France. Over the course of three years, reflectance data were measured on samples of two primary pavement types, very thin asphalt concrete (VTAC) and surface dressing (SD). The investigators compared the research-obtained R-Tables with the standard R-Tables and found that discrepancies exist (in spite of “scaling the standard R-Table to match lightness values”). Ylinen, and colleagues (2010) conducted a similar investigation of pavement samples from roads in Finland. These researchers found discrepancies between the research-obtained R-Tables and the standard R-Tables as well. In addition, Khan’s (1998) investigation of relationship between pavement surfaces and light reflectance also found inadequacies in the use of standard R-Tables.

Adrian and Jobanputra (2005) conducted a study comparing reflectance properties of concrete with asphalt surfaces. **Table 4** below displays the average luminance (cd/m²) of two common pavement types, asphalt and concrete, when light output is held constant at 400 Watts. Adrian and Jobanputra measured the average luminance as 6.03 cd/m² in concrete and the average luminance as 3.40 cd/m² in asphalt. Study data, presented in **Table 4**, indicates that concrete surfaces reflect 1.77 ($6.03/3.40 = 1.77$) times more light than asphalt surfaces.

Table 4. Light Reflection of Asphalt and Concrete
(Source: Adrian and Jobanputra, 2005)

Pavement Type	Average Power (Watts)	Average Luminance (cd/m²)
Asphalt (R3)	400	3.40
Concrete (R1)	400	6.03

This study concluded that even while using the same light source at the same intensity the surface pavement type had a significant impact on the amount light reflected. Concrete surfaces significantly increased the overall light reflected in parking lots. This research indicated that concrete pavements can be up to twice as reflective compared to the typical asphalt pavement surface.

Hassan and colleagues (2008) conducted research documenting a statistically significant discrepancy between standard R-Tables and re-evaluated R-Tables. **Table 5** displays all the actual values that were reevaluated in the numerator of the table values. The bold values in the denominator are the equivalent values collected from the most commonly used R-Tables (R1, R2, and R3). **Table 5** displays the results of the R-Table reevaluation performed in the experimental study.

Table 5. Comparison of R-Tables to Measured Values
(Source: Hassan et al., 2008)

tan γ	β						
	90	105	120	135	150	165	180
(a) Standard surface R1							
0.50	503/517	503/542	503/603	503/638	503/697	503/738	503/781
0.75	371/382	371/408	371/458	371/489	386/541	395/574	395/606
1.00	269/169	269/199	269/232	269/254	278/297	278/318	278/333
(b) Standard surface R2							
0.50	281/245	271/312	271/405	271/458	260/577	260/635	260/640
0.75	206/230	206/280	206/348	206/387	206/473	206/516	206/523
1.00	152/206	152/231	152/259	141/277	141/311	141/329	141/341
(c) Standard surface R3							
0.50	204/269	199/313	199/356	199/373	199/418	194/438	194/436
0.75	149/215	149/249	149/284	145/300	136/338	136/358	140/361
1.00	100/131	100/148	100/171	100/187	100/215	100/231	100/245

A statistical analysis of the results is displayed in **Table 6** shown below. This table demonstrates a statistically significant difference between the experimentally collected values and in the original R2 and R3 tables (associated with asphalt). The R1 table (a) (first row) was validated as a representative source of data (associated with concrete).

Table 6. Statistical Analysis
(Source: Hassan et al., 2008)

Source of variation	F	P value	F crit	Interpretation
Standard surface R1	3.20	0.0808	4.084	Not significant
Standard surface R2	29.908	<0.001	4.084	Significant
Standard surface R3	40.02	<0.001	4.084	Significant

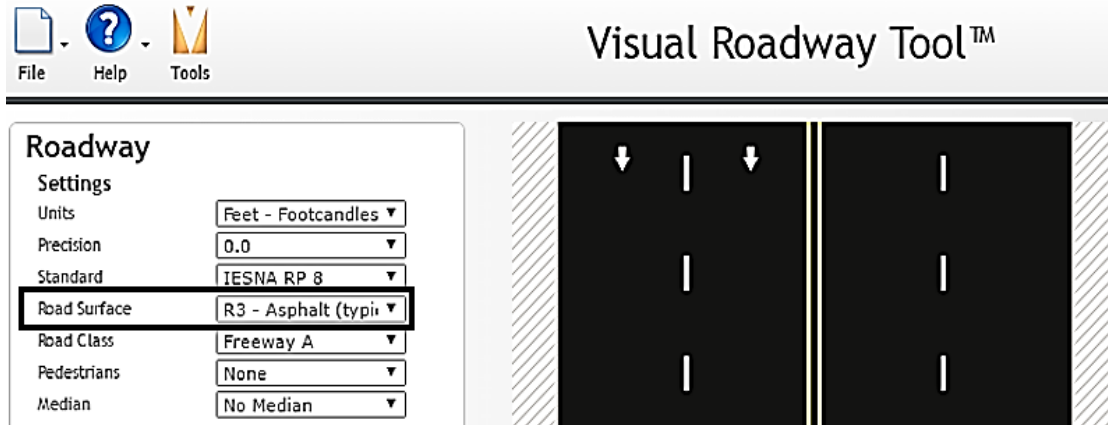


Figure 15. Road Surface R3 – Asphalt
(Source: Acuity Brands Lighting, 2016)

Despite research demonstrating sufficient evidence of the R-Table inadequacies, the standard R-Tables are still the foundation of road lighting calculations. Current road lighting design software continues to utilize these outdated tables. One example is displayed in **Figure 15** above. A computerized program for calculating pavement reflectance is the Visual Roadway Tool. This tool requires an initial selection of an appropriate table (R-Table) that is then used to make design calculations accordingly.

All light types (excluding LED's) were already in use prior to the creation of these R-Tables. This is why the incandescent light used in the experimental program is also referred to as “traditional”. Any type of light could have been originally used to develop the original R-Tables except LED lights. LED lights are the only light source invented after the development of the R-Tables. Yet, light designers continue to use the original R-Tables assuming these tables still apply to this relatively new lighting technology. Therefore, while the objective of the experimental program is to analysis the light reflectivity of concrete and asphalt it was also critical to compare new LED lights with the older (traditional) lights used to develop the original R-Tables.

III. EXPERIMENTAL PROGRAM

The following research programs are designed to test and perform measurements intended to record light reflectivity. The experimental program is separated into two stages of the design process. First, the laboratory test program is designed to perform measurements in a controlled laboratory environment. Second, the field test program is designed with the intentions of collecting data of “in-situ” pavement surfaces. **Figure 16** shows the separate programs of experimental testing.

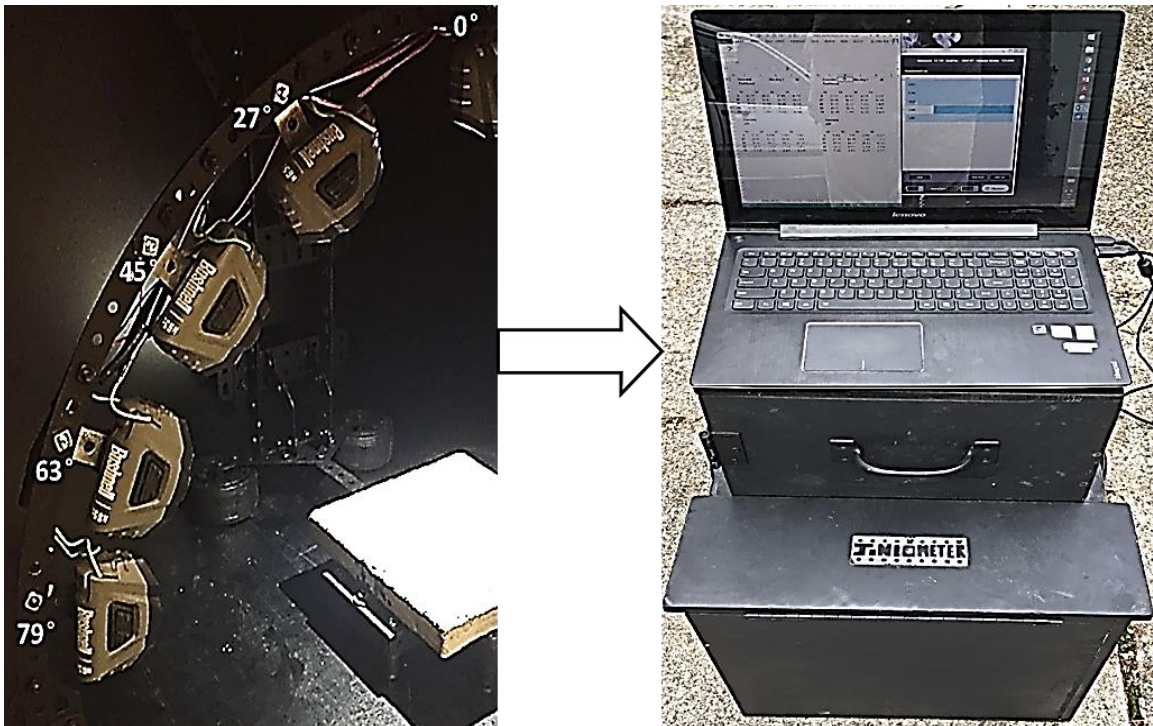


Figure 16. Lab (Left) and Field (Right) Programs

A. Lab Testing

The purposes of the experimental program is to design and fabricate a device capable of measuring angular light reflectivity. The following section presents the design process for developing a functional goniometer measurement program.

1. Goniometer Prototype Concept

A “goniometer” can be defined as an instrument for the precise measurement of angles. The initial design concept selected the most critical and feasible angle locations to place lights in order to best measure their reflective properties. The initial design concept is depicted in the **Figure 17** displayed below.

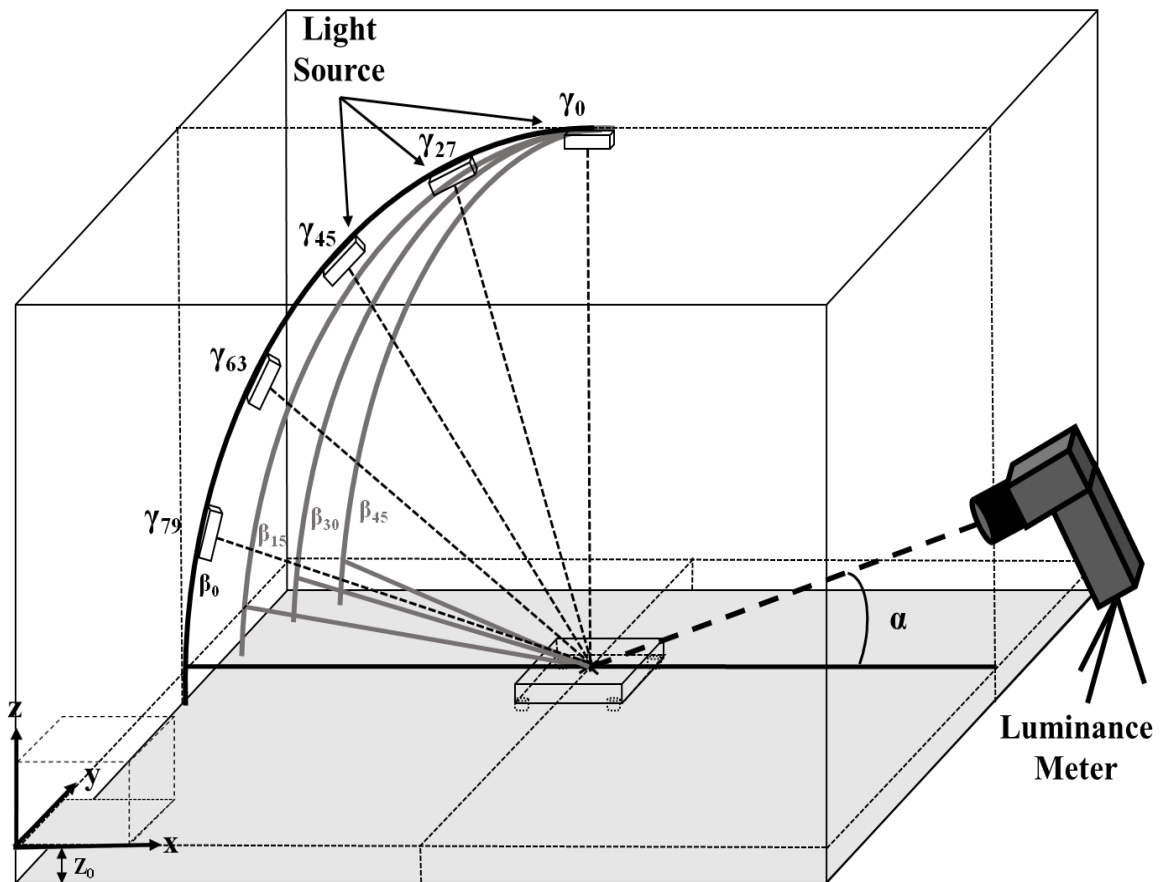


Figure 17. Goniometer Prototype Design

2. Measurement Tools

Two separate measurement tools are required for a proper experimental testing program. **Figure 18** shows the illuminance meter (AMPROBE LM-200LED) that was used to measure the initial amount of illuminated light on the sample stage.



Figure 18. Illuminance Meter

The second measurement tool required was a luminance meter. The required luminance meter (Konica Minolta LS-150) selected for these measurements is shown in **Figure 19**.



Figure 19. Luminance Meter

The luminance meter had the optional capabilities of storing the measured data internally. The use of a Data Management Program (CS-S20) allowed data to be directly displayed and recorded on an external portable lap top. A screen shot of this program is shown in **Figure 20**.

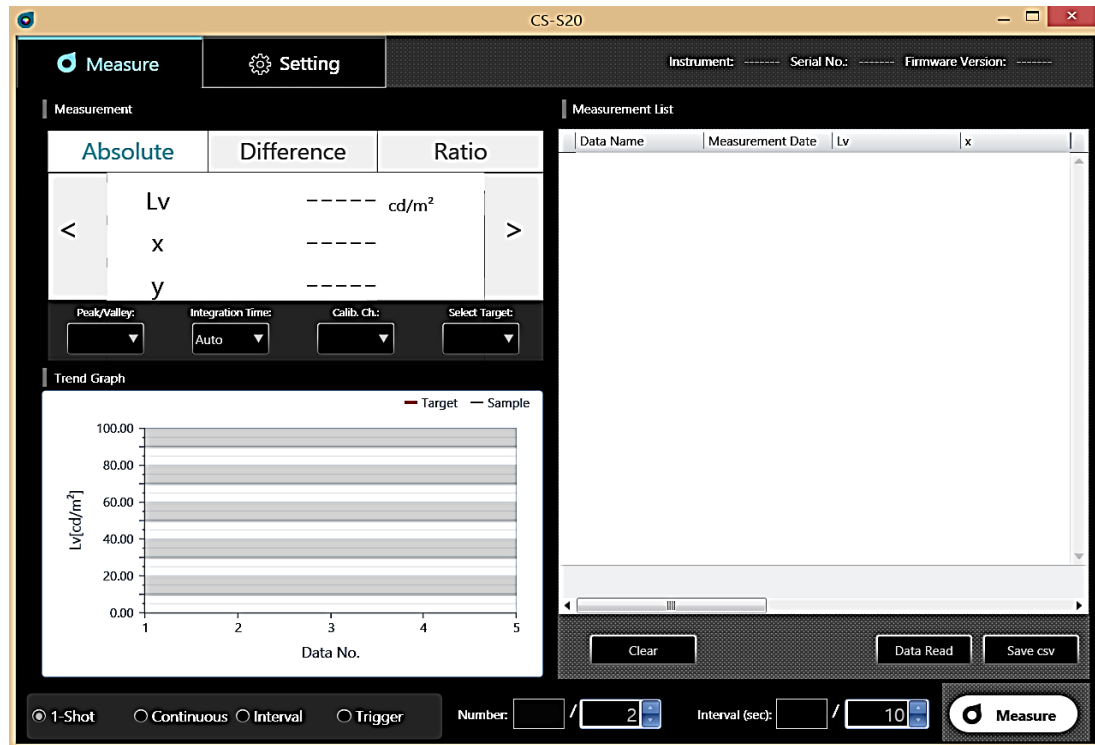


Figure 20. Data Management Program (CS-S20)

Luminance meters are typically designed for field measurements. This Luminance Meter (Konica Minolta LS-150) was initially selected because it not only had the capabilities of performing field measurements but also had the option of an additional Close-Up Lens that allowed much closer measurements. For example, the luminance meter had a no restriction on the maximum measurement distance but the minimum measurement distance was limited to approximately 3 ft. By utilizing an additional (attachment) lens much smaller measurement distances were achievable. The No. 122 Close-Up Lens allowed measurements to be taken around a distance of 9 in away from the target.

3. Lab Samples Tested

The ID assigned to each specimen is defined by the 1st letter representing the testing condition [either Lab (L) or Field (F) tests], 2nd letter represents the material pavement type [Concrete (C) or Asphalt (A) surfaces], and finally the two letter following the dash define the descriptions of those pavements where w/c = 0.40, 0.45, and 0.50 (40, 45, and 50, respectively) and Light and Dark (LT and DK, respectively). Each specimen is illuminated by “traditional” (Incandescent) light and LED light and is represented by the very last letter of the Specimen ID. The “traditional” (Incandescent) light is represented by the letter “T”. The LED lights are indicated by a letter “L”. For example, (LC-40_T) Specimen ID represents Lab tested, Concrete, with w/c = 0.40 properties, utilizing a “traditional” (Incandescent) light source. **Table 7** and **Table 8** presents the Specimen ID’s defined for each lab tested sample.

Table 7. Lab Traditional Light Specimen ID

Specimen ID	Test Condition	Pavement Type	Properties	Light Source
LC-40_T	Lab (L)	Concrete (C)	w/c = 0.40	Traditional (T)
LC-45_T			w/c = 0.45	
LC-50_T			w/c = 0.50	
LA-LT_T		Asphalt (A)	Light (LT)	
LA-DK_T	Dark (DK)			

***Specimen ID = (Test Condition)(Pavement Type)-(Properties)_(Light Source)**

Table 8. Lab LED Light Specimen ID

Specimen ID	Test Condition	Pavement Type	Properties	Light Source
LC-40_L	Lab (L)	Concrete (C)	w/c = 0.40	LED (L)
LC-45_L			w/c = 0.45	
LC-50_L			w/c = 0.50	
LA-LT_L		Asphalt (A)	Light (LT)	
LA-DK_L	Dark (DK)			

***Specimen ID = (Test Condition)(Pavement Type)-(Properties)_(Light Source)**

Concrete lab specimens were developed with the intention of varying w/c ratios to adjust the surface “lightness” of each sample. Visual inspection of each different w/c concrete sample showed little variation to the human eye. Test results made it clear that the varying w/c ratio had little effect on the concrete. On the other hand, the visual inspection of the asphalt samples showed noticeable difference in color lightness of each. Equivalent pictures are shown in **Figure 21**.

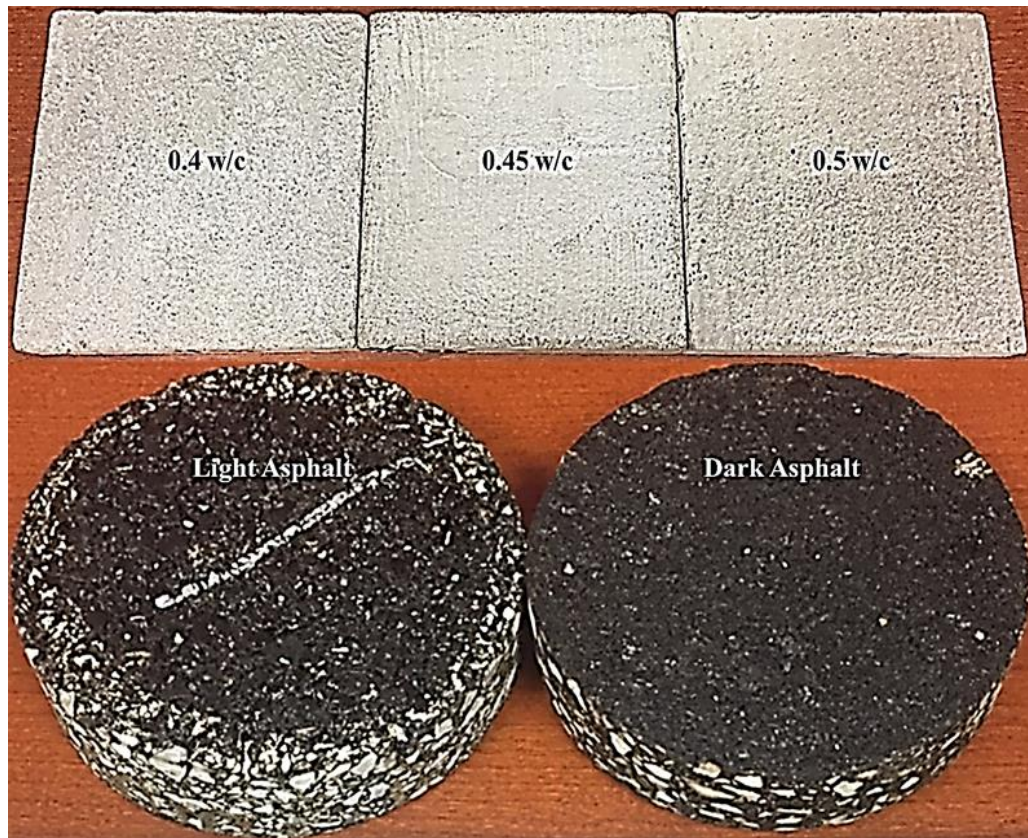


Figure 21. Lab Specimen ID

4. Lab Goniometer Testing Program

The original R-Tables have multiple γ angles at which light reflectivity is measured. The γ angles of 63° and 0° are needed in order to calculate specularity (S_1). Therefore, these angles were initially selected as absolutely critical for design.

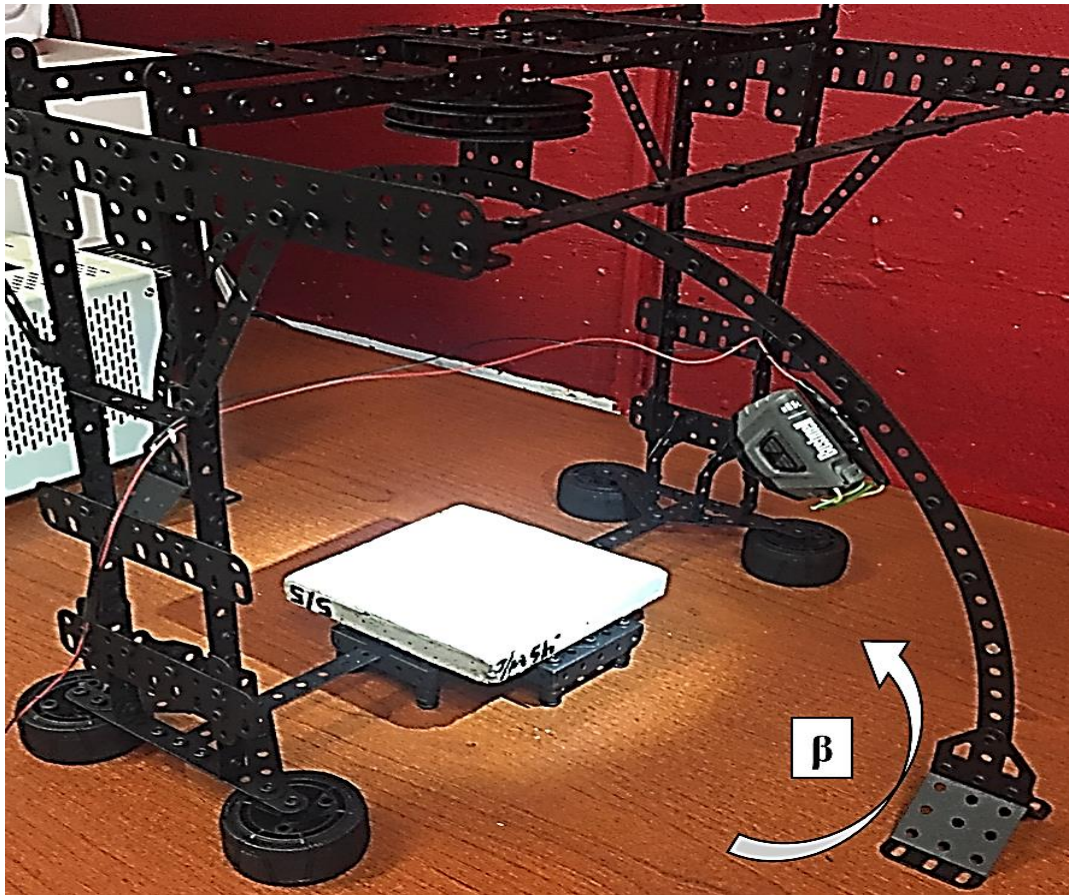


Figure 22. Goniometer Prototype Structure

Figure 22 shows the goniometer prototype structure which was fabricated according to the initial design concepts. The prototype provided a structure capable of rotating mounted lights at specific β angles. **Figure 22** only shows one specific mounted light but the following figure shows all the lights mounted along the arch (γ) in the final design. The angles ultimately selected for mounting lights (γ) were at 0° , 27° , 45° , 63° , and 79° along the arch.

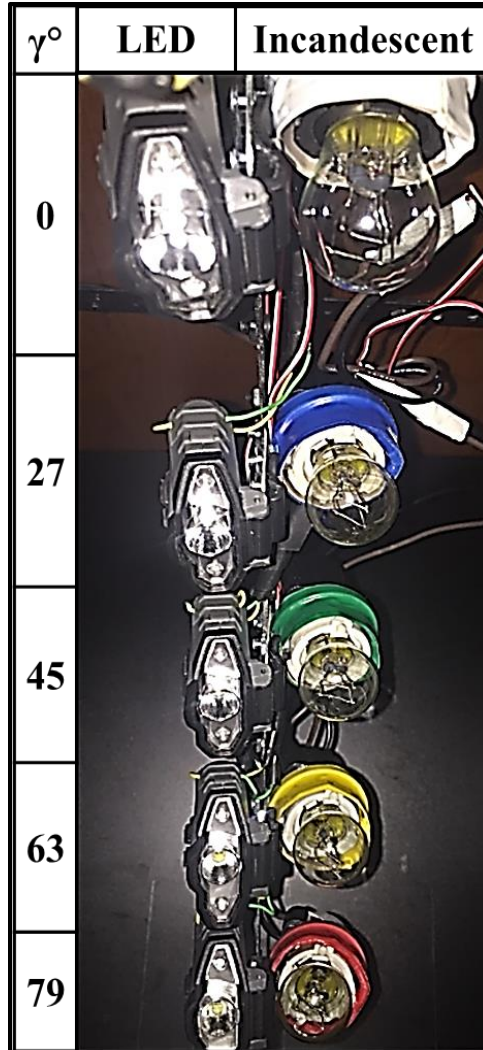


Figure 23. LED Lights and Incandescent Lights

Figure 23 shows a picture of all the lights mounted along the arch in the final design. LED lights and “traditional” lights were mounted adjacently at the same γ angles along the arch. The term traditional light is referring to any and all light sources prior to the advent of LED light sources. The “traditional” light source selected for use in the goniometer design was an incandescent type light. The final lab goniometer utilized incandescent light bulbs as the equivalent representative of a “traditional” source. The design incorporates miniature LED lights as the representative for LED light sources.

Table 9. Specified Luminous Flux

Incandescent Bulb	LED Light Source
188 lumens	65 lumens

Table 9 defines the intended light intensity of each respective light source. The displayed manufacture lumens are the bulb intensity intended for use. For example, the LED light is meant to be powered by a single AAA battery. For testing purposes, these batteries were removed from all the LED lights and electrical (+/-) wires were appropriately attached to each light source which was connected to a Power Supply Unit (BK Precision). This power supply unit was used to control the amount of power being supplied to the light source. Even though the LED lights were intended to produce only 65 Lumens this light intensity could be easily manipulated utilizing this power supply unit. Each of these light sources (Incandescent and LED) run on different amounts of power which is the primary interest of LED lights (very efficient). For example, the LED light was supplied a small amount of power and the traditional was supplied a large amount of power. The LED light requires much less power because the technology uses the power more efficiently than the older “traditional” technology does. Therefore, equivalent light intensity of each light source is achieved by supplying different amounts of power. This concept is better illustrated in **Figure 24** and **Figure 25**.

Initial calibration is performed in order to maintain equivalent light intensity (output) from each of the respective light sources (Incandescent and LED). The B&K Precision Corporation (2016) states: “maximum output current is proportional to the output voltage, rather than supplying the rated current at any output voltage.” Therefore, Volts supplied is proportional to Watts because the meter maintains a constant 3 Amp current.



Figure 24. Calibration of Traditional Lights

Figure 24 shows the Volts required $[(12.8V) (3A) = (38.4W)]$ in order for the traditional (incandescent) light source to achieve the intensity of 300 lux.



Figure 25. Calibration of LED Lights

Figure 25 shows the Volts required $[(0.55V) (3A) = (1.65W)]$ in order for the LED light source to achieve a light intensity of 300 lux. Therefore, the traditional (incandescent) lights required more than 23 times the amount of power (input) than the LED lights just to provide the exact same level of light intensity (output).

The manufacture claims were verified by manually angling the illuminance meter towards each light. As long as there was a constant amount of power supplied to each light source the intensity would stay approximately close to 300 lux. Manually angling the illuminance meter is not a feasible or accurate method of maintaining constant light intensity. It was assumed that this light calibrated intensity remained constant at the other lights (27° , 45° , 63° , and 79°) as long as the power supply was continually maintained.

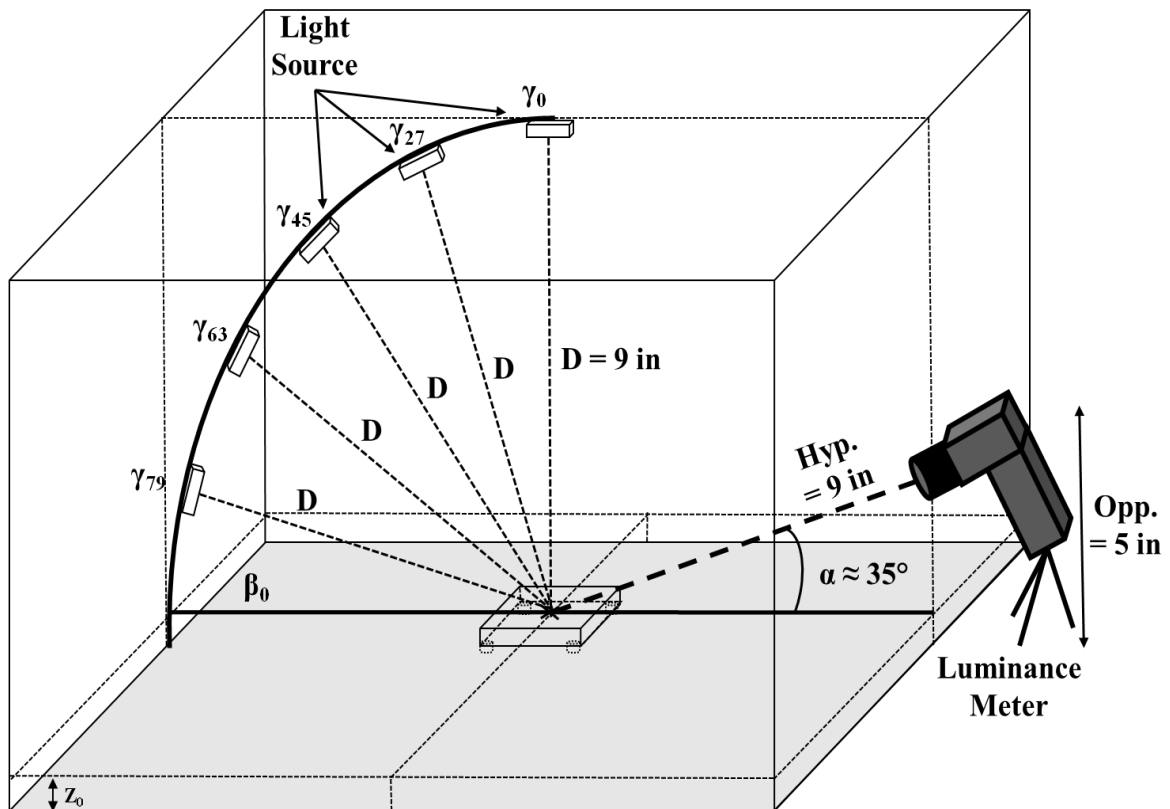


Figure 26. Final Lab Goniometer Design

Figure 26 illustrates the final design light distance (9 in) from each angled light source to the sample being measured. The Close-Up lens ultimately determined the dimensions of the luminance meter. Where the luminance meter viewing distance or hypotenuse (Hyp.) was 9 in away from the sample and was approximately 5 in (Opp.) tall. Therefore, the 35° observation angle was also determined according to these dimensions.

There were a total of 20 measurements required for 5 different samples and 3 separate trials of each was desired. There was a total of 300 lab measurement data points collected. **Figure 27** is a visual representation of all the varying locations each light was placed to take corresponding measurements. The luminance meter is depicted as the grey looking camera on a tripod on the right hand side of the figure. The testing measurement process began at $\beta = 0$ and each of the 5 lights (desired γ angles) were individually turned on by supplying power appropriately. The arch was rotated to achieve a new β angle and the same process was repeated until all the desired measurements were achieved.

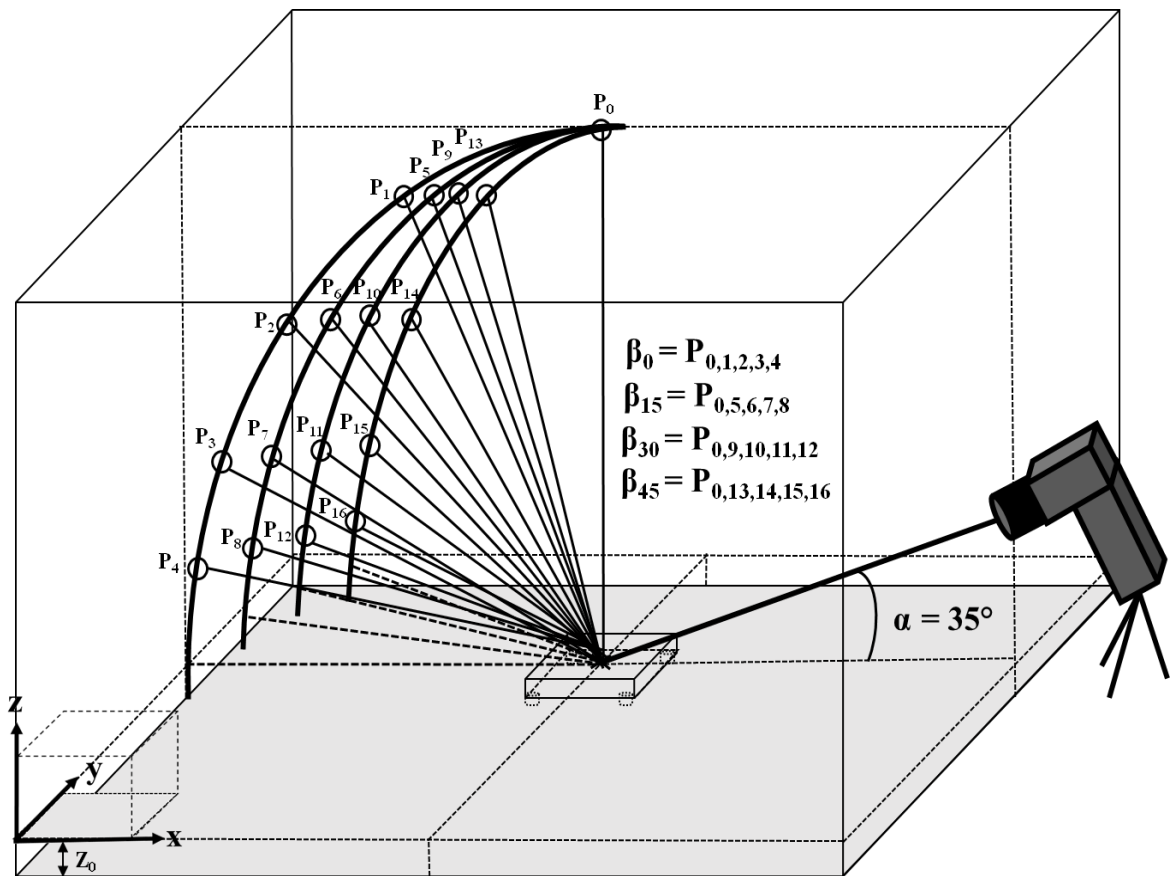


Figure 27. Visual of Angle Combinations

Table 10. Angle Combination Points

α°	β°	γ°	P
35	0	0	P ₀
		27	P ₁
		45	P ₂
		63	P ₃
		79	P ₄
	15	0	P ₀
		27	P ₅
		45	P ₆
		63	P ₇
		79	P ₈
	30	0	P ₀
		27	P ₉
		45	P ₁₀
		63	P ₁₁
		79	P ₁₂
	45	0	P ₀
27		P ₁₃	
45		P ₁₄	
63		P ₁₅	
79		P ₁₆	

Table 10 is a matrix showing all the required combinations of angular measurements. The right side column (P) correlate with each measurement point corresponding to the equivalent visual display in **Figure 27**. Each time β is rotated a measurement is taken with the top light ($\gamma = 0$) but the physical location of that point does not change. P₀ is repeated for all β angles but should be considered a separate measurement. Therefore, while the data points (P) range from the subscript number of 0 to 16 there are actually 20 measurements performed because P₀ is repeated for each β angle. The same angles and respective measurement points were utilized in the field testing program.

B. Field Testing

This field testing section presents the design process that ultimately provided a functional portable goniometer. First, the portable goniometer design modifications will be outlined. Second, the field samples tested will be defined. Last, an overview of the portable goniometer testing program will be presented.

1. Portable Goniometer Design

The data collected in the lab experimental testing program demonstrated the design was adequate of providing accurate and reliable results. The primary objective of the experimental program was to ultimately develop a test program which could be utilized for “in-situ” field measurements. To achieve this objective a few modifications are made to the prototype used in the lab testing program. The primary modifications are listed as follows:

- Housing structure was developed to provide portability and block out light;
- “In-situ” measurements were achieved by replacing the previous sample stage with an opening in the floor that allowed the surface below to be measured;
- It was also desirable to develop an alternative observation angle method for comparison.

The final portable goniometer has the capabilities of measuring data for both 15° and 35° observation angles. Therefore, both designs are presented in the following two sections.

a. Observation Angle of 15 Degrees

The field testing has the same observation angle as the lab testing to have comparable data. It was also desirable to develop an option for a small observation angle. This is typically achieved utilizing a mirror system due to closely spaced equipment.

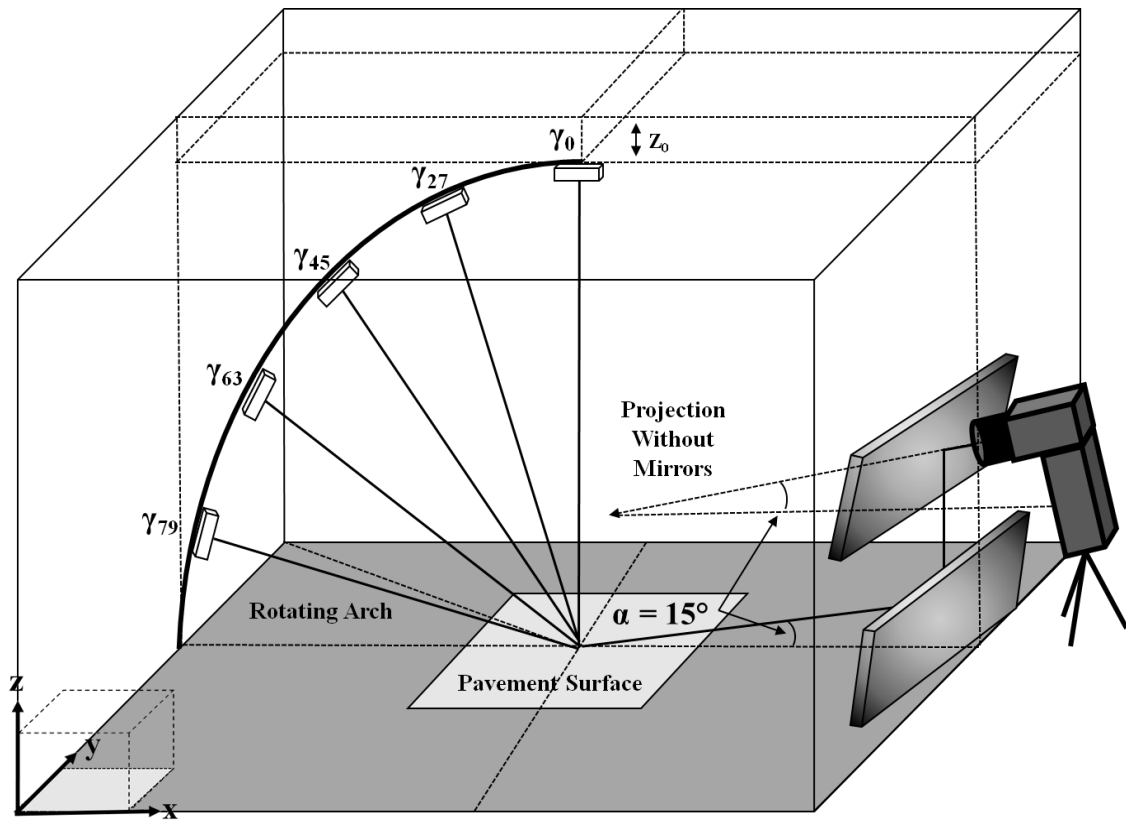


Figure 28. Portable Goniometer Mirror System

A two-way mirror system was installed in the goniometer to have a 15° observation angle to be achieved by simply adjusting the angle of the luminance meter. This design modification is displayed in **Figure 28**. The modifications of the portable goniometer enable testing to measure the same β and γ angles at both 15° and 35° observation angles. Parking lot viewing angles tend to be much steeper compared to drivers on high speed highways. Therefore, the 35° observation angle was ultimately selected as the acceptable representative approach for recreating the parking lot scenario.

b. Observation Angle of 35 Degrees

The primary objective of a portable goniometer is to eliminate the pavement samples tested in the previous lab procedure. The purpose is to develop a method to achieve the same procedure used in the lab tests but on any desired pavement surface.

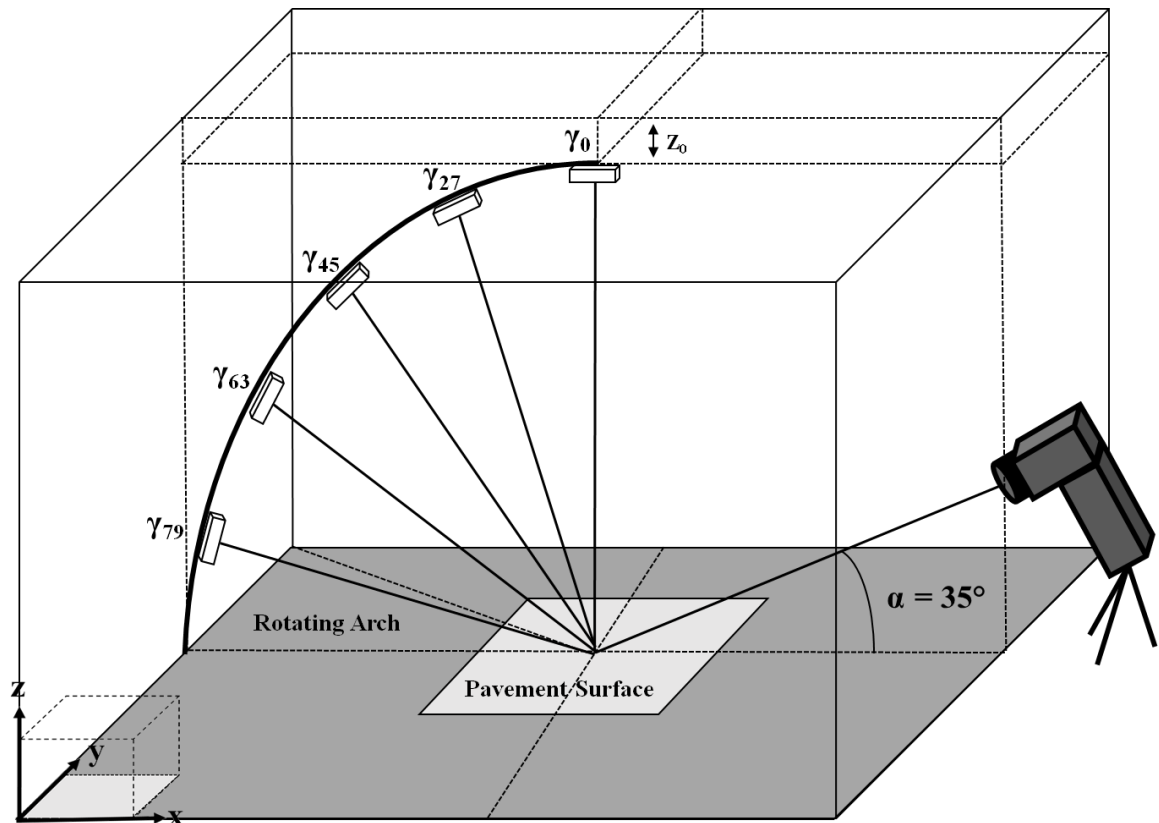


Figure 29. Portable Goniometer Design

Figure 29 illustrates the final portable goniometer design. In contrast to the laboratory testing that measured an elevated specimen surface (Z_0) (see **Figure 17**), this goniometer design enables measurement directly onto the pavement surface (in-situ). Therefore, the axis origin is adjusted accordingly ($Z = 0$). Shown in **Figure 29** the dark grey is the floor of the goniometer and the light grey square in the middle is the floor opening which allows viewing of the “in-situ” pavement surface below.

2. Field Sampled Tested

The primary purpose of the “portable” goniometer is to easily re-locate to the field and perform “in-situ” pavement testing. The tested samples are not cored to obtain each individual sample like those tested in the lab. Each of the field samples are actual “in-situ” pavement surfaces where they have been exposed to aging effects. Each of the field sample Specimen ID’s are associated to the pictures shown in **Figure 30**. The same nomenclature is applied to the field samples that was used in the lab testing and each of the corresponding Specimen ID’s are displayed in **Table 11** and **Table 12**.

Table 11. Field Traditional Light Specimen ID

Specimen ID	Test Condition	Pavement Type	Properties	Light Source
FC-SP_T	Field (F)	Concrete (C)	Specular (SP)	Traditional (T)
FC-DF_T			Diffused (DF)	
FA-DK_T		Asphalt (A)	Dark (DK)	

*Specimen ID = (Test Condition)(Pavement Type)-(Properties)_(Light Source)

Table 12. Field LED Light Specimen ID

Specimen ID	Test Condition	Pavement Type	Properties	Light Source
FC-SP_L	Field (F)	Concrete (C)	Specular (SP)	LED (L)
FC-DF_L			Diffused (DF)	
FA-DK_L		Asphalt (A)	Dark (DK)	

*Specimen ID = (Test Condition)(Pavement Type)-(Properties)_(Light Source)



Figure 30. Field Specimen ID

3. Portable Goniometer Testing Program

Figure 31 shows the final portable goniometer. The right side shows the opening to the lower level where the primary goniometer testing is located. The front flap opening allows the user to easily access the goniometer light fixtures inside as well as the mirror system towards the back. The door is then closed during testing to eliminate all the outside light from leaking into the system. There is a hole in the backside that allows the luminance meter to measure the luminance of target location.



Figure 31. Final Portable Goniometer

Figure 31 illustrates the upper level of the goniometer that houses both of the power supply units and the additional Multimeters (see **Figure 32**). Each power supply unit had power cords that ran out a hole in the back of the upper section and is powered by using any standard electrical plug. A portable car power inverter is a feasible option for testing in remote locations.



Figure 32. Upper Level Power Control Section

Figure 32 shows the front face of the upper housing level with the door open. The power supply unit on the left controlled the traditional (incandescent) lights and the power supply unit on the right controlled the LED lights. Each measurement of varying γ angles (0° , 27° , 45° , 63° , and 79°) was separately wired into a 5 button control switch. The two separate power supply boxes provided constant power to each light source. Each separate light source is selectively supplied power (desired γ angle) by pressing the each button accordingly (small switch device sitting below the large power supply box).

The portable goniometer program utilized the same testing procedure as the lab program. Equivalent light intensities from each light source is initialized (300 lux). Once the light intensities of both sources are matched the primary task of the user is to simply switch on and off each desired light and monitor the supplied power accordingly.



Figure 33. Initial Calibration Process

The portable goniometer testing program is shown in **Figure 33**. As shown in the picture, data could be collected even in the mid-day sun. Light pollution entering the box is measured by simply taking a recording when all the lights are turned off. Even in the worst case scenario there was only around 1 to 2 cd/m^2 resulting from light pollution. Even with minimal error the device is not recommended or intended for use in extreme sunlight. The portable goniometer design performed as intended and actually exceeded initial expectations. More results are discussed in following sections.

IV. TEST RESULTS AND ANALYSIS

This chapter presents the data measured from the testing programs. Following the results section the analysis will be presented accordingly.

A. Test Results

This section consists of two sections. The first section will present the overview of the luminance data of each pavement type and light source. The following section presents the more detailed effect of α , β , and γ angular parameters on the luminance data.

1. Luminance Results

This section presents the luminance values of the different pavement surfaces exposed to different light sources. This initial section does not consider the variation of angular parameters (α , β , and γ). The range of luminance data are compared with respect to pavement type and light source. These results represent the overall reflective behavior. The median line is a fair representation of the general behavior of the given parameter. Therefore, the excess of outliers do not represent error but are intended to display the range of luminance values collected.

a. Lab Results

To understand the effect of the considered variables on the luminance values, each dataset of each specimen is used to estimate statistics (median, 1st and 3rd quartiles, and the maximum and minimum values).

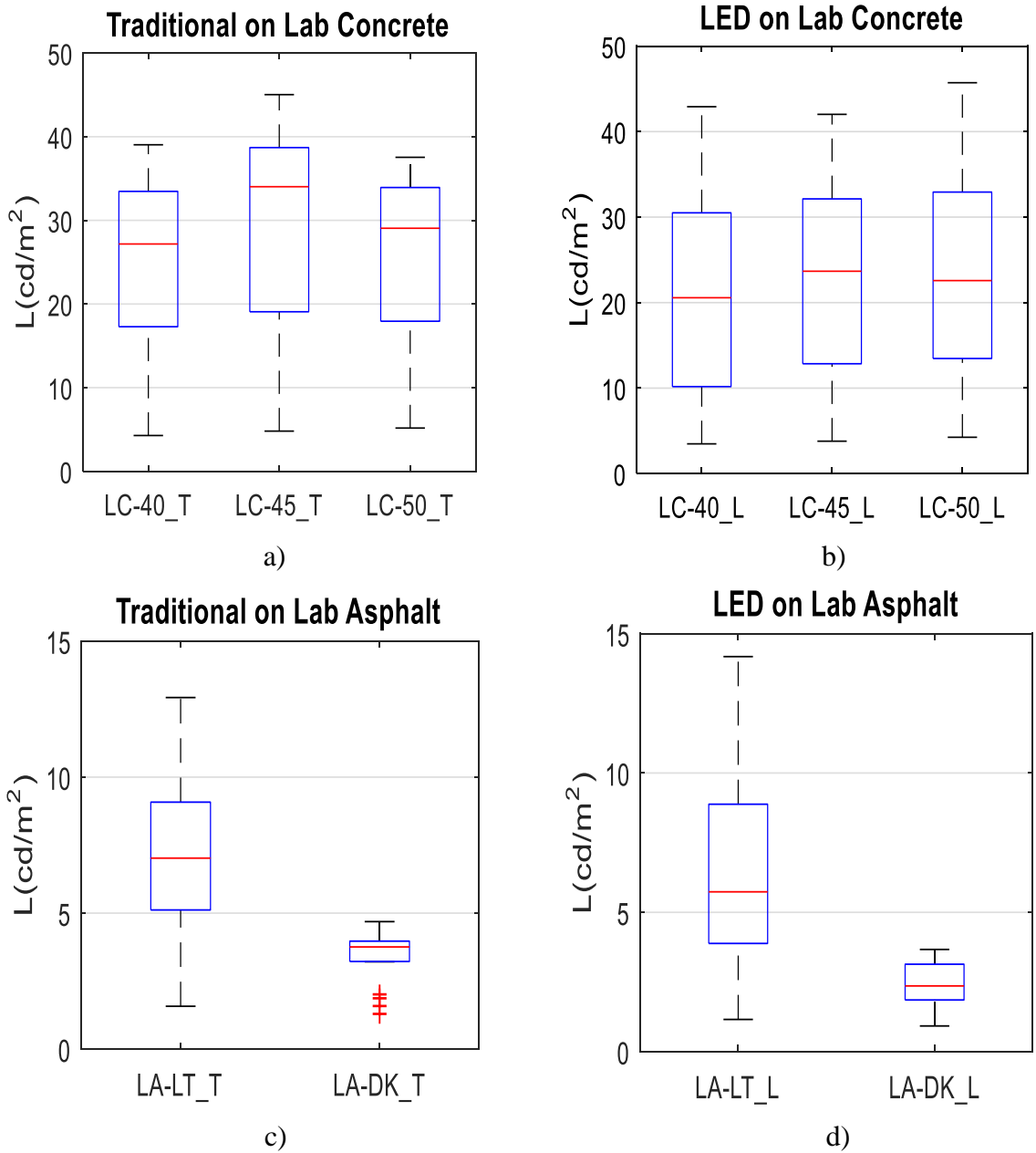


Figure 34. Lab Luminance Results

- a) Traditional on Lab Concrete b) LED on Lab Concrete
c) Traditional on Lab Asphalt d) LED on Lab Asphalt

Figure 34 shows the luminance values used to compare both pavement types illuminated by each light source. **Figure 34 a)** is a boxplot of the luminance (cd/m^2) values of the LC series illuminated by the incandescent (traditional) light. **Figure 34 b)** shows the exact same LC series illuminated by LED light. **Figure 34 c)** is the LA series illuminated by the incandescent light. Lastly, **Figure 34 d)** shows the same LA series except illuminated by LED light. Each of the luminance boxplots shows the data median (middle line), the 1st and 3rd quartile (top and bottom edges of the box), the maximum and minimum values (dotted extension lines), and outliers are represented by a separate cross. For example, in **Figure 34 a)** there appears to be a large range in data. This is due to the effect of the β and γ angles on averaged luminance values. The purpose of this statistical analysis is to compare the collective dataset of each group of specimens.

Results indicated that w/c ratios ranging from 0.40 to 0.50 had no significant difference when they were illuminated by the same light. Therefore, it is justifiable to select the 0.40 w/c ratio sample for the simplicity of further analysis. On the other hand, the two asphalt samples exhibited a significant difference in luminance values. The LC series consistently presented high values of reflectivity as compared to the LA series that demonstrated relatively inconsistent results.

Both pavements showed consistently higher luminance values when illuminated by the incandescent light. For example, the average median luminance value of the LC series when illuminated by the incandescent light was about 30 cd/m^2 whereas the LED light only produced about 23 cd/m^2 on the same series. This difference was even more significant in the LA series in which the incandescent nearly produced double the light when compared to the LED.

b. Field Results

A similar presentation of the Lab results are provided for Field results as follows.

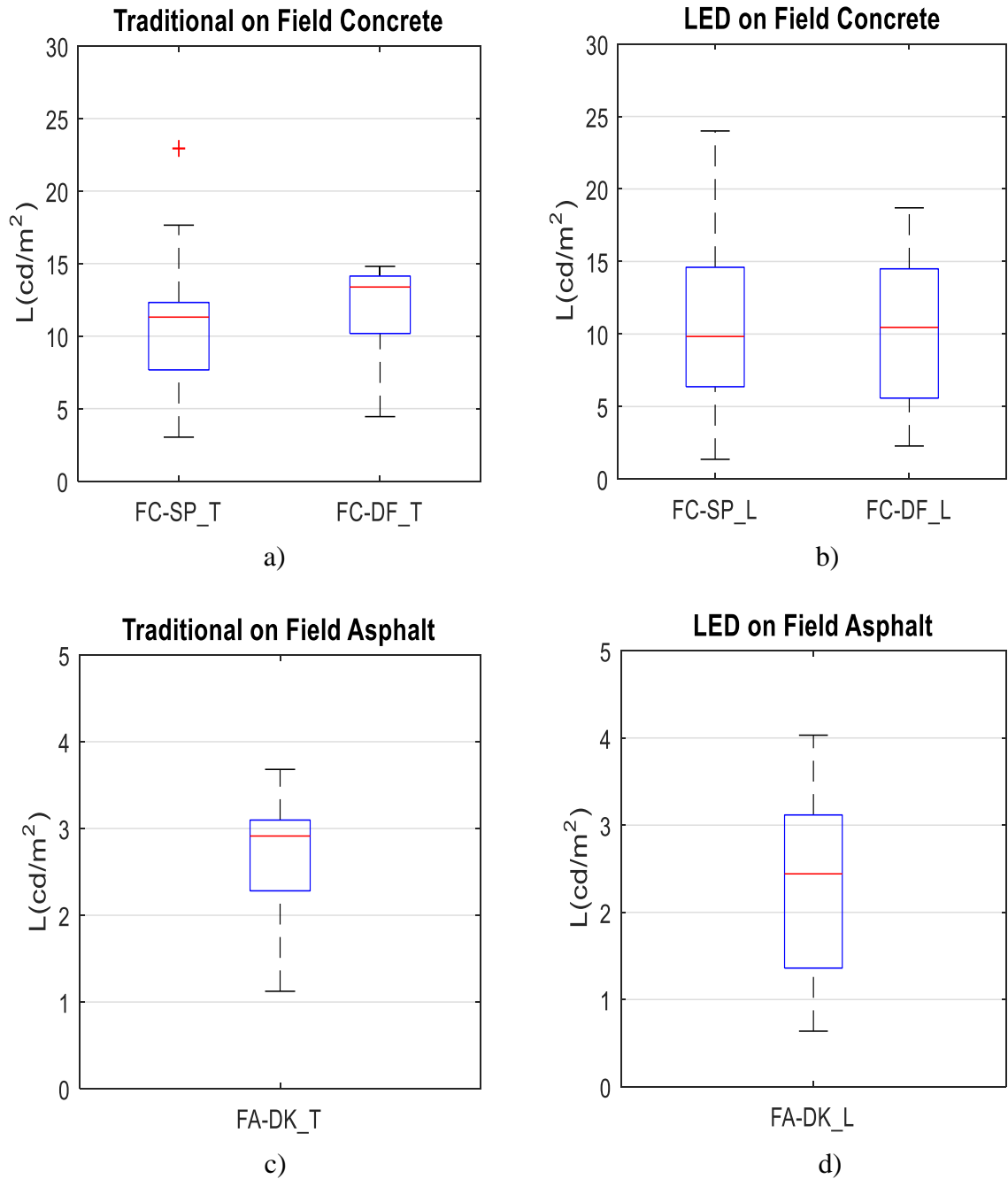


Figure 35. Field Luminance Results

- a) Traditional on Field Concrete b) LED on Field Concrete
c) Traditional on Field Asphalt d) LED on Field Asphalt

Figure 35 presents the luminance values collected for the field data. The graphical display of data uses the same layout as the previous lab results. Incandescent light on concrete pavement is presented in **Figure 35 a)**, LED on concrete is presented in **Figure 35 b)**, incandescent on asphalt is presented in **Figure 35 c)**, and lastly LED on asphalt is presented in **Figure 35 d)**. Both samples of concrete had a median value around 10 to 15 (cd/m^2) and the asphalt sample had a median value between 2.5 to 3 (cd/m^2). The lab concrete samples (LC series) had very similar results when illuminated by each independent light source.

The field results also presented a significant range in maximum and minimum values provided by each illuminating light **Figure 35 a) vs. b)**. For example, the highest median values occur with the incandescent light but the maximum values are greater with the LED light. Both concrete samples show a median above $12 \text{ cd}/\text{m}^2$ for incandescent (**Figure 35 a)** and below $12 \text{ cd}/\text{m}^2$ for the same samples for the LED (**Figure 35 b)**. Inversely, both samples present higher maximum values for the LED light compared to incandescent light. Therefore, the illumination of the incandescent effectively distributes light more evenly than the LED does.

While this influence of lighting is clearly apparent regardless of pavement type, each individual concrete sample did not exhibit the same pattern change. For example, the specular concrete (FC-SP) and diffused concrete (FC-DF) both shared similar median values with respect to the light source. Whereas, the range of values varied with respect to the surface material type (i.e., specular or diffused). **Figure 35 b)** demonstrates each surface achieved the same ($10 \text{ cd}/\text{m}^2$) median value but the range of values was much greater for the specular surface than the range of the diffused surface.

c. Summary

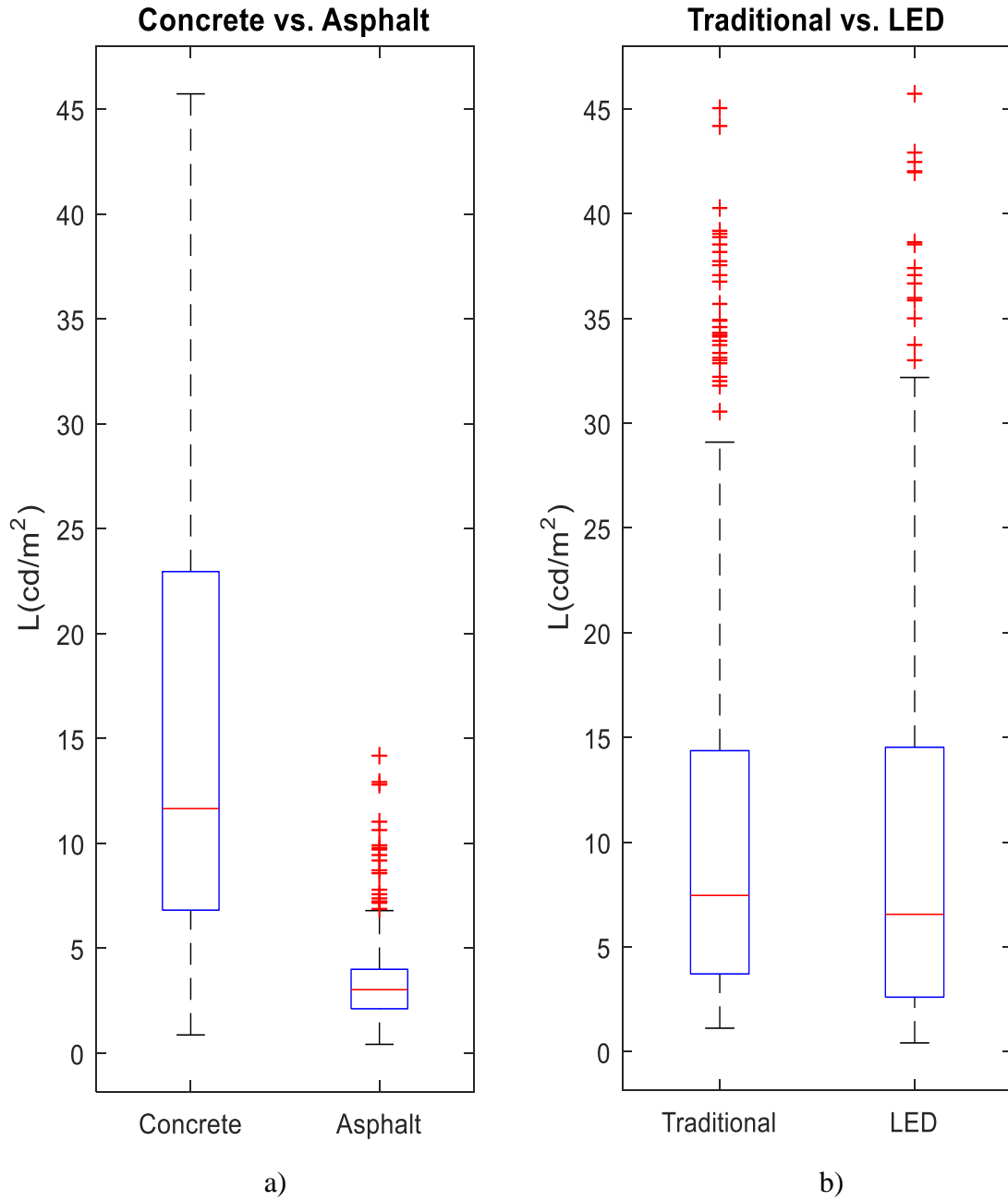


Figure 36. Summary of Luminance Results

a) Traditional vs. LED b) Concrete vs. Asphalt

Figure 36 presents a summary of luminance values from both the lab and field testing. **Figure 36 a)** shows the collective results of all the luminance values of concrete and asphalt. The concrete group is composed of the LC series (**Figure 34 a and b**) and the FC series (**Figure 35 a and b**). Similarly, the collective asphalt group is composed of both the LA series (**Figure 34 c and d**) and the FA series (**Figure 35 c and d**). The median values of each concrete and asphalt are about 12 and 4 (cd/m²) respectively. The results indicate that concrete surfaces exhibited up to 3 times higher luminance values than the asphalt surfaces.

Figure 36 b) compares the luminance values between incandescent and LED lights regardless of the pavement type. This boxplot indicates little variation between the average luminance values of each light source. **Figure 36 b)** indicates that in general (regardless of the pavement surface) incandescent and LED lights seem to provide the same average luminance values. It should be noted that the datasets of each traditional (incandescent) and LED light sources include both pavements. Therefore, a comparison not considering different pavement types can possibly be misrepresentative of the light reflectiveness of each light source.

Figure 35 a) vs. b) present evidence that the light source can have an impact on the characteristics of the results. The same effect is not apparent in the general luminance values (**Figure 36 b**). This is evidence that further (more detailed) analysis of the data is required and is presented accordingly in the following section.

2. Luminance Results at Varied Angles

This section presents the data results collected in the testing programs with consideration of the angular components (β and γ). The R-Tables are so critical to design because they represent the angular behavior of different surfaces with respect to β and γ . The proceeding results display the angular results collected in each of the experimental programs (lab and field respectively).

A more representative analysis of each specimen under one light is achieved by considering the specific angular data. Critical samples were selected to present the most representative data for each type of pavement. The LC series exhibits higher luminance values (around 30 cd/m²) than expected for typical concrete. Inversely, the FC series had lower luminance values (20 cd/m²) than was initially expected. Therefore, the LC series was determined to be representative of lighter concrete and the FC series represents a darker concrete pavement type.

The light asphalt lab sample (LA series) had higher luminance values (15 cd/m²) than the dark asphalt sample. Therefore, the light asphalt sample was selected for the LA series as a relatively adequate representation of lighter asphalt. The FA series resulted in expected luminance values (about 5 cd/m²) and therefore appeared to be a fairly adequate representation of darker asphalt. These results were considered to select a representative range of pavement types to analyze at the angular level.

a. Lab Results

Table 13. Selected Lab Samples

Specimen ID	Test Condition	Pavement Type	Properties
LC-40	Lab (L)	Concrete (C)	w/c = 0.40
LA-LT		Asphalt (A)	Light (LT)

***Specimen ID = (Test Condition)(Pavement Type)-(Properties)**

Table 13 presents the two lab samples selected to further analyze at varied angles of β and γ . Previous results concluded minimal variation in the LC series. Therefore, the LC-40 (w/c = 0.40) was selected to represent the LC series for further analysis. On the other hand, the LA series did present a significant variation in the results. The lighter asphalt sample was selected to represent the LA series for further analysis. Both the LC series and lighter LA sample produced higher than expected luminance values. These were selected as the best case reflective representation for each respective pavement type.

Figure 37 a) and b) presents the luminance of an incandescent light on the LC sample. **Figure 38** a) and b) presents the luminance of the LED light on the exact same LC sample. For example, each graph on the left a) is a 3D Surface of luminance (cd/m^2) as the z-axis, the β angle (degrees) is the x-axis (axis on the right side), and the γ angle (degrees) is the y-axis (axis on the left side). The right side of each figure also presents a Contour Plot b) of those same results just displayed in a different manner. Similarly, on the Contour Plots, the β angle (degrees) is the x-axis (axis on bottom side), the γ angle (degrees) is the y-axis (axis on the left side), and the numbers of each contour represent the respective luminance (cd/m^2) values. This exact same layout is used for all following figures and is intended to make comparison of all the plots relatively easy for the reader.

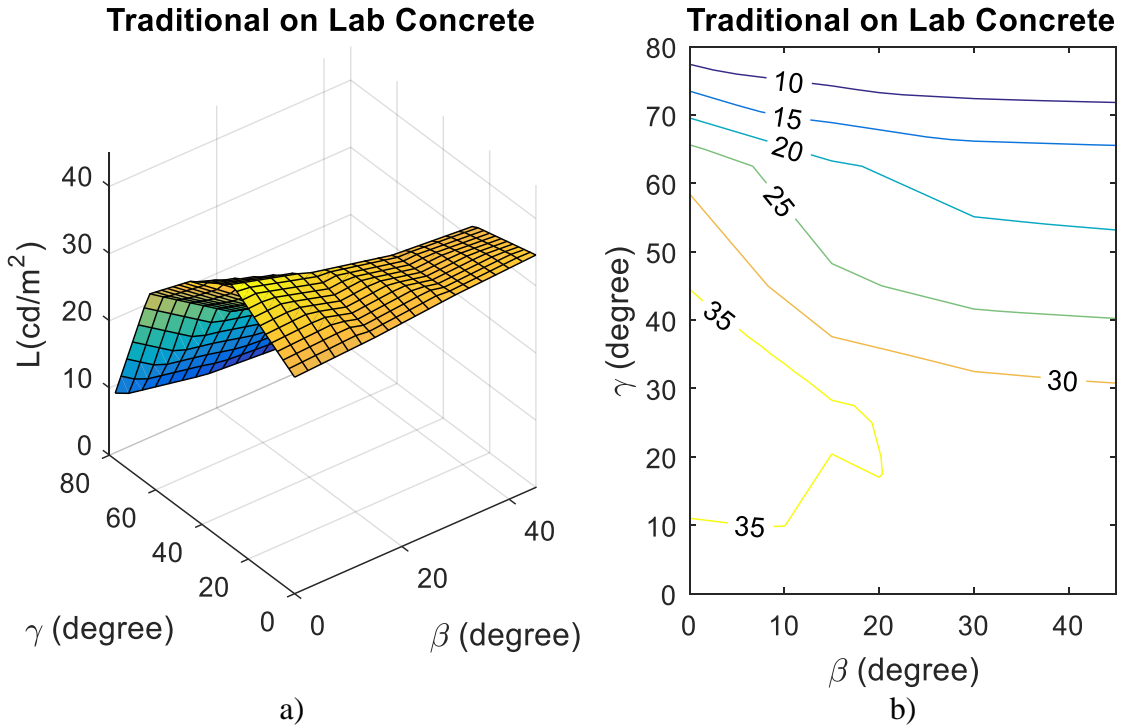


Figure 37. Incandescent Luminance on Lab Concrete

a) 3D Surface b) Contour Plot

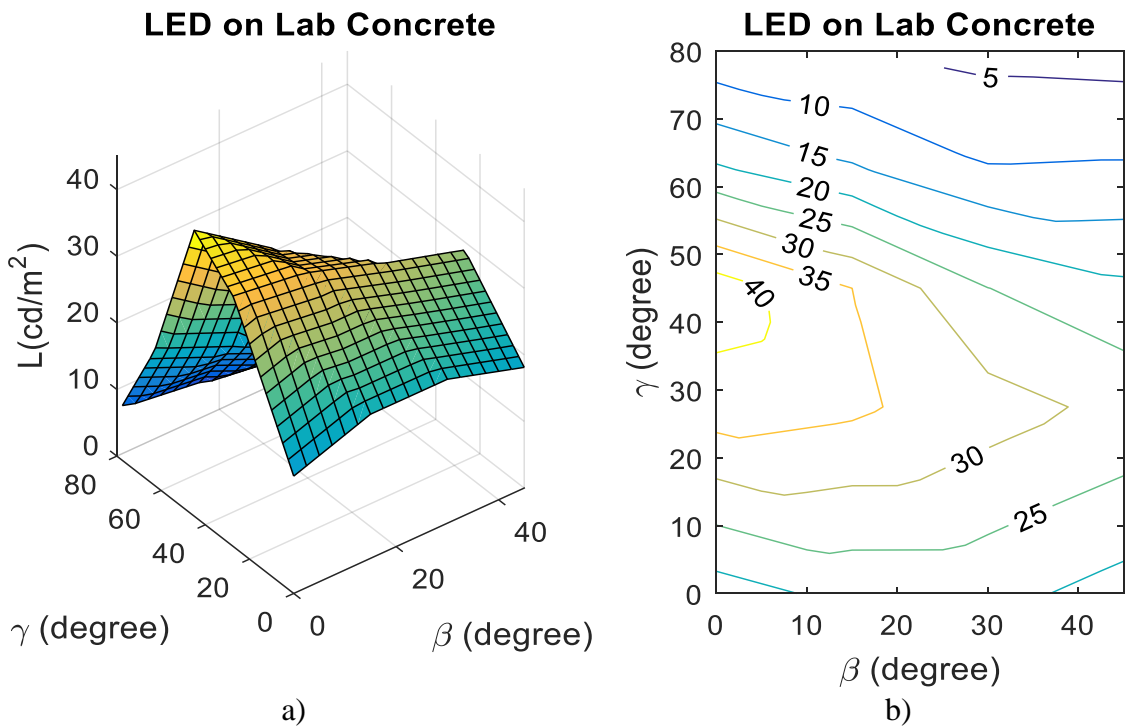


Figure 38. LED Luminance on Lab Concrete

a) 3D Surface b) Contour Plot

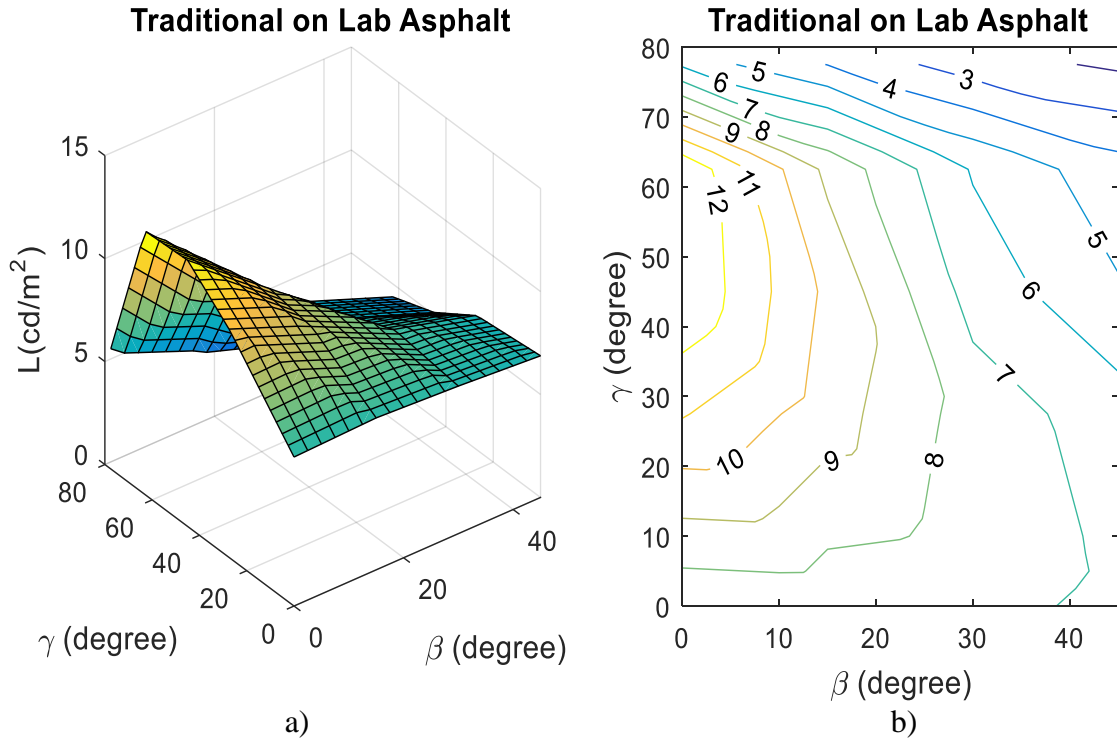


Figure 39. Incandescent Luminance on Lab Asphalt

a) 3D Surface b) Contour Plot

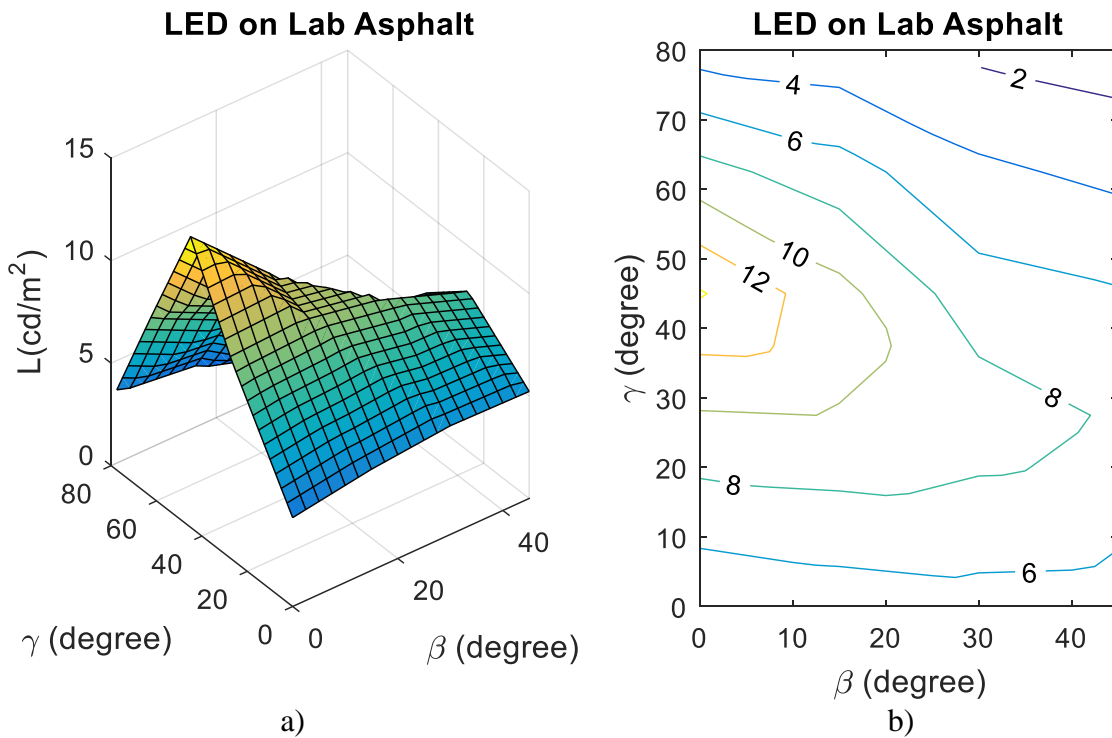


Figure 40. LED Luminance on Lab Asphalt

a) 3D Surface b) Contour Plot

Figure 37 a) and b) as well as **Figure 38** a) and b) both present a significant difference between the luminance values collected from the LED light than that of the incandescent light. The incandescent luminance values show a more normalized pattern than that of the LED light. Concrete is also expected to be less sensitive to a change in the β angle (according to the original R1 table values). This behavior is clearly presented in the luminance results. The smooth flowing downward pattern of the incandescent is the shape to be expected for the concrete surface (according to R-Tables). This consistent “smooth” behavior is not seen in any of the LED luminance results. As shown in all the 3D Surface luminance plots, there seems to be a consistent “spike” in luminance values as the γ angle approaches about 45 degrees.

Figure 39 a) and b) as well as **Figure 40** a) and b) both present similar patterns from the previous LC series except these are the luminance values from the LA series. Once again, the same pattern variation can be seen between the incandescent and LED luminance results. There is another significantly noticeable “spike” in the LED luminance results. Inverse to the behavior of concrete, asphalt is expected to be more influenced by the β angle. The luminance results validate this expected behavior. This can be seen as the β angle increases the luminance value decreases accordingly. This β angle effect on asphalt is still less than the effect of the γ angle on the luminance results. A combination of both influences from the β and γ angle create what will be described as a “twisting” effect that can be seen in the 3D Surface luminance plots.

b. Field Results

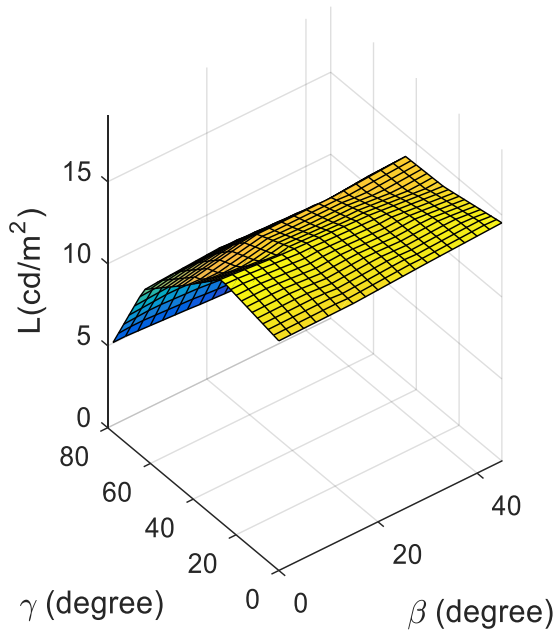
Table 14. Selected Field Samples

Specimen ID	Test Condition	Pavement Type	Properties
FC-DF	Field (F)	Concrete (C)	Diffused (DF)
FA-DK		Asphalt (A)	Dark (DK)

***Specimen ID = (Test Condition)(Pavement Type)-(Properties)**

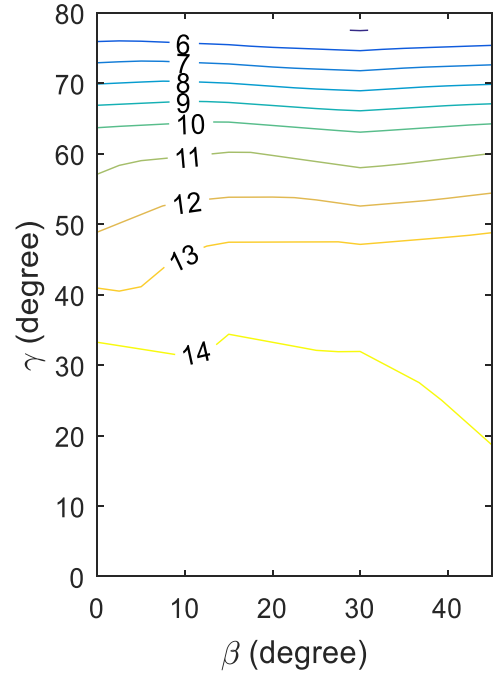
Table 14 presents the two field samples selected for further analysis at varied angular values. The two concrete samples tested in the field (FC) are intentionally selected due to each of their unique surface textures. Typically, concrete is more diffused in nature and therefore this sample is selected to represent the FC series. The variations in the behavior of the specular and diffused surfaces will be discussed later in terms of different observation angles. Only one sample of asphalt was tested in the field and therefore is used to represent the FA series. Both the FC series and FA series produced lower luminance values than expected. Previously defined selected lab specimens exhibit higher reflective performance for each pavement type. The selected field specimens exhibit lower reflective performance for each pavement type. Therefore both sets of selected specimens are a relatively accurate representations of high and low reflective performance for each pavement type. The following figures will present the results from the FC and FA series in the same layout as before.

Traditional on Field Concrete



a)

Traditional on Field Concrete

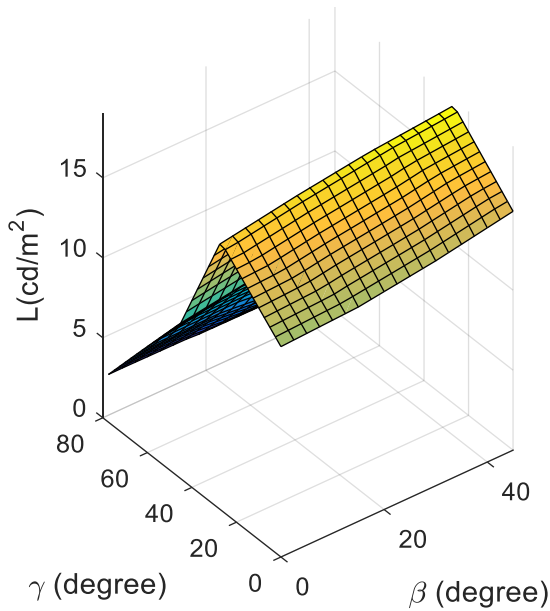


b)

Figure 41. Incandescent Luminance on Field Concrete

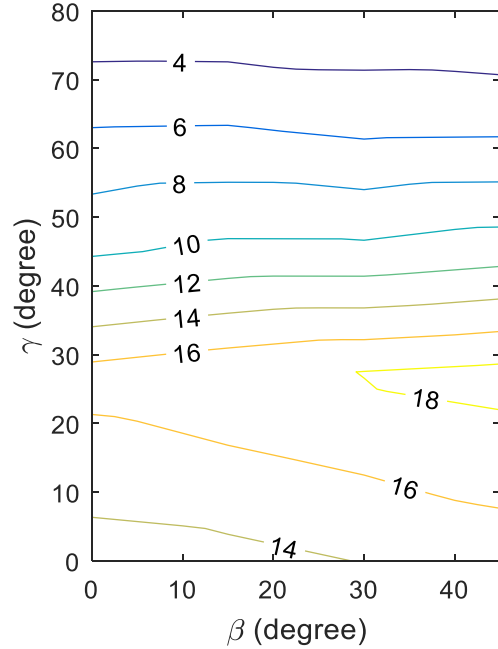
a) 3D Surface b) Contour Plot

LED on Field Concrete



a)

LED on Field Concrete



b)

Figure 42. LED Luminance on Field Concrete

a) 3D Surface b) Contour Plot

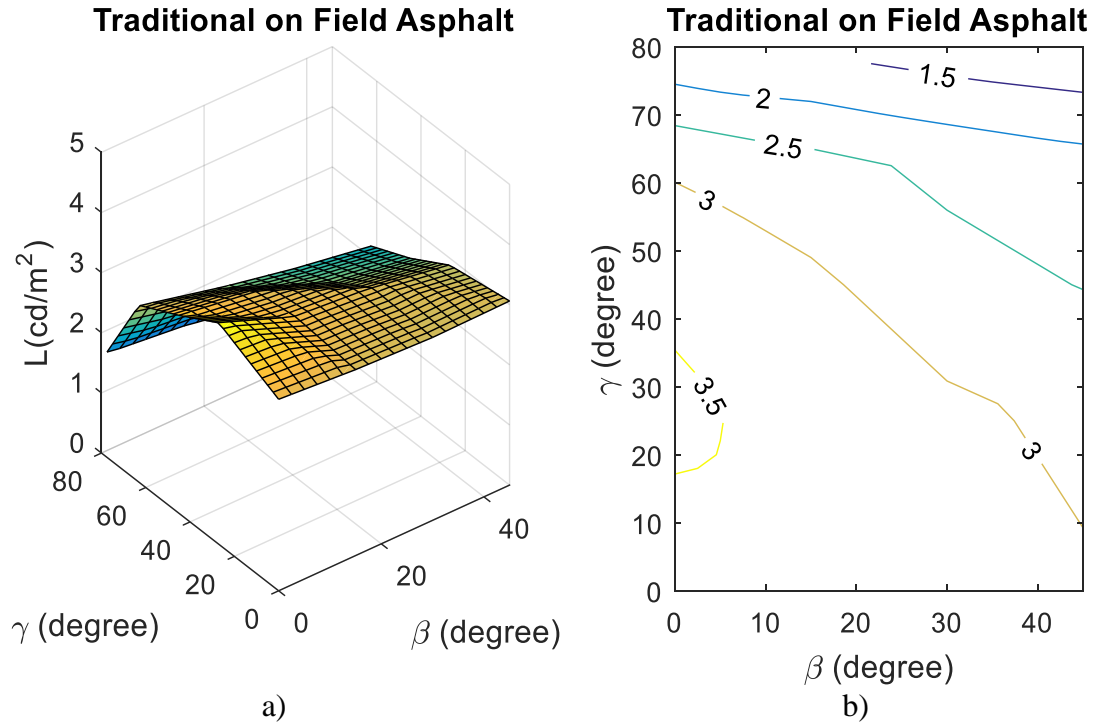


Figure 43. Incandescent Luminance on Field Asphalt

a) 3D Surface b) Contour Plot

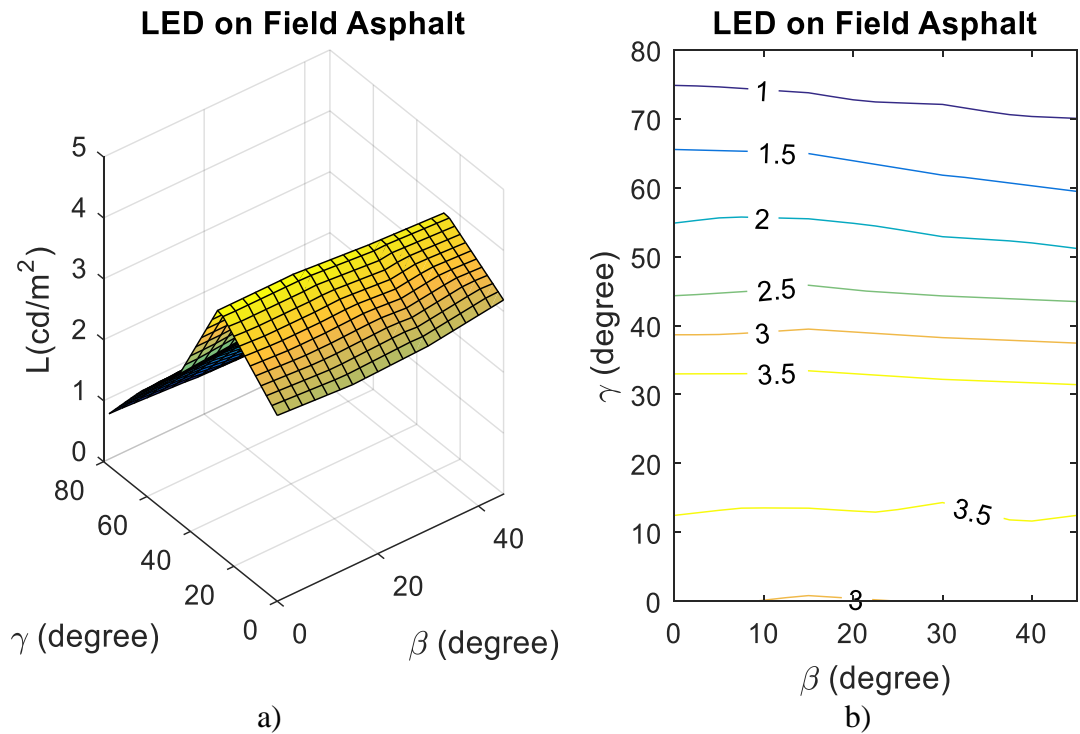


Figure 44. LED Luminance on Field Asphalt

a) 3D Surface b) Contour Plot

Figure 41 and **Figure 42** presents the luminance results from the FC series illuminated by both independent light sources. Luminance values have a much lower range than that of the previous lab samples, but as stated, this was the intention of the selected samples. Despite the scale of each graph the exact same “spike” pattern can be seen from the concrete field sample results.

Figure 43 and **Figure 44** presents the luminance results from the FA series illuminated by both independent light sources. The FA series (asphalt) illuminated by the incandescent light appropriately demonstrates the “twisting” effect previously mentioned. The back right of the FA (asphalt) 3D Surface luminance plot has a darker shade than the FC (concrete) 3D Surface luminance plot. This confirms the expected behavior of asphalt as reported by the original R-Tables. The results from the FA series also indicate that regardless of the surface type the exact same “spike” behavior is demonstrated when illuminated by the LED.

B. Analysis

In general lighting parameters are pre-determined prior to actual construction and therefore do not have the future “in-situ” pavement surface to measure luminance values. R-Values are utilized by designers to calculate and predict the minimum luminance values required for a certain area. Common design practice is to calculate luminance from pre-defined R-Values. This is the exact opposite process used in this research. Therefore, the following analysis section will outline the procedure used to calculate the R-Values from the luminance values collected in the experimental testing program. The converted R-Values will be displayed in a similar manner as the previous 3D Surface and Contour Plots except are now presented as R-Values instead of the previous luminance values.

Utilizing the equations previously defined in the literature (*Eq.4*) each R-Value is calculated accordingly. *Eq.4* presents $[R = ((h^2/I)(L))]$. Where L is the luminance value collected in the experimental tests and (h^2/I) is calculated as shown in **Table 15**. Intensity is converted from lux to cd in order to use the equation. For example, the intensity used in the experimental testing was held constant at 300 lux which is equivalent to 15.7 cd.

Table 15. Converting Luminance to R-Values

γ°	D (m)	h (m)	I (cd)	h^2 / I
0°	0.229	0.22860	15.7	0.00333
27°	0.229	0.20368	15.7	0.00264
45°	0.229	0.16164	15.7	0.00166
63°	0.229	0.10378	15.7	0.00069
79°	0.229	0.04362	15.7	0.00012

***(I = 300 lux = 15.7 cd)**

1. R-Values of Selected Samples

Table 16. Simplified Factors for Respective γ Angle

R =	(h²/I)	*L
R ₀ =	33.33	*L ₀
R ₂₇ =	26.46	*L ₂₇
R ₄₅ =	16.67	*L ₄₅
R ₆₃ =	6.87	*L ₆₃
R ₇₉ =	1.21	*L ₇₉

***10,000**

Table 16 displays simplified factors (h^2/I) that correspond with each of the varied γ angles used in each of the experimental programs. The calculations for the (h^2/I) factors are previously presented in **Table 15** except the factors presented in **Table 16** are all multiplied by 10,000 for ease of use. This is exactly what is done in the original R-Tables and therefore allows simple conversions of equivalent values. For example, looking back to **Figure 37 b)** the maximum luminance value defined on the contour map is 35 cd/m² and occurs approximately at the $\gamma = 0^\circ$ angle and therefore must use the 33.33 factor (**Table 16**) to calculate the corresponding R-Value. The following is an example of the simplified calculation where:

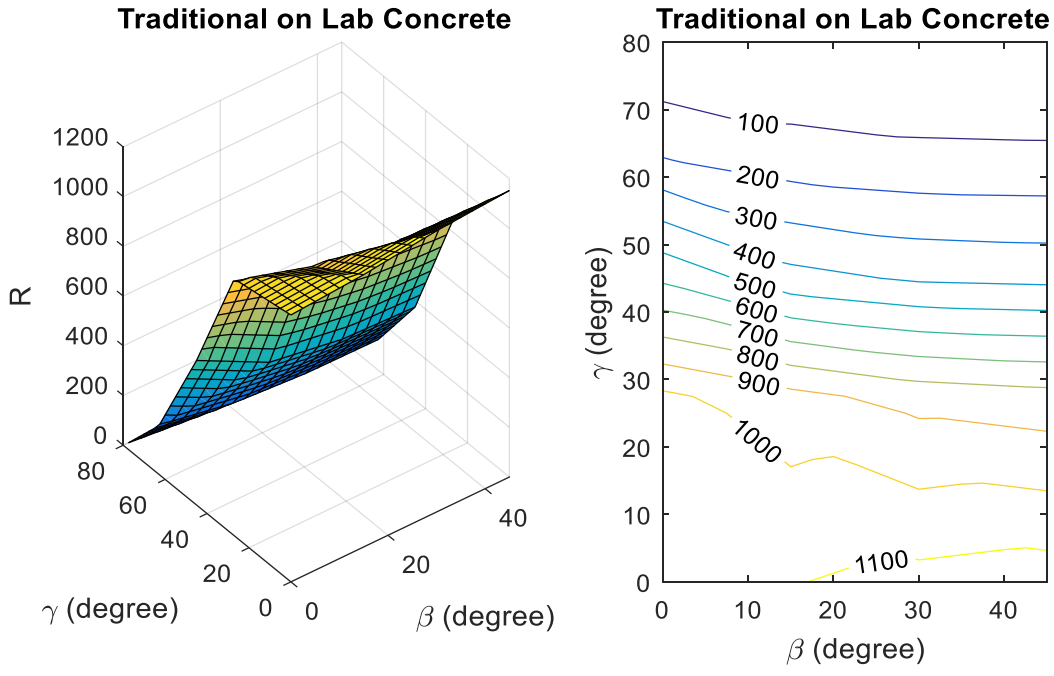
$$R_0 = (h^2/I)(L_0) = (33.33)(35) \approx 1,100$$

Looking forward to **Figure 45 b)** the corresponding maximum R-Value is 1,100 which is approximately equal to the value calculated above.

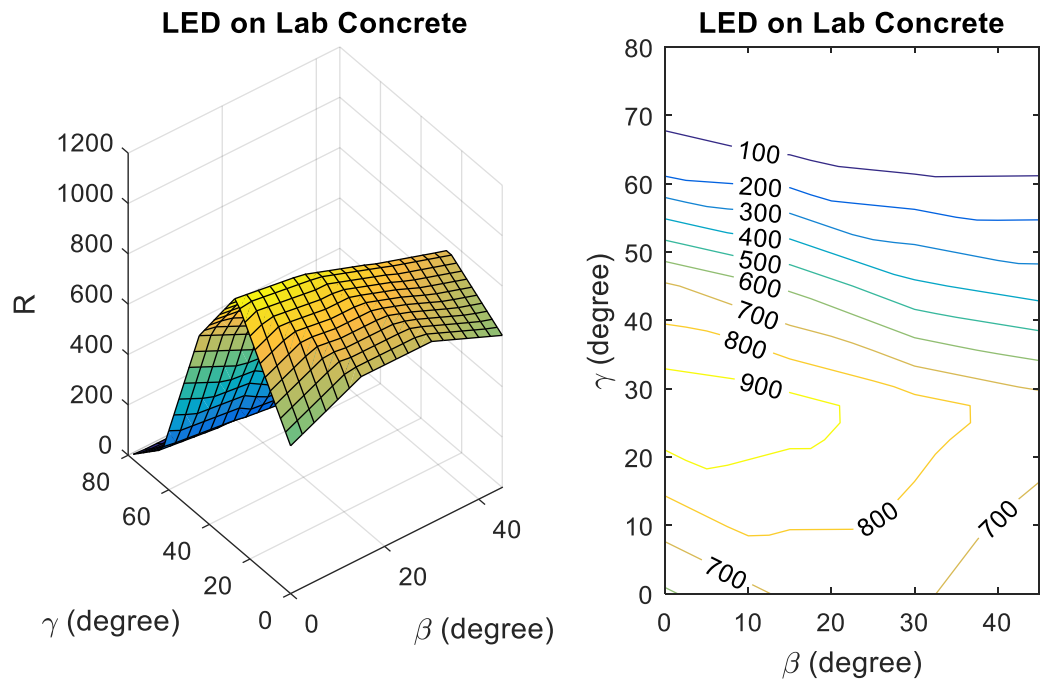
a. Lab R-Values

This conversion procedure was utilized to calculate the corresponding R-Values of all the data reported in the previous results section. The graphs are displayed in the same consistent manner as used in the results (luminance) section. The only difference in the proceeding section is that each 3D Surface and Contour Plots are presented in terms of R-Values instead of luminance values (as previously reported). These values repeat similar patterns as described in the results section but are presented with the objective of comparing them with the original R-Table graphs. The following section presents the converted R-Values calculated from the previously reported lab luminance results. The first two figures (**Figure 45** and **Figure 46**) display the equivalent R-Values of the concrete lab sample (LC). The next (**Figure 47** and **Figure 48**) two figures similarly represent the equivalent R-Values of the asphalt lab sample (LA).

As presented in **Figure 45**, **Figure 46**, **Figure 47**, and **Figure 48** the R-Values consistently decrease as the γ angle increases regardless of the change in the β angle. Typically, the R-Values are much higher for concrete pavements than asphalt pavements. Interestingly, the overall shape of the 3D Surface R-Value plots are similar between concrete and asphalt illuminated by the incandescent light source as shown in **Figure 45** and **Figure 47**. Also the overall shape of the 3D Surface R-Value plot are similar between concrete and asphalt specimens illuminated by the LED light source as shown in **Figure 46** and **Figure 48**. This indicates that the light source is a significant parameter that will impact the R-Value with respect to the γ angle.



a) b)
Figure 45. Incandescent R-Value on Lab Concrete
 a) 3D Surface b) Contour Plot



a) b)
Figure 46. LED R-Value on Lab Concrete
 a) 3D Surface b) Contour Plot

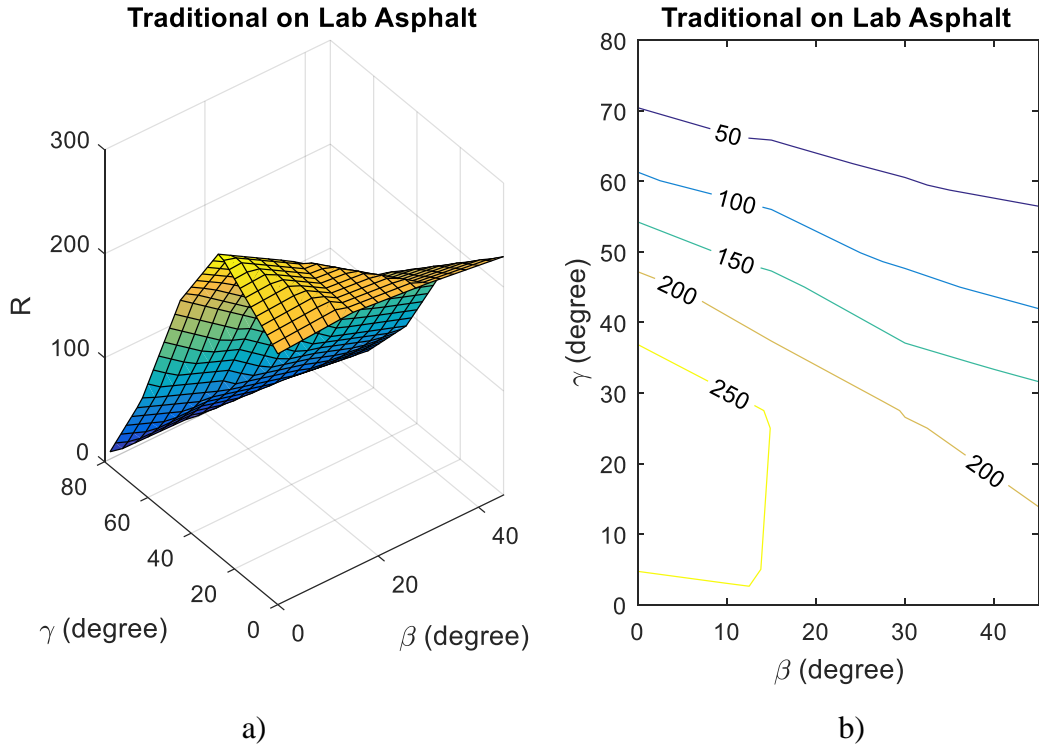


Figure 47. Incandescent R-Value on Lab Asphalt
a) 3D Surface b) Contour Plot

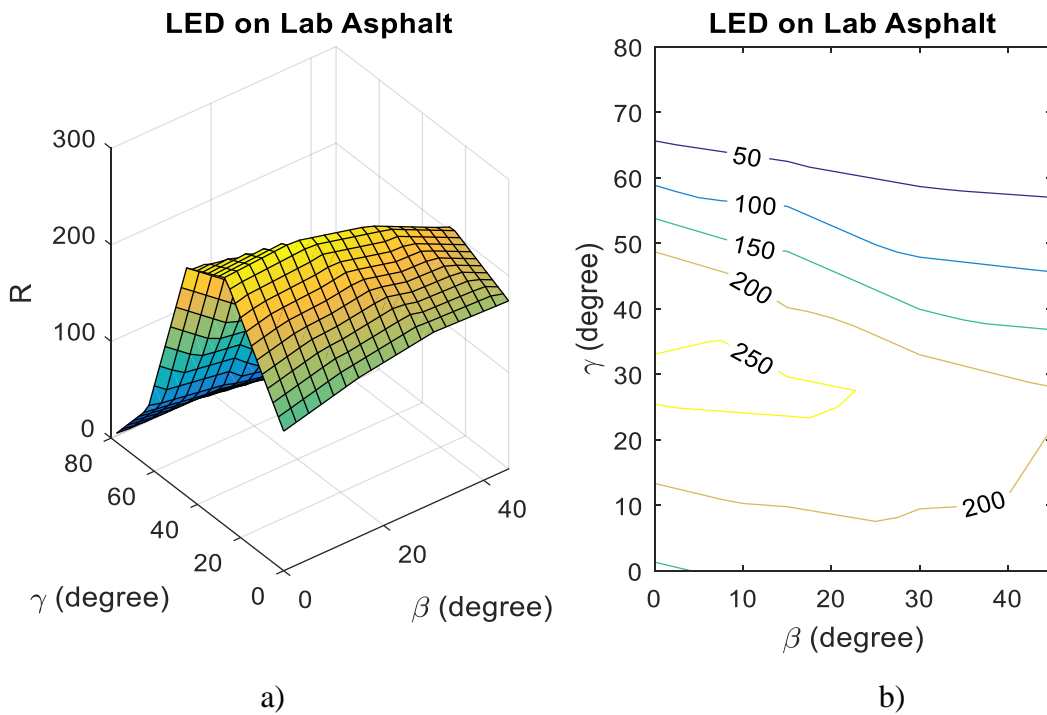


Figure 48. LED R-Value on Lab Asphalt
a) 3D Surface b) Contour Plot

b. Field R-Values

Same as the previous lab R-Value section, the following section presents the converted R-Values calculated from the previous results in the field luminance section. The first two figures (**Figure 49** and **Figure 50**) display equivalent R-Values of the concrete field sample (FC). The following (**Figure 51** and **Figure 52**) two figures present the equivalent R-Values of the asphalt field sample (FA).

As presented in **Figure 49**, **Figure 50**, **Figure 51**, and **Figure 52** the R-Values consistently decrease as the γ angle increases regardless of the change in the β angle. Typically, the R-Values are much higher for concrete than for asphalt pavement types. Interestingly, the overall shape of the 3D Surface R-Value plots are similar between concrete and asphalt illuminated by the incandescent light source as shown in **Figure 49** and **Figure 51**. Also the overall shape of the 3D Surface R-Value plot is similar between concrete and asphalt specimens illuminated by the LED light source as shown in both **Figure 50** and **Figure 52**. This indicates that the light source is a significant parameter that will impact the R-Value with respect to the γ angle.

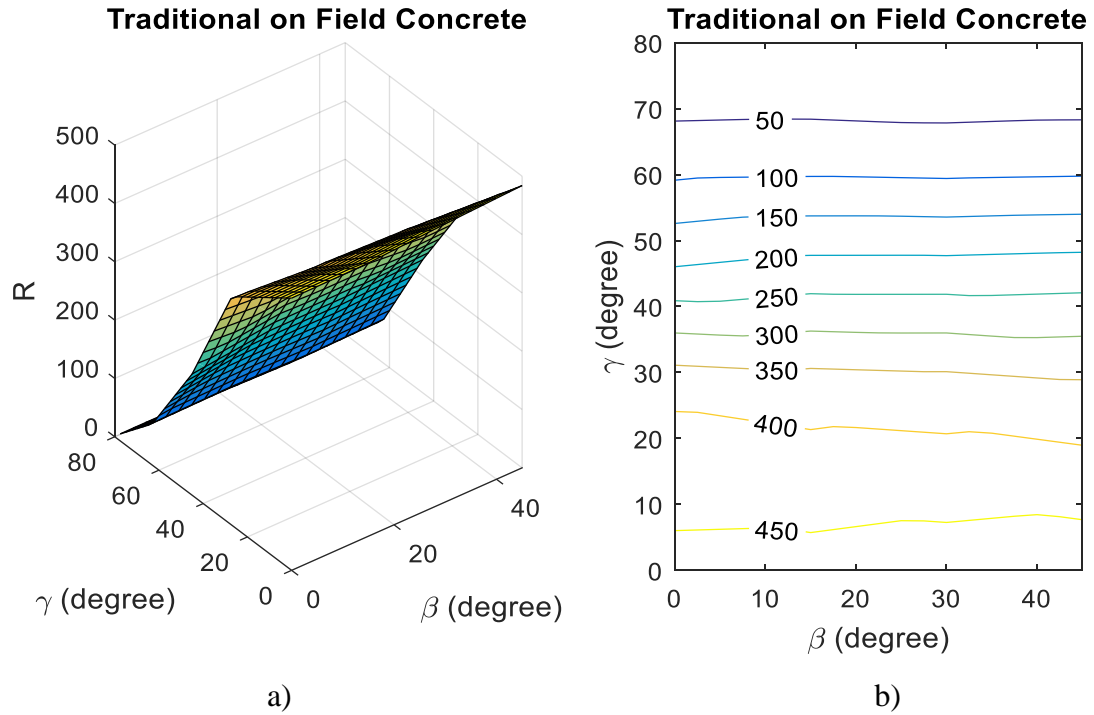


Figure 49. Incandescent R-Value on Field Concrete
a) 3D Surface b) Contour Plot

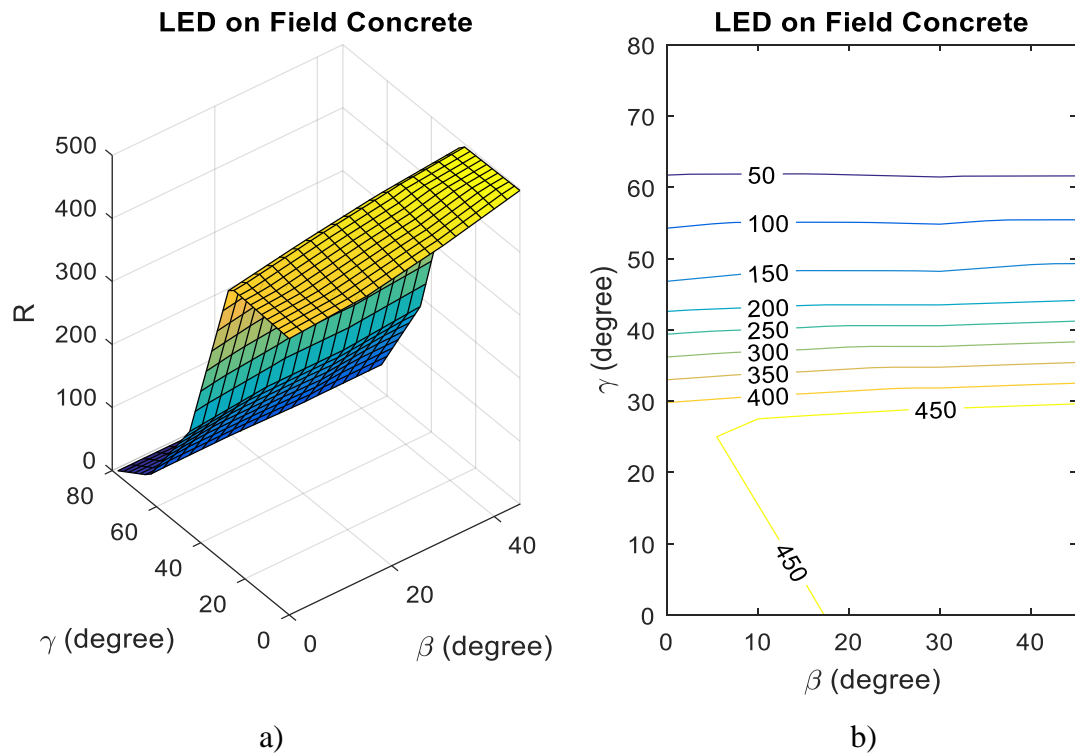


Figure 50. LED R-Value on Field Concrete
a) 3D Surface b) Contour Plot

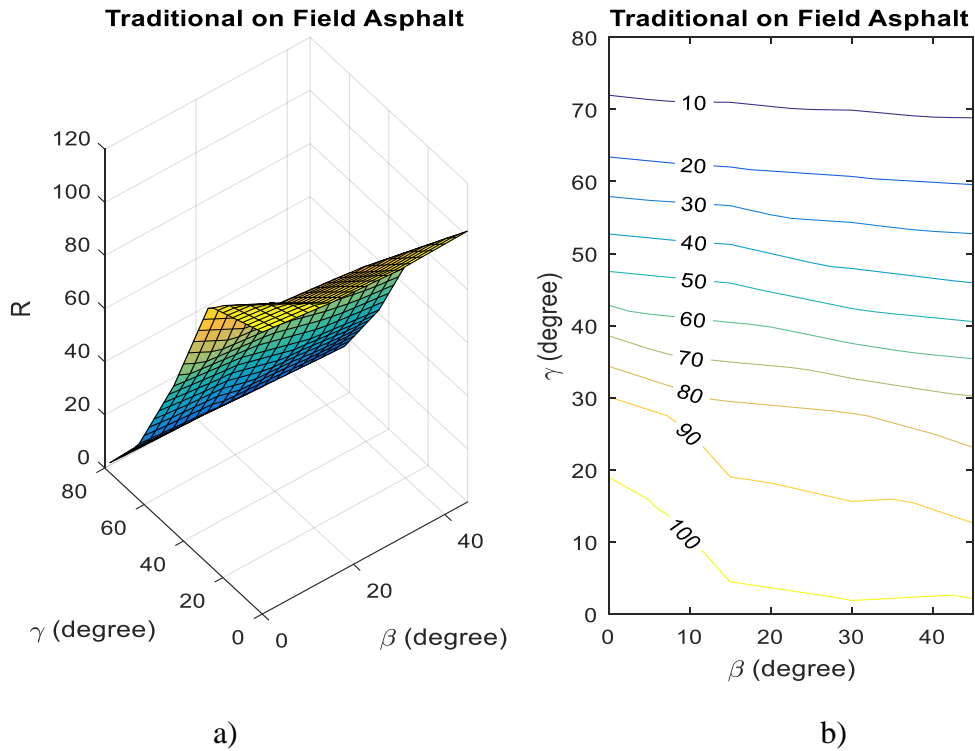


Figure 51. Incandescent R-Value on Field Asphalt
 a) 3D Surface b) Contour Plot

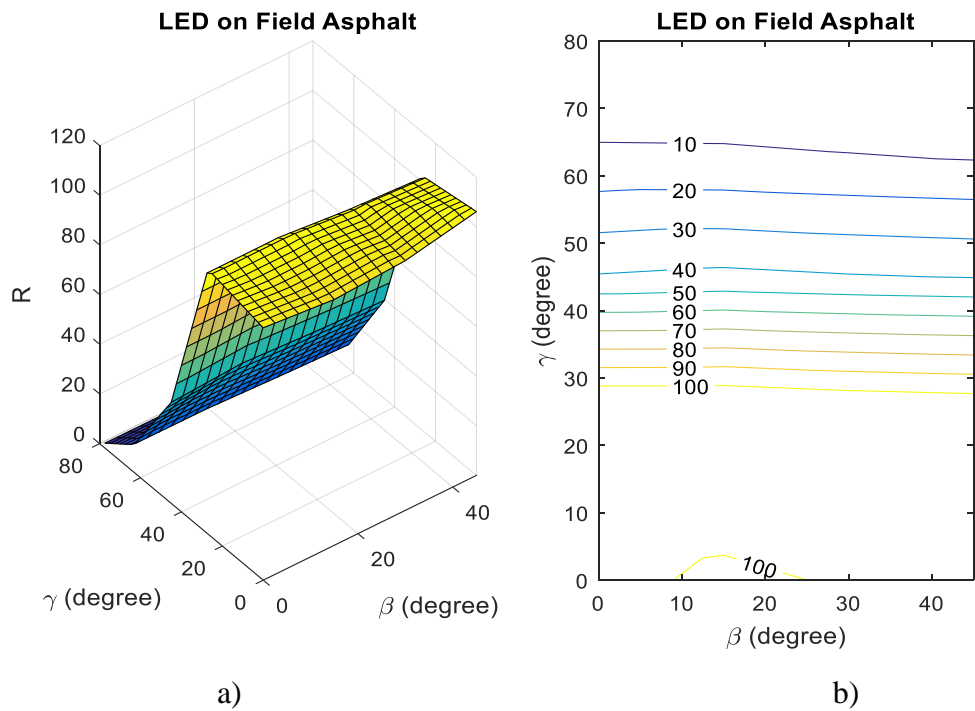


Figure 52. LED R-Value on Field Asphalt
 a) 3D Surface b) Contour Plot

2. R-Values Compared to Original R1 and R3

The following section presents simplified data pulled from the original R-Tables and are compared to the converted R-Values determined from the experimental program. The original R-Tables have more angle combinations than those selected for testing in the experimental program. Therefore, the R-Values at the selected angle combinations were pulled out of the original R-Table in order to make a fair comparison. The utilized selective R-Table values are displayed in simplified tables at the end of the appendix. Only two of the original R-Tables are selected for this comparative analysis. The R1 table represents a concrete surface and R3 table represents a typical asphalt surface. The R2 table is the intermediate table that shares properties resembling concrete and asphalt. The R4 table is not typically used and is intended to represent the very extreme specular cases for asphalt surfaces. The R1 and R3 tables are selected because they are the most commonly used R-Tables in design practice.

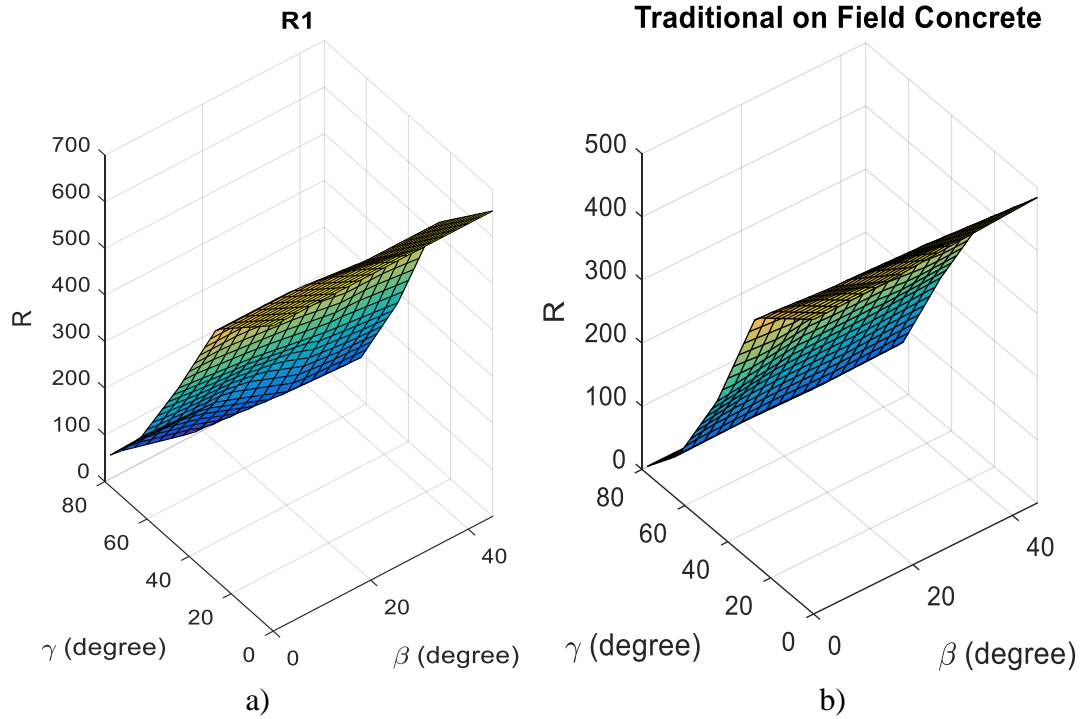


Figure 53. Incandescent Light Comparing R1 (Concrete)
 a) Original R1 b) Equivalent R1

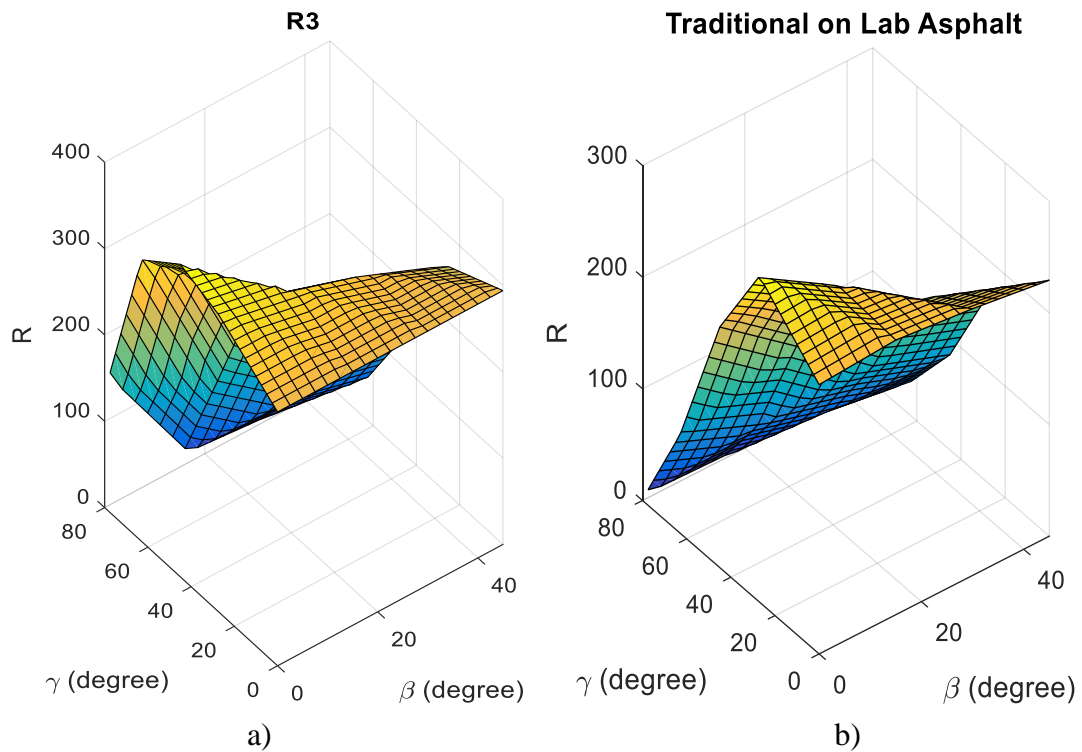


Figure 54. Incandescent Light Comparing R3 (Asphalt)
 a) Original R3 b) Equivalent R3

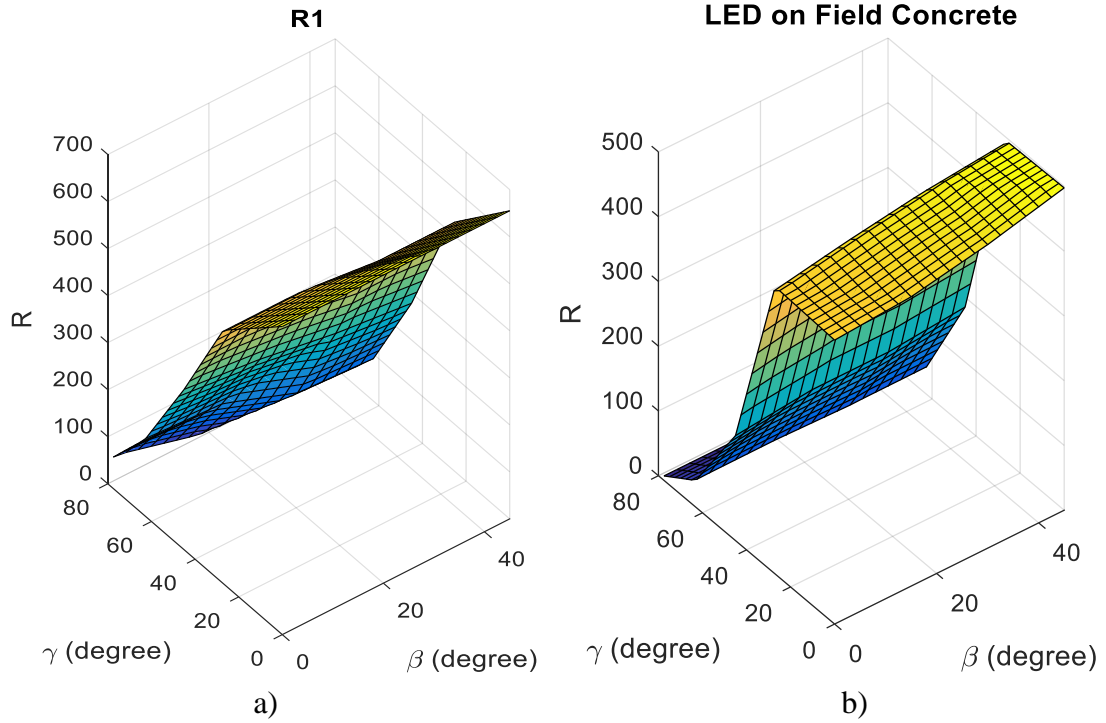


Figure 55. LED Light Comparing R1 (Concrete)

a) Original R1 b) Equivalent R1

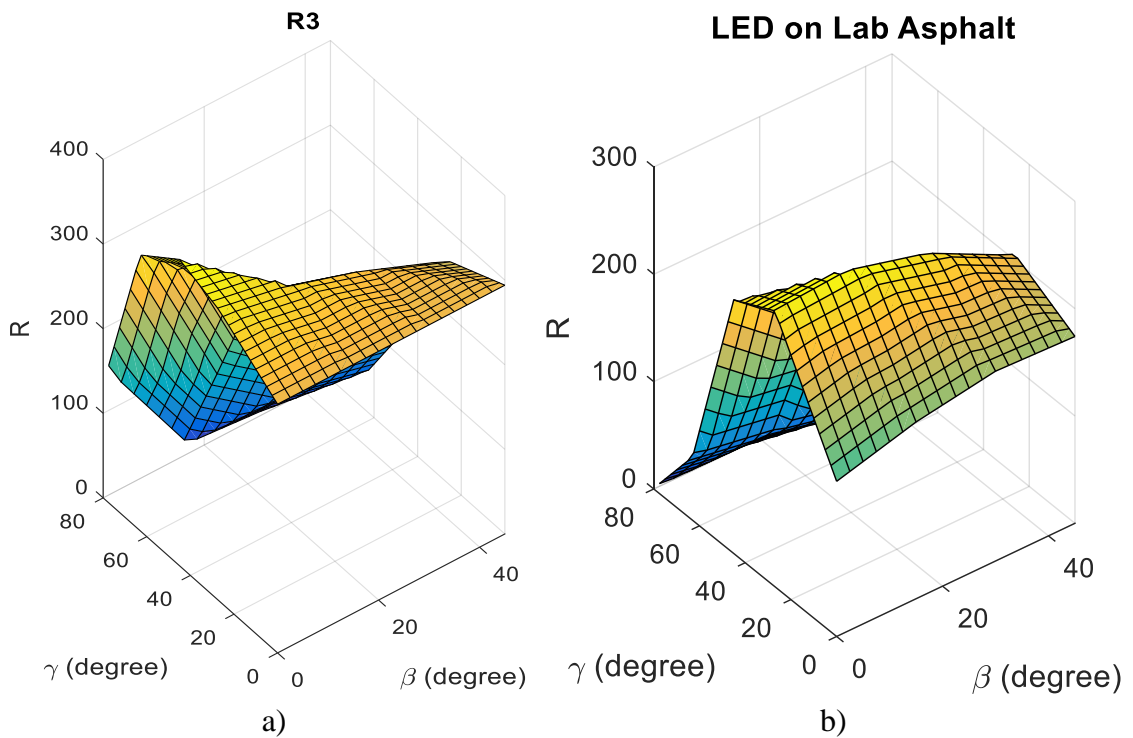


Figure 56. LED Light Comparing R3 (Asphalt)

a) Original R3 b) Equivalent R3

Figure 53 and **Figure 54** both present the R-Value data collected from using a traditional (incandescent) light source. **Figure 53 a)** presents the R1 (concrete) data as it is intended to look. **Figure 53 b)** is the equivalent concrete data collected utilizing the traditional (incandescent) light. Likewise, **Figure 54 a)** presents the R3 (asphalt) data as it is intended to look. **Figure 54 b)** is the equivalent asphalt data collected utilizing the traditional (incandescent) light. Comparing a) and b) in both figures it is very apparent that the two plots have very similar trends.

Figure 55 and **Figure 56** present the same information except for LED lights. The side by side comparison of a) and b) in both figures (asphalt and concrete) clearly shows that LED lights do not produce the same trends as seen with traditional (incandescent) light sources. This is shown by the consistently repeating “spike” in the LED R-Values.

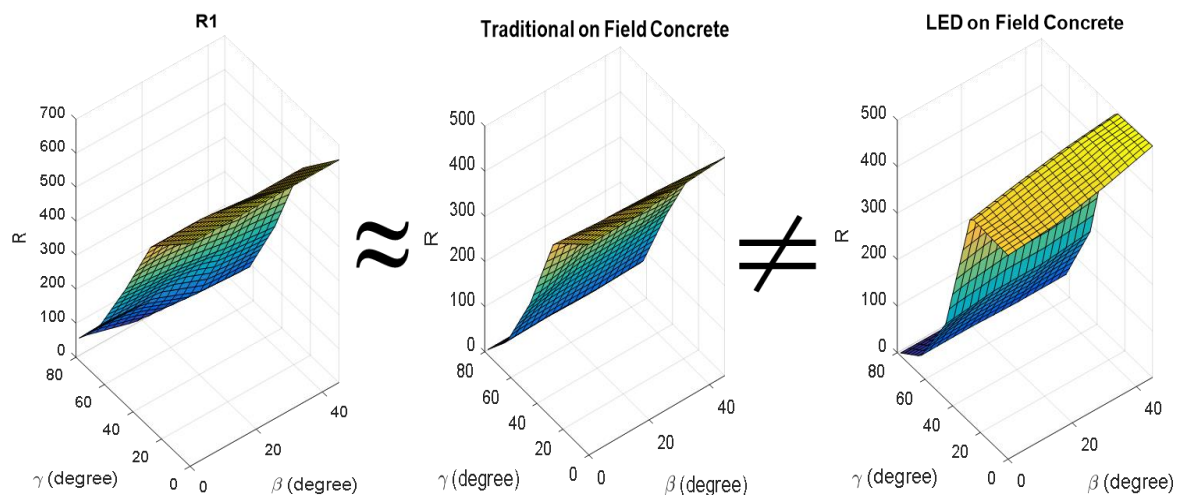


Figure 57. R1 vs. Incandescent vs. LED

Figure 57 indicates R-Values are representative of traditional (incandescent) lights but are not representative of the behavior of LED lights. This indicates that the light reflectivity of concrete and asphalt are not the same with respect to the light source.

3. S1 Values Compared to Original R1, R2, R3, and R4

Table 17. S1 Values of Original R-Tables

Pavement Type	R-Table	(S1)
Concrete	R1	0.25
Asphalt	R2	0.58
	R3	1.11
	R4	1.55

Table 18. S1 Values of Constant Observation Angle

Test Location	Pavement Type	Description	Incandescent (S1)	LED (S1)
Lab ($\alpha = 35^\circ$)	Concrete	w/c = 0.40	0.18	0.24
		w/c = 0.45	0.21	0.25
		w/c = 0.50	0.20	0.33
	Asphalt	Light	0.36	0.41
		Dark	0.26	0.31
Field ($\alpha = 35^\circ$)	Concrete	Specular	0.19	0.25
		Diffused	0.15	0.09
	Asphalt	Dark	0.19	0.11

Table 19. S1 Values of Varied Observation Angles

Light Type	Pavement Type	Description	$\alpha = 15^\circ$ (S1)	$\alpha = 35^\circ$ (S1)
Incandescent	Concrete	Specular	0.39	0.19
		Diffused	0.20	0.15
	Asphalt	Dark	0.32	0.19
LED	Concrete	Specular	0.58	0.25
		Diffused	0.11	0.09
	Asphalt	Dark	0.21	0.11

Table 17 presents all the specularity (S1) values associated with each of the corresponding original R-Tables, as previously defined. It is important to note that the original R-Tables were developed under an observation angle $\alpha = 1^\circ$ and the majority of the experimental test results were developed utilizing an observation angle at $\alpha = 35^\circ$ for lab and field testing and $\alpha = 15^\circ$ for only the field testing.

Table 18 presents all the S1 values calculated from the calculated R-Values. The equation for S1 was previously presented (*Eq.8*) which utilizes the converted R-Values at corresponding angles. For example, the R-Value at $\beta = 0^\circ$ and $\gamma = 63^\circ$ is divided by the R-Value at $\beta = 0^\circ$ and $\gamma = 0^\circ$ angles which are derived from measured luminance values. One of the noticeable conclusions is that S1 was consistently higher with the LED lights than it was with the incandescent lights. This was true for every sample except for the last two rows of field samples.

Table 19 displays the S1 values calculated from only the field tests. The diffused concrete values are bolded in **Table 18** and **Table 19** with the intentions of detailing the critical differences between the two tables. **Table 19** presents both observation angles tested in the field ($\alpha = 15^\circ$ and $\alpha = 35^\circ$) and therefore the columns do not represent the different light sources but instead compare varying observation angles. As observation angles lower the S1 values begin to approach the expected values presented in the original R-Tables. Typically concrete is not very specular but is more of a diffused pavement surface. The specular concrete sample measured in the field is not very representative of typical concrete pavement surfaces. This sample showed the variation of the observation angle is much more influential on specular surfaces (S1=0.58-0.25) than it is on diffused surfaces (S1=0.11-0.09) specifically under the LED light.

4. Specular and Diffused at Varied Observation Angles

Table 20. Specular vs. Diffused at Varied Observation Angles

LIGHT TYPE	SPECULAR VS. DIFFUSED	$\alpha = 15^\circ$ (S1)	$\alpha = 35^\circ$ (S1)
Incandescent	Specular	0.39	0.19
	Diffused	0.20	0.15
LED	Specular	0.58	0.25
	Diffused	0.11	0.09

Table 20 presents the same data as shown previously in **Table 19** but simplified down to the specular and diffused concrete samples. The specular concrete sample tested is a very rare case and is not very representative of a concrete pavement. The previous analysis indicates significant variations between concrete and asphalt with respect to the light source. This variation is influenced by each respective pavements “lightness” (Q_0) and “specularity” (S1). These two concrete samples are selected for analysis with the intention of eliminating the “lightness” (Q_0) influence. Each concrete sample is analyzed assuming similar “lightness” (Q_0) but varied “specularity” (S1). Influence of specularity is demonstrated with respect to the two different observation angles. This comparison is presented in the following Contour Plots.

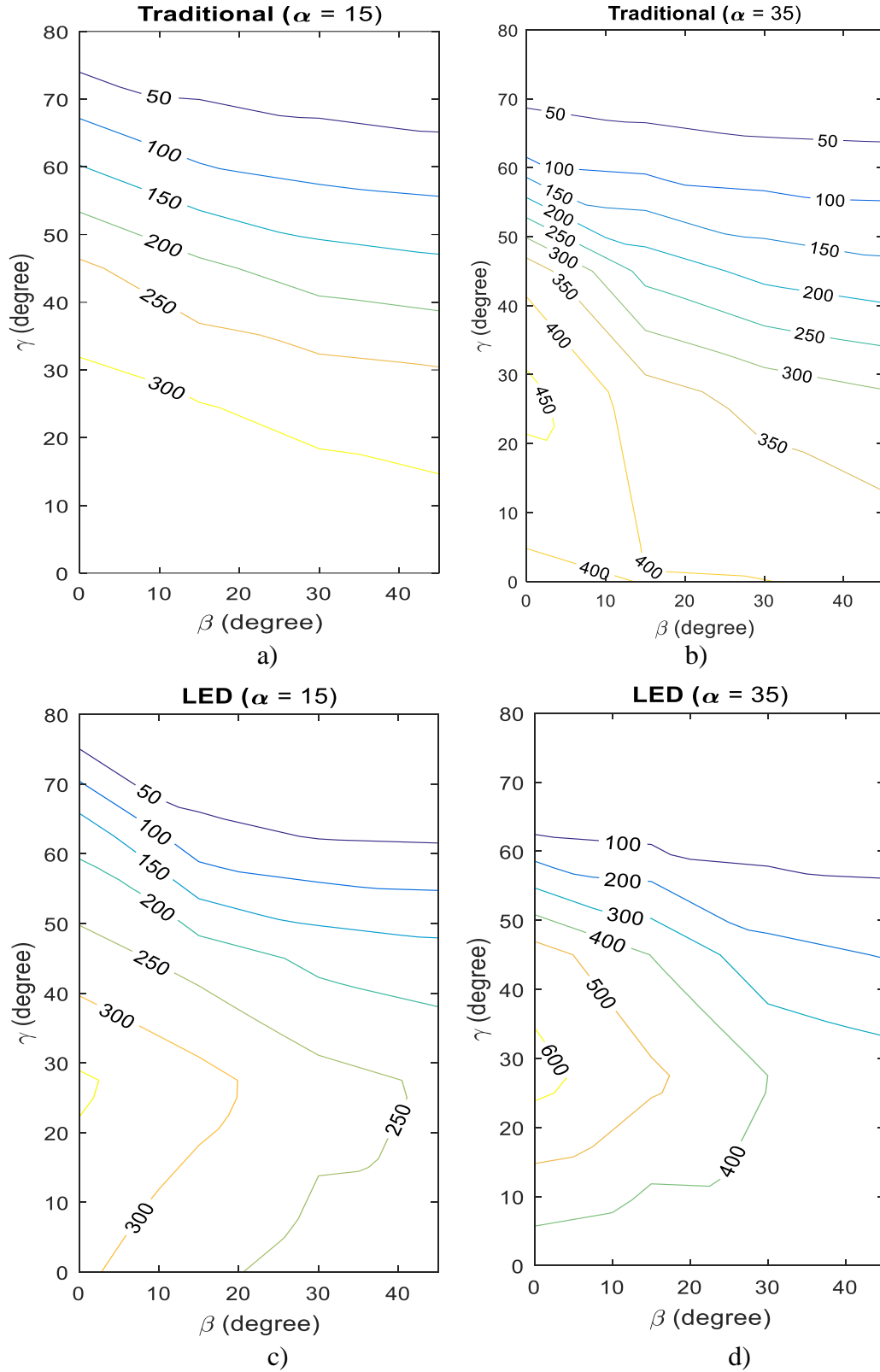


Figure 58. Specular Concrete Contour Plots

a) Incandescent $\alpha = 15^\circ$ b) Incandescent $\alpha = 35^\circ$

c) LED $\alpha = 15^\circ$ d) LED $\alpha = 35^\circ$

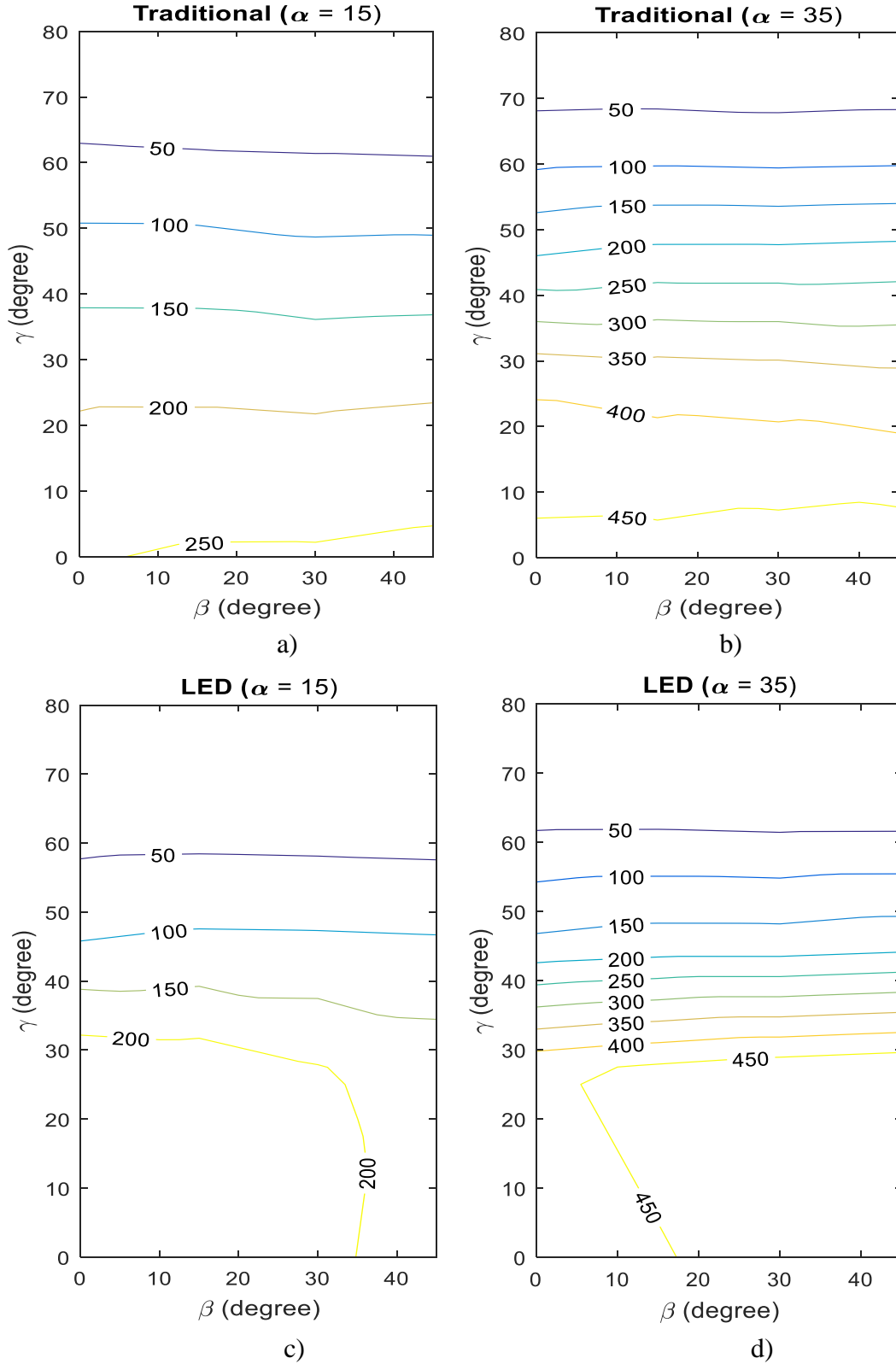


Figure 59. Diffused Concrete Contour Plots
 a) Incandescent $\alpha = 15^\circ$ b) Incandescent $\alpha = 35^\circ$
 c) LED $\alpha = 15^\circ$ d) LED $\alpha = 35^\circ$

Figure 58 presents the specular surface where a) and b) represent the traditional (incandescent) light measured at observation angles of 15° and 35° respectively. This same comparison of the observation angles are presented in c) and d) for the LED light measurements. **Figure 58** indicates that the change in the observation angle influences the decrease in the R-Values with respect to the β and γ angle. This is demonstrated by the amplification of decreasing R-Values in both the β and γ angle axis directions with respect to each of the varied observation angles.

Figure 59 presents the diffused surface where a) and b) represent the traditional (incandescent) light measured at observation angles of 15° and 35° respectively. This same comparison of the observation angles are presented in c) and d) for the LED light measurements. **Figure 59** does not present the same effect as seen in the specular surface. While there still is the same amplifying effect in the decreasing R-Values it only occurs in the γ angle axis direction with respect to the observation angle. This amplified pattern change is exhibited in similar manners regardless of the light source.

Therefore, the previous R-Value comparison indicated the significant influence the light source had on the R-Value data but did not seem to impact the specular analysis. The results indicate that specular behavior is entirely dependent on different surface types (i.e., specular or diffused) but is not influenced by the light source.

V. CONCLUSION AND RECOMMENDATIONS

The experimental program testing consisted of two different types of pavement surfaces (i.e., concrete and asphalt) and two different light sources (i.e., incandescent and LED). The luminance values were measured at varied angles, β and γ , in order to compare the results with the original R-Values used in light design practices. The potential changes of current R-Values are investigated using a goniometer developed for laboratory and field application. The tested laboratory specimens considered concrete with varying w/c ratios (w/c = 0.40, 0.45, and 0.50) and two different apparent asphalt surfaces (Dark and Light). Field tests considered diffused and specular concrete as well as asphalt pavement surface. This closing chapter presents the overall summary of the research outcomes and findings. The initial section will summarize the ultimate conclusion of the analysis results. Lastly, the final section outlines the most logical and feasible recommendations.

A. Conclusion

Concrete exhibited a median luminance value around 12 cd/m^2 compared to the asphalt pavements 4 cd/m^2 median luminance value. These results indicate that regardless of the angular contributions and type of light, concrete is up to 3 times more reflective than asphalt pavements. This conclusion is concurrent with the previous research that states asphalt has become less reflective since the R-Tables were originally developed.

When compared regardless of angular contributions, the two varied light sources appear to have no significant influence on reflectivity. But when angular contributions are considered the true reflective behavior becomes apparent. The incandescent light source exhibited the exact same behavior as defined by the original R-Values but the LED light source did not. There is clearly a different pattern in the data collected using the incandescent light source as compared to the LED light source. Even though both light sources reflect approximately the same amount of average light. This overall light reflected is not distributed in a similar manner. The uneven distribution of reflected light is represented by the amplification (spike) in LED light data with respect to the γ angle.

Even though, different light sources demonstrate significantly different behavior on the same pavements, the behavior of that surface is also influenced by “lightness” (Q_0) and “specularity” (S_1). Therefore, the two concrete surfaces with varied specularity were further investigated to evaluate the pavement interaction with light. The specular concrete demonstrated a decrease in R-Values with respect to changes in both the β and γ angles. The diffused concrete also demonstrated a decrease in R-Values, but with respect to only the changes in the γ angle. Both amplification patterns, caused by the variation in the two observation angles, were exhibited regardless of the light source illuminating the surface. This indicates the change in the γ angle influences the R-Values regardless of pavement characteristics. Whereas, the change in the β angle specifically influences R-Values with respect to surface specularity.

In conclusion, the pavement surface specularity influences the light distribution with respect to the change in the β angle, but the light source influences the distribution of reflected light with respect to the change in the γ angle.

B. Recommendations

The original R-Tables only consider the pavement type as a factor of reflectivity. The original values claim that more specular surfaces will have greater influences on the reduced luminance coefficient as the β angle changes. The original values also state that concrete and asphalt have varying influences on the reduced luminance coefficient as the γ angle changes. The original R-Tables define both of these fundamental patterns with respect to variations in pavement surfaces but completely disregard any influence of different light sources.

Future evaluation studies should be aware that different light sources influence the angular behavior of reflected light. Further research can assume that incandescent lights will behave as expected according to the original R-Tables but the same behavior cannot be assumed for LED light sources. Therefore, further assessment is needed to compare incandescent light sources with other traditional light sources (HPS and others) to determine if they behave in the same angular manner.

In conclusion, incandescent lights can be adequately designed according to the currently accepted design method, but assuming the same design method still applies to LED lights will produce inaccurate calculations. This will lead to incorrect pole spacing, light mounting heights, and required levels of supplied power. Inefficient calculations ultimately result in increased energy consumption and costs. LED lights are by far the most energy efficient light but in order to maximize their efficiency as a light source more research is needed to further evaluate their reflective behavior. If LED lights are designed appropriately they will ultimately provide extremely cost efficient lighting for all roadway and parking lot scenarios.

REFERENCES

- Acuity Brands Lighting (2016). Visual roadway tool. *Acuity Brands Lighting*. <http://www.visual-3d.com/tools/roadway/> (accessed October 1, 2016).
- Adrian, W. and Jobanputra, R. (2005). Influence of pavement reflectance on lighting for parking lots. *Portland Cement Association*, PCA R&D Serial No. 2458: 46.
- B&K Precision Corporation (2016). B&K precision power supply guide. *B&K Precision Corporation*. <http://www.bkprecision.com/support/downloads/power-supply-guide.html> (accessed November 1, 2016).
- Dumont, E., Paumier, J., and Ledoux, V. (2008). Are standard R-tables still representative of road surface photometric characteristics in France? *Proceedings of CIE International Symposium on Road Surface Photometric Characteristics, Measurement Systems and Results*. Torino, Italy, 9 – 10 July 2008: 8.
- Ekrias, A., Ylinen, A., Eloholma, M and Hlonen, L. (2008). Effects of pavement lightness and colour on road lighting performance. *Proceedings of CIE International Symposium on Road Surface Photometric Characteristics: Measurement Systems and Results*. Torino, Italy, 9 – 10 July 2008: 8.
- EPA (2005). Reducing urban heat islands: Compendium of strategies: Cool pavements. *U.S. Environmental Protection Agency's Office of Atmospheric Programs*, <https://www.epa.gov/sites/production/files/2014-06/documents/basicscompendium.pdf> (accessed October 1, 2016).
- Fotios, S., Boyce, P., and Ellis, C. (2006). The effect of pavement material on road lighting performance. *Lighting Journal*, 71(2), 35-40.
- Hassan, M., Elseifi, M., Wakim, J., and El-Rayes, K. (2008). Measurement of pavement surface reflectance for a balloon lighting system. *Journal of Transportation Engineering*, 134(10), 432-437.
- Kelly, G. (2013). Understand color science to maximize success with LEDs – part 4. *LEDs Magazine*: 9.
- Khan, M. H. (1998). *Influence of pavement surface characteristics on light reflectance properties*. Master's Thesis, Texas Tech University, Lubbock, Texas.

- Lutkevich, P., McLean, D. and Cheung, J. (2012). *FHWA Lighting Handbook*. U.S. Dept. of Transportation, Federal Highway Administration, Washington, D.C.: 96.
- PIER Buildings Program (2011). Bi-level LED parking garage luminaires. *California Energy Commission's Public Interest Energy Research Program: 4*. <http://cltc.ucdavis.edu/sites/default/files/files/publication/pier-bilevel-led-parking-garage.pdf> (accessed October 1, 2016).
- Van Bommel, W. (2015). *Road lighting: Fundamentals, technology and application*. Springer International Publishing, Cham, Switzerland: 343.
- Ylinen, A, Poulakka, M. and Halonen, L (2010). Road surface reflection properties and applicability of the R-tables for today's pavement materials in Finland. *Light & Engineering*, 18(1): 78-90.

APPENDIX

MATLAB Data ($\alpha = 35^\circ$)

Name	Light	Material	alpha	beta	gamma	Luminance	R-value
LC-40	Traditional	Concrete	35	0	0	32.2	1073.7
LC-40	Traditional	Concrete	35	0	27	39.0	1033.1
LC-40	Traditional	Concrete	35	0	45	34.9	581.5
LC-40	Traditional	Concrete	35	0	63	28.3	194.7
LC-40	Traditional	Concrete	35	0	79	8.0	9.7
LC-40	Traditional	Concrete	35	15	0	32.9	1095.2
LC-40	Traditional	Concrete	35	15	27	35.7	944.5
LC-40	Traditional	Concrete	35	15	45	26.0	433.4
LC-40	Traditional	Concrete	35	15	63	20.5	140.6
LC-40	Traditional	Concrete	35	15	79	5.6	6.8
LC-40	Traditional	Concrete	35	30	0	33.9	1131.0
LC-40	Traditional	Concrete	35	30	27	33.0	873.4
LC-40	Traditional	Concrete	35	30	45	23.1	385.8
LC-40	Traditional	Concrete	35	30	63	17.5	120.5
LC-40	Traditional	Concrete	35	30	79	4.7	5.7
LC-40	Traditional	Concrete	35	45	0	34.6	1152.8
LC-40	Traditional	Concrete	35	45	27	32.0	847.0
LC-40	Traditional	Concrete	35	45	45	22.5	374.6
LC-40	Traditional	Concrete	35	45	63	17.0	117.0
LC-40	Traditional	Concrete	35	45	79	4.3	5.2
LC-40	LED	Concrete	35	0	0	17.6	586.9
LC-40	LED	Concrete	35	0	27	37.4	989.7
LC-40	LED	Concrete	35	0	45	42.9	715.2
LC-40	LED	Concrete	35	0	63	20.1	138.3
LC-40	LED	Concrete	35	0	79	7.0	8.5
LC-40	LED	Concrete	35	15	0	21.6	721.1
LC-40	LED	Concrete	35	15	27	35.9	949.0
LC-40	LED	Concrete	35	15	45	35.0	583.3
LC-40	LED	Concrete	35	15	63	15.2	104.1
LC-40	LED	Concrete	35	15	79	5.5	6.7
LC-40	LED	Concrete	35	30	0	21.6	720.1
LC-40	LED	Concrete	35	30	27	32.2	851.6
LC-40	LED	Concrete	35	30	45	25.1	417.9

LC-40	LED	Concrete	35	30	63	10.0	68.6
LC-40	LED	Concrete	35	30	79	3.9	4.8
LC-40	LED	Concrete	35	45	0	18.1	603.9
LC-40	LED	Concrete	35	45	27	28.8	762.8
LC-40	LED	Concrete	35	45	45	21.0	350.2
LC-40	LED	Concrete	35	45	63	10.4	71.2
LC-40	LED	Concrete	35	45	79	3.5	4.2
LC-45	Traditional	Concrete	35	0	0	37.7	1257.7
LC-45	Traditional	Concrete	35	0	27	44.2	1169.1
LC-45	Traditional	Concrete	35	0	45	45.0	750.6
LC-45	Traditional	Concrete	35	0	63	38.2	262.2
LC-45	Traditional	Concrete	35	0	79	10.0	12.2
LC-45	Traditional	Concrete	35	15	0	38.5	1284.2
LC-45	Traditional	Concrete	35	15	27	40.3	1065.6
LC-45	Traditional	Concrete	35	15	45	33.1	552.1
LC-45	Traditional	Concrete	35	15	63	25.1	172.6
LC-45	Traditional	Concrete	35	15	79	6.6	8.0
LC-45	Traditional	Concrete	35	30	0	38.9	1296.0
LC-45	Traditional	Concrete	35	30	27	37.1	980.8
LC-45	Traditional	Concrete	35	30	45	25.8	430.6
LC-45	Traditional	Concrete	35	30	63	19.8	135.7
LC-45	Traditional	Concrete	35	30	79	5.0	6.1
LC-45	Traditional	Concrete	35	45	0	39.2	1306.0
LC-45	Traditional	Concrete	35	45	27	34.9	924.3
LC-45	Traditional	Concrete	35	45	45	24.5	407.8
LC-45	Traditional	Concrete	35	45	63	18.4	126.3
LC-45	Traditional	Concrete	35	45	79	4.8	5.8
LC-45	LED	Concrete	35	0	0	23.0	765.6
LC-45	LED	Concrete	35	0	27	42.0	1110.7
LC-45	LED	Concrete	35	0	45	38.5	642.2
LC-45	LED	Concrete	35	0	63	28.3	194.4
LC-45	LED	Concrete	35	0	79	10.1	12.3
LC-45	LED	Concrete	35	15	0	24.9	831.1
LC-45	LED	Concrete	35	15	27	42.0	1112.0
LC-45	LED	Concrete	35	15	45	27.2	453.3
LC-45	LED	Concrete	35	15	63	23.2	159.1
LC-45	LED	Concrete	35	15	79	7.4	9.0
LC-45	LED	Concrete	35	30	0	26.5	883.8
LC-45	LED	Concrete	35	30	27	38.6	1022.4
LC-45	LED	Concrete	35	30	45	16.6	276.6
LC-45	LED	Concrete	35	30	63	14.9	102.2
LC-45	LED	Concrete	35	30	79	4.4	5.3
LC-45	LED	Concrete	35	45	0	24.2	806.2

LC-45	LED	Concrete	35	45	27	36.0	952.0
LC-45	LED	Concrete	35	45	45	20.9	348.9
LC-45	LED	Concrete	35	45	63	10.8	74.3
LC-45	LED	Concrete	35	45	79	3.8	4.6
LC-50	Traditional	Concrete	35	0	0	33.4	1111.7
LC-50	Traditional	Concrete	35	0	27	36.8	972.6
LC-50	Traditional	Concrete	35	0	45	37.5	625.7
LC-50	Traditional	Concrete	35	0	63	31.8	218.4
LC-50	Traditional	Concrete	35	0	79	9.2	11.2
LC-50	Traditional	Concrete	35	15	0	33.7	1124.2
LC-50	Traditional	Concrete	35	15	27	34.2	905.3
LC-50	Traditional	Concrete	35	15	45	29.0	483.7
LC-50	Traditional	Concrete	35	15	63	23.1	158.9
LC-50	Traditional	Concrete	35	15	79	6.7	8.1
LC-50	Traditional	Concrete	35	30	0	34.1	1137.7
LC-50	Traditional	Concrete	35	30	27	30.6	808.4
LC-50	Traditional	Concrete	35	30	45	22.5	374.9
LC-50	Traditional	Concrete	35	30	63	18.5	127.3
LC-50	Traditional	Concrete	35	30	79	5.7	6.9
LC-50	Traditional	Concrete	35	45	0	34.3	1143.8
LC-50	Traditional	Concrete	35	45	27	29.1	769.9
LC-50	Traditional	Concrete	35	45	45	20.6	344.1
LC-50	Traditional	Concrete	35	45	63	17.4	119.2
LC-50	Traditional	Concrete	35	45	79	5.2	6.3
LC-50	LED	Concrete	35	0	0	18.0	600.4
LC-50	LED	Concrete	35	0	27	36.7	970.3
LC-50	LED	Concrete	35	0	45	45.7	762.0
LC-50	LED	Concrete	35	0	63	28.5	195.6
LC-50	LED	Concrete	35	0	79	8.6	10.5
LC-50	LED	Concrete	35	15	0	23.3	777.7
LC-50	LED	Concrete	35	15	27	37.1	980.8
LC-50	LED	Concrete	35	15	45	42.5	707.7
LC-50	LED	Concrete	35	15	63	18.2	124.8
LC-50	LED	Concrete	35	15	79	6.4	7.7
LC-50	LED	Concrete	35	30	0	22.6	752.2
LC-50	LED	Concrete	35	30	27	33.7	892.7
LC-50	LED	Concrete	35	30	45	23.3	388.1
LC-50	LED	Concrete	35	30	63	13.9	95.7
LC-50	LED	Concrete	35	30	79	4.7	5.7
LC-50	LED	Concrete	35	45	0	19.0	634.6
LC-50	LED	Concrete	35	45	27	32.1	850.2
LC-50	LED	Concrete	35	45	45	22.6	376.4
LC-50	LED	Concrete	35	45	63	13.0	89.3

LC-50	LED	Concrete	35	45	79	4.3	5.2
LA-LT	Traditional	Asphalt	35	0	0	7.2	241.1
LA-LT	Traditional	Asphalt	35	0	27	11.0	291.9
LA-LT	Traditional	Asphalt	35	0	45	12.9	215.4
LA-LT	Traditional	Asphalt	35	0	63	12.8	87.9
LA-LT	Traditional	Asphalt	35	0	79	5.1	6.2
LA-LT	Traditional	Asphalt	35	15	0	7.4	245.9
LA-LT	Traditional	Asphalt	35	15	27	9.4	249.9
LA-LT	Traditional	Asphalt	35	15	45	9.8	163.1
LA-LT	Traditional	Asphalt	35	15	63	8.7	59.9
LA-LT	Traditional	Asphalt	35	15	79	3.5	4.2
LA-LT	Traditional	Asphalt	35	30	0	7.2	238.8
LA-LT	Traditional	Asphalt	35	30	27	7.6	200.5
LA-LT	Traditional	Asphalt	35	30	45	6.6	110.2
LA-LT	Traditional	Asphalt	35	30	63	5.9	40.5
LA-LT	Traditional	Asphalt	35	30	79	2.2	2.6
LA-LT	Traditional	Asphalt	35	45	0	6.9	229.3
LA-LT	Traditional	Asphalt	35	45	27	6.5	172.2
LA-LT	Traditional	Asphalt	35	45	45	5.1	85.3
LA-LT	Traditional	Asphalt	35	45	63	4.4	29.9
LA-LT	Traditional	Asphalt	35	45	79	1.6	1.9
LA-LT	LED	Asphalt	35	0	0	4.3	144.5
LA-LT	LED	Asphalt	35	0	27	9.7	256.9
LA-LT	LED	Asphalt	35	0	45	14.2	236.3
LA-LT	LED	Asphalt	35	0	63	8.6	58.9
LA-LT	LED	Asphalt	35	0	79	3.4	4.2
LA-LT	LED	Asphalt	35	15	0	4.9	164.7
LA-LT	LED	Asphalt	35	15	27	9.9	262.3
LA-LT	LED	Asphalt	35	15	45	10.6	177.3
LA-LT	LED	Asphalt	35	15	63	6.7	46.3
LA-LT	LED	Asphalt	35	15	79	3.0	3.6
LA-LT	LED	Asphalt	35	30	0	5.3	176.9
LA-LT	LED	Asphalt	35	30	27	9.2	243.0
LA-LT	LED	Asphalt	35	30	45	6.8	113.3
LA-LT	LED	Asphalt	35	30	63	4.3	29.8
LA-LT	LED	Asphalt	35	30	79	1.8	2.2
LA-LT	LED	Asphalt	35	45	0	5.2	174.0
LA-LT	LED	Asphalt	35	45	27	7.8	206.2
LA-LT	LED	Asphalt	35	45	45	6.2	102.7
LA-LT	LED	Asphalt	35	45	63	3.4	23.5
LA-LT	LED	Asphalt	35	45	79	1.2	1.4
LA-DK	Traditional	Asphalt	35	0	0	3.7	124.9
LA-DK	Traditional	Asphalt	35	0	27	4.0	107.1

LA-DK	Traditional	Asphalt	35	0	45	4.0	66.6
LA-DK	Traditional	Asphalt	35	0	63	4.7	32.2
LA-DK	Traditional	Asphalt	35	0	79	2.0	2.4
LA-DK	Traditional	Asphalt	35	15	0	3.8	126.0
LA-DK	Traditional	Asphalt	35	15	27	4.0	105.8
LA-DK	Traditional	Asphalt	35	15	45	3.9	65.7
LA-DK	Traditional	Asphalt	35	15	63	4.5	30.8
LA-DK	Traditional	Asphalt	35	15	79	1.9	2.3
LA-DK	Traditional	Asphalt	35	30	0	3.8	125.6
LA-DK	Traditional	Asphalt	35	30	27	3.8	100.4
LA-DK	Traditional	Asphalt	35	30	45	3.6	60.2
LA-DK	Traditional	Asphalt	35	30	63	3.9	26.6
LA-DK	Traditional	Asphalt	35	30	79	1.6	1.9
LA-DK	Traditional	Asphalt	35	45	0	3.7	122.4
LA-DK	Traditional	Asphalt	35	45	27	3.6	95.9
LA-DK	Traditional	Asphalt	35	45	45	3.2	53.5
LA-DK	Traditional	Asphalt	35	45	63	3.2	22.2
LA-DK	Traditional	Asphalt	35	45	79	1.3	1.6
LA-DK	LED	Asphalt	35	0	0	2.1	69.4
LA-DK	LED	Asphalt	35	0	27	3.6	94.6
LA-DK	LED	Asphalt	35	0	45	2.0	33.9
LA-DK	LED	Asphalt	35	0	63	3.1	21.6
LA-DK	LED	Asphalt	35	0	79	1.3	1.5
LA-DK	LED	Asphalt	35	15	0	2.3	76.3
LA-DK	LED	Asphalt	35	15	27	3.6	96.5
LA-DK	LED	Asphalt	35	15	45	1.7	27.9
LA-DK	LED	Asphalt	35	15	63	3.1	21.5
LA-DK	LED	Asphalt	35	15	79	1.2	1.4
LA-DK	LED	Asphalt	35	30	0	2.4	80.9
LA-DK	LED	Asphalt	35	30	27	3.7	97.0
LA-DK	LED	Asphalt	35	30	45	2.6	42.6
LA-DK	LED	Asphalt	35	30	63	2.8	19.3
LA-DK	LED	Asphalt	35	30	79	1.0	1.2
LA-DK	LED	Asphalt	35	45	0	2.6	85.2
LA-DK	LED	Asphalt	35	45	27	3.6	94.6
LA-DK	LED	Asphalt	35	45	45	2.3	37.6
LA-DK	LED	Asphalt	35	45	63	2.2	15.3
LA-DK	LED	Asphalt	35	45	79	0.9	1.1
FC-SP	Traditional	Concrete	35	0	0	11.6	385.7
FC-SP	Traditional	Concrete	35	0	27	17.7	467.1
FC-SP	Traditional	Concrete	35	0	45	22.9	382.3
FC-SP	Traditional	Concrete	35	0	63	10.8	74.0
FC-SP	Traditional	Concrete	35	0	79	4.8	5.9

FC-SP	Traditional	Concrete	35	15	0	12.1	401.7
FC-SP	Traditional	Concrete	35	15	27	14.1	372.9
FC-SP	Traditional	Concrete	35	15	45	14.0	233.2
FC-SP	Traditional	Concrete	35	15	63	9.1	62.8
FC-SP	Traditional	Concrete	35	15	79	3.8	4.6
FC-SP	Traditional	Concrete	35	30	0	12.0	400.7
FC-SP	Traditional	Concrete	35	30	27	12.6	333.2
FC-SP	Traditional	Concrete	35	30	45	11.1	184.2
FC-SP	Traditional	Concrete	35	30	63	7.9	54.0
FC-SP	Traditional	Concrete	35	30	79	3.3	4.0
FC-SP	Traditional	Concrete	35	45	0	11.7	391.0
FC-SP	Traditional	Concrete	35	45	27	11.6	306.7
FC-SP	Traditional	Concrete	35	45	45	9.8	163.6
FC-SP	Traditional	Concrete	35	45	63	7.5	51.4
FC-SP	Traditional	Concrete	35	45	79	3.0	3.7
FC-SP	LED	Concrete	35	0	0	10.1	337.0
FC-SP	LED	Concrete	35	0	27	24.0	635.1
FC-SP	LED	Concrete	35	0	45	33.0	550.0
FC-SP	LED	Concrete	35	0	63	12.4	85.5
FC-SP	LED	Concrete	35	0	79	2.0	2.4
FC-SP	LED	Concrete	35	15	0	9.2	305.0
FC-SP	LED	Concrete	35	15	27	19.7	521.9
FC-SP	LED	Concrete	35	15	45	23.9	398.2
FC-SP	LED	Concrete	35	15	63	9.1	62.4
FC-SP	LED	Concrete	35	15	79	1.5	1.8
FC-SP	LED	Concrete	35	30	0	9.3	310.6
FC-SP	LED	Concrete	35	30	27	15.3	404.6
FC-SP	LED	Concrete	35	30	45	13.9	231.8
FC-SP	LED	Concrete	35	30	63	6.8	47.0
FC-SP	LED	Concrete	35	30	79	1.4	1.7
FC-SP	LED	Concrete	35	45	0	9.6	318.5
FC-SP	LED	Concrete	35	45	27	13.4	355.1
FC-SP	LED	Concrete	35	45	45	11.7	195.3
FC-SP	LED	Concrete	35	45	63	5.9	40.5
FC-SP	LED	Concrete	35	45	79	1.4	1.7
FC-DF	Traditional	Concrete	35	0	0	14.0	466.7
FC-DF	Traditional	Concrete	35	0	27	14.8	391.9
FC-DF	Traditional	Concrete	35	0	45	12.5	207.8
FC-DF	Traditional	Concrete	35	0	63	10.3	70.6
FC-DF	Traditional	Concrete	35	0	79	5.0	6.0
FC-DF	Traditional	Concrete	35	15	0	14.1	468.3
FC-DF	Traditional	Concrete	35	15	27	14.4	381.9
FC-DF	Traditional	Concrete	35	15	45	13.4	223.0

FC-DF	Traditional	Concrete	35	15	63	10.6	72.5
FC-DF	Traditional	Concrete	35	15	79	4.7	5.7
FC-DF	Traditional	Concrete	35	30	0	14.3	477.0
FC-DF	Traditional	Concrete	35	30	27	14.2	376.6
FC-DF	Traditional	Concrete	35	30	45	13.4	223.2
FC-DF	Traditional	Concrete	35	30	63	10.1	69.3
FC-DF	Traditional	Concrete	35	30	79	4.5	5.4
FC-DF	Traditional	Concrete	35	45	0	14.5	484.0
FC-DF	Traditional	Concrete	35	45	27	13.8	364.4
FC-DF	Traditional	Concrete	35	45	45	13.7	227.8
FC-DF	Traditional	Concrete	35	45	63	10.5	71.9
FC-DF	Traditional	Concrete	35	45	79	4.7	5.7
FC-DF	LED	Concrete	35	0	0	13.2	438.3
FC-DF	LED	Concrete	35	0	27	16.8	443.5
FC-DF	LED	Concrete	35	0	45	9.7	162.1
FC-DF	LED	Concrete	35	0	63	6.0	41.3
FC-DF	LED	Concrete	35	0	79	2.7	3.2
FC-DF	LED	Concrete	35	15	0	13.4	446.7
FC-DF	LED	Concrete	35	15	27	17.6	465.0
FC-DF	LED	Concrete	35	15	45	10.5	174.3
FC-DF	LED	Concrete	35	15	63	6.1	41.7
FC-DF	LED	Concrete	35	15	79	2.6	3.2
FC-DF	LED	Concrete	35	30	0	14.1	468.7
FC-DF	LED	Concrete	35	30	27	18.3	483.0
FC-DF	LED	Concrete	35	30	45	10.5	174.2
FC-DF	LED	Concrete	35	30	63	5.6	38.2
FC-DF	LED	Concrete	35	30	79	2.6	3.1
FC-DF	LED	Concrete	35	45	0	14.9	497.7
FC-DF	LED	Concrete	35	45	27	18.7	494.9
FC-DF	LED	Concrete	35	45	45	11.1	184.8
FC-DF	LED	Concrete	35	45	63	5.6	38.5
FC-DF	LED	Concrete	35	45	79	2.3	2.8
FA-DK	Traditional	Asphalt	35	0	0	3.2	106.1
FA-DK	Traditional	Asphalt	35	0	27	3.7	97.4
FA-DK	Traditional	Asphalt	35	0	45	3.3	54.9
FA-DK	Traditional	Asphalt	35	0	63	2.9	20.2
FA-DK	Traditional	Asphalt	35	0	79	1.6	2.0
FA-DK	Traditional	Asphalt	35	15	0	3.1	103.1
FA-DK	Traditional	Asphalt	35	15	27	3.2	84.5
FA-DK	Traditional	Asphalt	35	15	45	3.1	51.7
FA-DK	Traditional	Asphalt	35	15	63	2.6	18.2
FA-DK	Traditional	Asphalt	35	15	79	1.5	1.8
FA-DK	Traditional	Asphalt	35	30	0	3.0	101.4

FA-DK	Traditional	Asphalt	35	30	27	3.1	81.7
FA-DK	Traditional	Asphalt	35	30	45	2.7	44.6
FA-DK	Traditional	Asphalt	35	30	63	2.4	16.4
FA-DK	Traditional	Asphalt	35	30	79	1.3	1.5
FA-DK	Traditional	Asphalt	35	45	0	3.1	102.0
FA-DK	Traditional	Asphalt	35	45	27	2.9	76.3
FA-DK	Traditional	Asphalt	35	45	45	2.5	41.4
FA-DK	Traditional	Asphalt	35	45	63	2.2	14.9
FA-DK	Traditional	Asphalt	35	45	79	1.1	1.4
FA-DK	LED	Asphalt	35	0	0	3.0	101.6
FA-DK	LED	Asphalt	35	0	27	4.0	106.6
FA-DK	LED	Asphalt	35	0	45	2.4	40.7
FA-DK	LED	Asphalt	35	0	63	1.6	11.2
FA-DK	LED	Asphalt	35	0	79	0.8	0.9
FA-DK	LED	Asphalt	35	15	0	3.0	98.9
FA-DK	LED	Asphalt	35	15	27	4.0	106.7
FA-DK	LED	Asphalt	35	15	45	2.5	42.4
FA-DK	LED	Asphalt	35	15	63	1.6	11.1
FA-DK	LED	Asphalt	35	15	79	0.7	0.9
FA-DK	LED	Asphalt	35	30	0	3.0	100.5
FA-DK	LED	Asphalt	35	30	27	3.9	104.0
FA-DK	LED	Asphalt	35	30	45	2.4	40.7
FA-DK	LED	Asphalt	35	30	63	1.4	9.9
FA-DK	LED	Asphalt	35	30	79	0.7	0.8
FA-DK	LED	Asphalt	35	45	0	3.2	106.2
FA-DK	LED	Asphalt	35	45	27	3.9	102.3
FA-DK	LED	Asphalt	35	45	45	2.4	39.6
FA-DK	LED	Asphalt	35	45	63	1.3	8.8
FA-DK	LED	Asphalt	35	45	79	0.6	0.8

MATLAB Data ($\alpha = 15^\circ$)

Name	Light	Material	alpha	beta	gamma	Luminance	R-value
FC-SP	Traditional	Concrete	15	0	0	9.9	331.5
FC-SP	Traditional	Concrete	15	0	27	11.9	314.9
FC-SP	Traditional	Concrete	15	0	45	15.6	259.9
FC-SP	Traditional	Concrete	15	0	63	19.0	130.2
FC-SP	Traditional	Concrete	15	0	79	10.9	13.3
FC-SP	Traditional	Concrete	15	15	0	10.3	342.7
FC-SP	Traditional	Concrete	15	15	27	11.2	297.1
FC-SP	Traditional	Concrete	15	15	45	12.7	211.3
FC-SP	Traditional	Concrete	15	15	63	12.0	82.5
FC-SP	Traditional	Concrete	15	15	79	6.3	7.6
FC-SP	Traditional	Concrete	15	30	0	10.2	339.9
FC-SP	Traditional	Concrete	15	30	27	10.6	281.2
FC-SP	Traditional	Concrete	15	30	45	10.6	176.2
FC-SP	Traditional	Concrete	15	30	63	9.6	65.7
FC-SP	Traditional	Concrete	15	30	79	4.6	5.6
FC-SP	Traditional	Concrete	15	45	0	10.0	334.7
FC-SP	Traditional	Concrete	15	45	27	10.2	270.8
FC-SP	Traditional	Concrete	15	45	45	9.7	162.3
FC-SP	Traditional	Concrete	15	45	63	8.3	57.0
FC-SP	Traditional	Concrete	15	45	79	3.9	4.7
FC-SP	LED	Concrete	15	0	0	9.3	308.8
FC-SP	LED	Concrete	15	0	27	13.6	358.9
FC-SP	LED	Concrete	15	0	45	16.5	275.0
FC-SP	LED	Concrete	15	0	63	26.3	180.5
FC-SP	LED	Concrete	15	0	79	6.3	7.7
FC-SP	LED	Concrete	15	15	0	7.8	261.3
FC-SP	LED	Concrete	15	15	27	12.0	318.8
FC-SP	LED	Concrete	15	15	45	13.8	230.7
FC-SP	LED	Concrete	15	15	63	8.9	61.0
FC-SP	LED	Concrete	15	15	79	2.1	2.6
FC-SP	LED	Concrete	15	30	0	6.9	230.9
FC-SP	LED	Concrete	15	30	27	10.1	268.3
FC-SP	LED	Concrete	15	30	45	11.3	187.8
FC-SP	LED	Concrete	15	30	63	6.3	43.2
FC-SP	LED	Concrete	15	30	79	1.3	1.6
FC-SP	LED	Concrete	15	45	0	6.8	228.2
FC-SP	LED	Concrete	15	45	27	9.3	245.2
FC-SP	LED	Concrete	15	45	45	10.3	171.6
FC-SP	LED	Concrete	15	45	63	5.7	39.4
FC-SP	LED	Concrete	15	45	79	1.1	1.3

FC-DF	Traditional	Concrete	15	0	0	7.4	246.6
FC-DF	Traditional	Concrete	15	0	27	7.2	189.9
FC-DF	Traditional	Concrete	15	0	45	7.4	124.1
FC-DF	Traditional	Concrete	15	0	63	7.2	49.3
FC-DF	Traditional	Concrete	15	0	79	3.9	4.8
FC-DF	Traditional	Concrete	15	15	0	7.7	255.5
FC-DF	Traditional	Concrete	15	15	27	7.2	189.7
FC-DF	Traditional	Concrete	15	15	45	7.4	123.7
FC-DF	Traditional	Concrete	15	15	63	6.7	45.8
FC-DF	Traditional	Concrete	15	15	79	3.4	4.1
FC-DF	Traditional	Concrete	15	30	0	7.7	255.7
FC-DF	Traditional	Concrete	15	30	27	7.1	186.6
FC-DF	Traditional	Concrete	15	30	45	6.9	114.5
FC-DF	Traditional	Concrete	15	30	63	6.4	43.7
FC-DF	Traditional	Concrete	15	30	79	2.7	3.3
FC-DF	Traditional	Concrete	15	45	0	7.9	262.6
FC-DF	Traditional	Concrete	15	45	27	7.2	190.5
FC-DF	Traditional	Concrete	15	45	45	7.0	116.5
FC-DF	Traditional	Concrete	15	45	63	6.1	41.6
FC-DF	Traditional	Concrete	15	45	79	2.6	3.1
FC-DF	LED	Concrete	15	0	0	7.3	244.2
FC-DF	LED	Concrete	15	0	27	9.0	238.9
FC-DF	LED	Concrete	15	0	45	6.2	103.4
FC-DF	LED	Concrete	15	0	63	4.1	27.8
FC-DF	LED	Concrete	15	0	79	1.6	1.9
FC-DF	LED	Concrete	15	15	0	6.8	226.3
FC-DF	LED	Concrete	15	15	27	8.7	231.3
FC-DF	LED	Concrete	15	15	45	6.7	111.8
FC-DF	LED	Concrete	15	15	63	4.2	29.0
FC-DF	LED	Concrete	15	15	79	1.4	1.7
FC-DF	LED	Concrete	15	30	0	6.1	202.8
FC-DF	LED	Concrete	15	30	27	7.7	204.6
FC-DF	LED	Concrete	15	30	45	6.6	110.8
FC-DF	LED	Concrete	15	30	63	4.0	27.4
FC-DF	LED	Concrete	15	30	79	1.1	1.3
FC-DF	LED	Concrete	15	45	0	5.8	194.1
FC-DF	LED	Concrete	15	45	27	6.8	179.8
FC-DF	LED	Concrete	15	45	45	6.5	107.8
FC-DF	LED	Concrete	15	45	63	3.6	25.1
FC-DF	LED	Concrete	15	45	79	0.9	1.1
FA-DK	Traditional	Asphalt	15	0	0	2.7	91.5
FA-DK	Traditional	Asphalt	15	0	27	3.2	84.3
FA-DK	Traditional	Asphalt	15	0	45	4.2	69.3

FA-DK	Traditional	Asphalt	15	0	63	4.3	29.5
FA-DK	Traditional	Asphalt	15	0	79	2.9	3.5
FA-DK	Traditional	Asphalt	15	15	0	2.7	91.5
FA-DK	Traditional	Asphalt	15	15	27	3.0	79.4
FA-DK	Traditional	Asphalt	15	15	45	3.6	59.4
FA-DK	Traditional	Asphalt	15	15	63	3.6	24.8
FA-DK	Traditional	Asphalt	15	15	79	1.9	2.3
FA-DK	Traditional	Asphalt	15	30	0	2.7	90.7
FA-DK	Traditional	Asphalt	15	30	27	2.9	75.8
FA-DK	Traditional	Asphalt	15	30	45	2.9	48.3
FA-DK	Traditional	Asphalt	15	30	63	2.7	18.6
FA-DK	Traditional	Asphalt	15	30	79	1.4	1.7
FA-DK	Traditional	Asphalt	15	45	0	2.7	91.6
FA-DK	Traditional	Asphalt	15	45	27	2.8	73.4
FA-DK	Traditional	Asphalt	15	45	45	2.6	42.7
FA-DK	Traditional	Asphalt	15	45	63	2.3	15.5
FA-DK	Traditional	Asphalt	15	45	79	1.2	1.5
FA-DK	LED	Asphalt	15	0	0	2.2	74.9
FA-DK	LED	Asphalt	15	0	27	3.3	87.8
FA-DK	LED	Asphalt	15	0	45	3.1	52.0
FA-DK	LED	Asphalt	15	0	63	2.3	16.1
FA-DK	LED	Asphalt	15	0	79	1.1	1.4
FA-DK	LED	Asphalt	15	15	0	1.9	64.2
FA-DK	LED	Asphalt	15	15	27	2.8	74.8
FA-DK	LED	Asphalt	15	15	45	3.1	51.4
FA-DK	LED	Asphalt	15	15	63	2.1	14.2
FA-DK	LED	Asphalt	15	15	79	0.8	0.9
FA-DK	LED	Asphalt	15	30	0	1.7	57.3
FA-DK	LED	Asphalt	15	30	27	2.4	64.5
FA-DK	LED	Asphalt	15	30	45	2.8	46.2
FA-DK	LED	Asphalt	15	30	63	1.7	11.6
FA-DK	LED	Asphalt	15	30	79	0.6	0.7
FA-DK	LED	Asphalt	15	45	0	1.6	53.1
FA-DK	LED	Asphalt	15	45	27	1.9	51.6
FA-DK	LED	Asphalt	15	45	45	2.4	40.5
FA-DK	LED	Asphalt	15	45	63	1.4	9.7
FA-DK	LED	Asphalt	15	45	79	0.4	0.5

Original R-Table Data ($\alpha = 1^\circ$)

Name	Light	Material	alpha	beta	gamma	Luminance	R-value
R1	Traditional	Concrete	1	0	0	0	655
R1	Traditional	Concrete	1	0	27	0	539
R1	Traditional	Concrete	1	0	45	0	341
R1	Traditional	Concrete	1	0	63	0	162
R1	Traditional	Concrete	1	0	79	0	57
R1	Traditional	Concrete	1	15	0	0	655
R1	Traditional	Concrete	1	15	27	0	539
R1	Traditional	Concrete	1	15	45	0	323
R1	Traditional	Concrete	1	15	63	0	153
R1	Traditional	Concrete	1	15	79	0	14
R1	Traditional	Concrete	1	30	0	0	655
R1	Traditional	Concrete	1	30	27	0	521
R1	Traditional	Concrete	1	30	45	0	296
R1	Traditional	Concrete	1	30	63	0	94
R1	Traditional	Concrete	1	30	79	0	9
R1	Traditional	Concrete	1	45	0	0	655
R1	Traditional	Concrete	1	45	27	0	521
R1	Traditional	Concrete	1	45	45	0	278
R1	Traditional	Concrete	1	45	63	0	85
R1	Traditional	Concrete	1	45	79	0	8.7
R2	Traditional	Asphalt	1	0	0	0	390
R2	Traditional	Asphalt	1	0	27	0	411
R2	Traditional	Asphalt	1	0	45	0	335
R2	Traditional	Asphalt	1	0	63	0	227
R2	Traditional	Asphalt	1	0	79	0	106
R2	Traditional	Asphalt	1	15	0	0	390
R2	Traditional	Asphalt	1	15	27	0	403
R2	Traditional	Asphalt	1	15	45	0	292
R2	Traditional	Asphalt	1	15	63	0	117
R2	Traditional	Asphalt	1	15	79	0	8.2
R2	Traditional	Asphalt	1	30	0	0	390
R2	Traditional	Asphalt	1	30	27	0	379
R2	Traditional	Asphalt	1	30	45	0	238
R2	Traditional	Asphalt	1	30	63	0	67
R2	Traditional	Asphalt	1	30	79	0	5
R2	Traditional	Asphalt	1	45	0	0	390
R2	Traditional	Asphalt	1	45	27	0	325
R2	Traditional	Asphalt	1	45	45	0	173
R2	Traditional	Asphalt	1	45	63	0	45
R2	Traditional	Asphalt	1	45	79	0	4.5
R3	Traditional	Asphalt	1	0	0	0	294
R3	Traditional	Asphalt	1	0	27	0	344

R3	Traditional	Asphalt	1	0	45	0	362
R3	Traditional	Asphalt	1	0	63	0	326
R3	Traditional	Asphalt	1	0	79	0	145
R3	Traditional	Asphalt	1	15	0	0	294
R3	Traditional	Asphalt	1	15	27	0	326
R3	Traditional	Asphalt	1	15	45	0	276
R3	Traditional	Asphalt	1	15	63	0	136
R3	Traditional	Asphalt	1	15	79	0	16
R3	Traditional	Asphalt	1	30	0	0	294
R3	Traditional	Asphalt	1	30	27	0	298
R3	Traditional	Asphalt	1	30	45	0	204
R3	Traditional	Asphalt	1	30	63	0	71
R3	Traditional	Asphalt	1	30	79	0	8.2
R3	Traditional	Asphalt	1	45	0	0	294
R3	Traditional	Asphalt	1	45	27	0	262
R3	Traditional	Asphalt	1	45	45	0	140
R3	Traditional	Asphalt	1	45	63	0	48
R3	Traditional	Asphalt	1	45	79	0	6.1
R4	Traditional	Asphalt	1	0	0	0	264
R4	Traditional	Asphalt	1	0	27	0	330
R4	Traditional	Asphalt	1	0	45	0	396
R4	Traditional	Asphalt	1	0	63	0	409
R4	Traditional	Asphalt	1	0	79	0	277
R4	Traditional	Asphalt	1	15	0	0	264
R4	Traditional	Asphalt	1	15	27	0	330
R4	Traditional	Asphalt	1	15	45	0	290
R4	Traditional	Asphalt	1	15	63	0	145
R4	Traditional	Asphalt	1	15	79	0	13
R4	Traditional	Asphalt	1	30	0	0	264
R4	Traditional	Asphalt	1	30	27	0	284
R4	Traditional	Asphalt	1	30	45	0	198
R4	Traditional	Asphalt	1	30	63	0	71
R4	Traditional	Asphalt	1	30	79	0	6.3
R4	Traditional	Asphalt	1	45	0	0	264
R4	Traditional	Asphalt	1	45	27	0	251
R4	Traditional	Asphalt	1	45	45	0	145
R4	Traditional	Asphalt	1	45	63	0	45
R4	Traditional	Asphalt	1	45	79	0	5

Simplified R-Tables

R1-Table

γ°	$\beta = 0^\circ$	$\beta = 15^\circ$	$\beta = 30^\circ$	$\beta = 45^\circ$
0°	655	655	655	655
27°	539	539	521	521
45°	341	323	296	278
63°	162	153	94	85
79°	57	14	9	8.7

R2-Table

γ°	$\beta = 0^\circ$	$\beta = 15^\circ$	$\beta = 30^\circ$	$\beta = 45^\circ$
0°	390	390	390	390
27°	411	403	379	325
45°	335	292	238	173
63°	227	117	67	45
79°	106	8.2	5	4.5

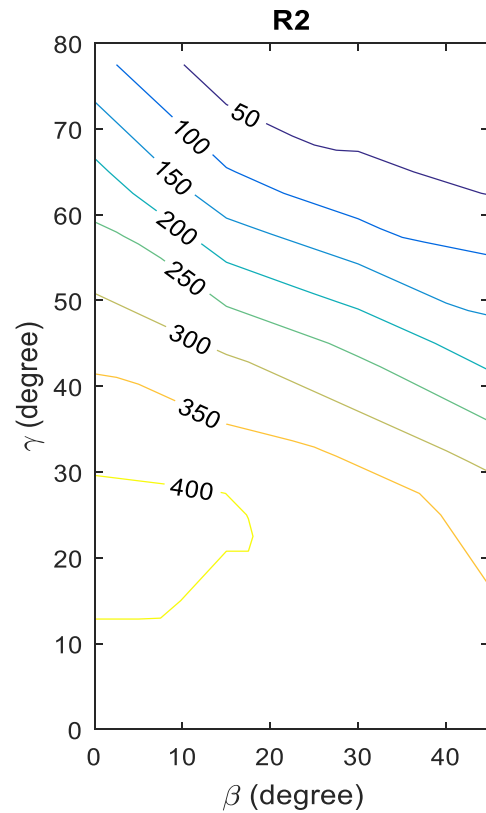
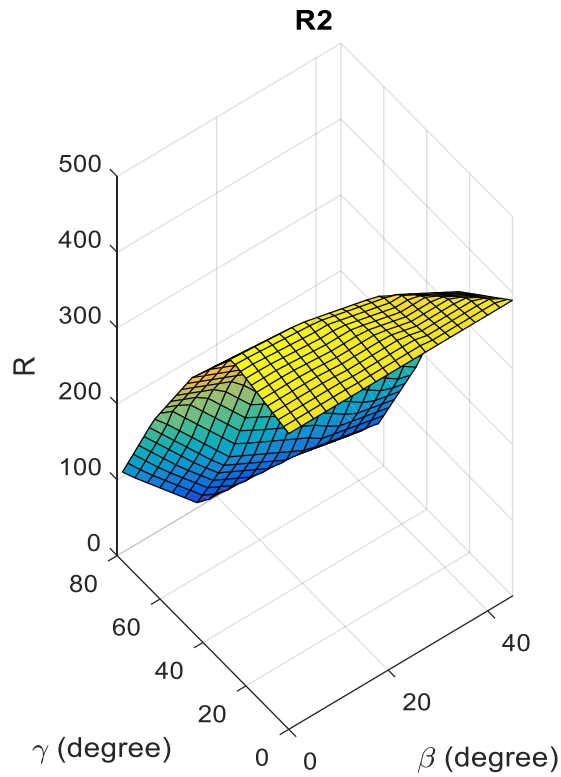
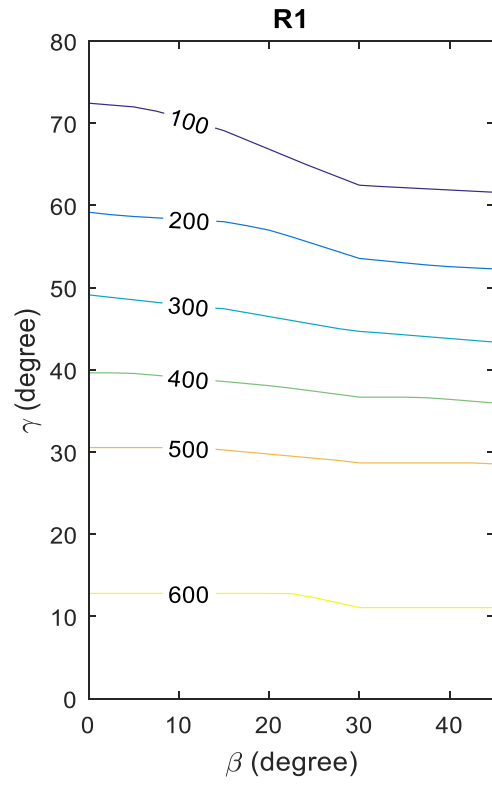
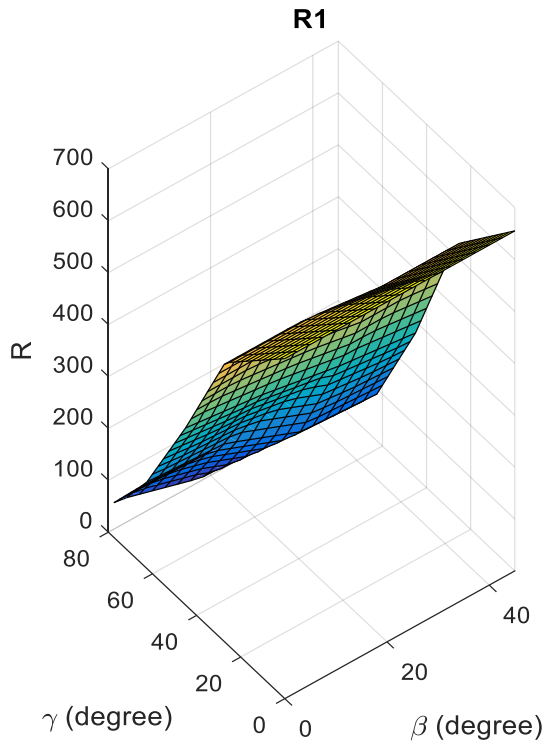
R3-Table

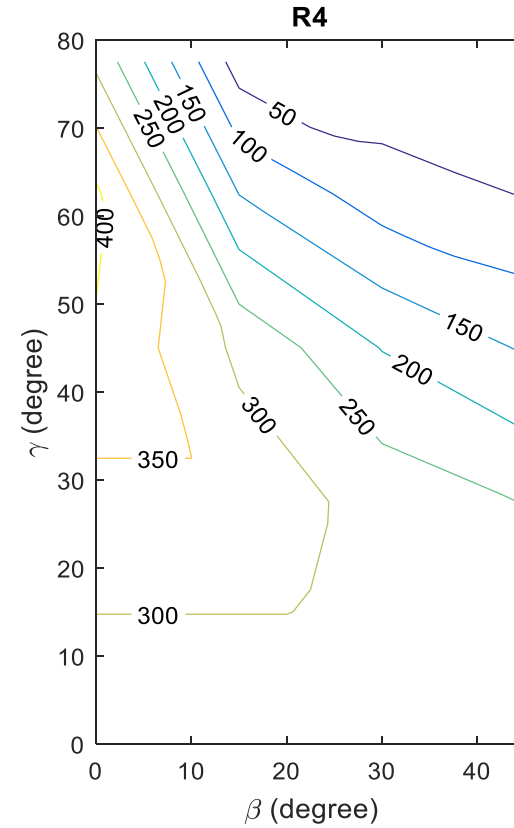
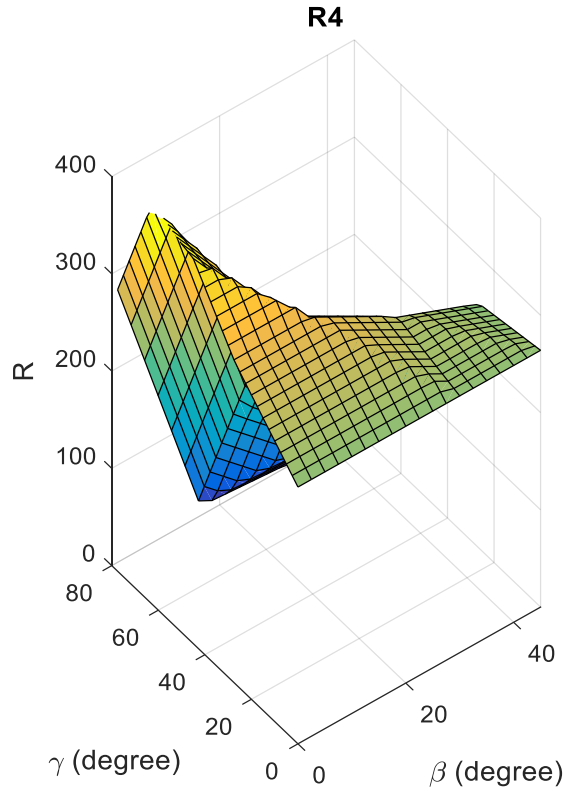
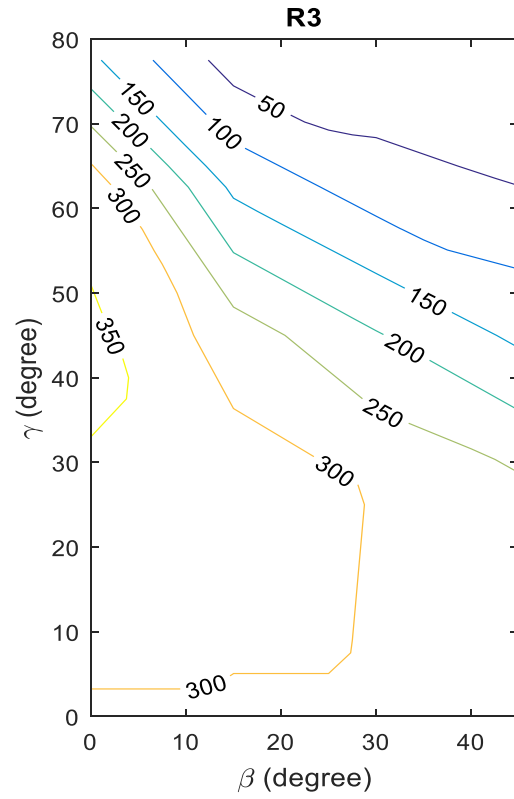
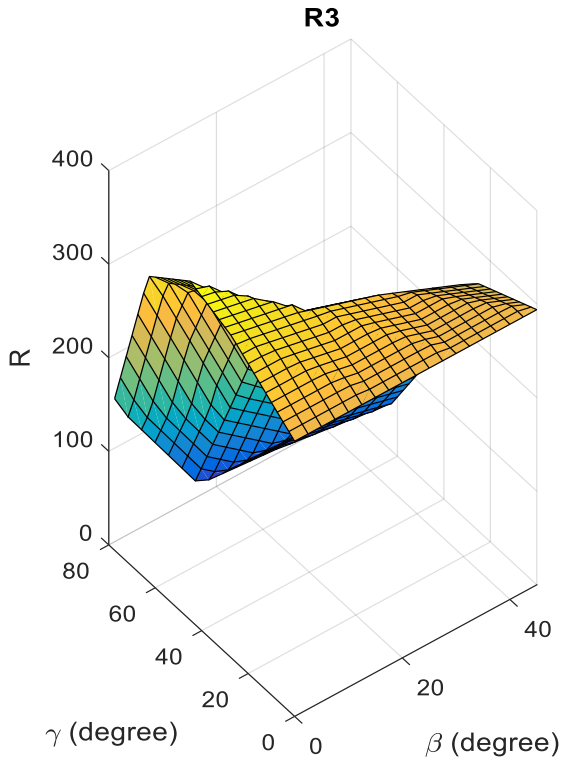
γ°	$\beta = 0^\circ$	$\beta = 15^\circ$	$\beta = 30^\circ$	$\beta = 45^\circ$
0°	294	294	294	294
27°	344	326	298	262
45°	362	276	204	140
63°	326	136	71	48
79°	145	16	8.2	6.1

R4-Table

γ°	$\beta = 0^\circ$	$\beta = 15^\circ$	$\beta = 30^\circ$	$\beta = 45^\circ$
0°	264	264	264	264
27°	330	330	284	251
45°	396	290	198	145
63°	409	145	71	45
79°	277	13	6.3	5

Simplified R-Graphs





CURRICULUM VITA

NAME: Jeremy Elliott Rice
Phone: 502-648-3574
Email: jericengineer@gmail.com

ADDRESS: 13803 Lakewoods Ct.
Prospect, KY 40059

DATE OF BIRTH: November 8, 1992

EDUCATION: B.S., Civil Engineering
University of Memphis
2011-2015

M.S., Civil Engineering
University of Louisville
2015-2016

AWARDS AND TITLES EARNED: Passed F.E. Exam in 2014
Became E.I.T. in 2015
Graduate M.S.C.E in 2016

STRUCTURAL ENGINEERING DESIGN CLASS: Steel Design
Reinforced Concrete Design
Prestressed Concrete Design
Masonry Design
Timber Design

REAL WORK EXPERIENCE: Data Analyst for Memphis Area Transit Authority (MATA)
Contact: John Lancaster (jlancaster@matatransit.com)

Research Assistant for the University of Louisville (U of L)
Contact: Young Hoon Kim (yhkim005@louisville.edu)